

# **For Reference**

---

**NOT TO BE TAKEN FROM THIS ROOM**



Ex LIBRIS  
UNIVERSITATIS  
ALBERTAENSIS
















Digitized by the Internet Archive  
in 2022 with funding from  
University of Alberta Library

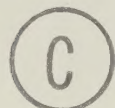
<https://archive.org/details/lwuagwu1979>



THE UNIVERSITY OF ALBERTA

DIAGENESIS OF THE BASAL BELLY RIVER SANDSTONE  
RESERVOIR, PEMBINA FIELD, ALBERTA, CANADA

by



CHUKWUMA JULIAN IWUAGWU

A THESIS

SUBMITTED TO THE FACULTY OF GRADUATE STUDIES AND RESEARCH  
IN PARTIAL FULFILMENT OF THE REQUIREMENTS FOR THE DEGREE  
OF MASTER OF SCIENCE

DEPARTMENT OF GEOLOGY

EDMONTON, ALBERTA

SPRING, 1979







## DEDICATION

To my parents, Chief and Mrs. James I. Iwuagwu, brothers ChikaA, Ugo, Oguledo, Onyebuchi and beloved sisters Evangeline (late), Patricia, Anthonia, Margret, Eugenia and Agnes for their love, help and encouragement which have been sources of inspiration to me.





## ABSTRACT

Techniques involving stereoscopic examination, thin sections, scanning electron microscopy and x-ray diffraction were used to study the petrography and diagenesis of the basal Belly River sandstone petroleum reservoir in the Pembina Keystone "B" pool. The project was initiated to study the cause of the anomalously low water/oil production ratio from a reservoir with high water saturation measured by mechanical logs and Core Laboratory analysis. The basal Belly River sandstone in the area of study is 50 to 70 feet (17-21 meters) thick, and is a fine- to medium grained, well to very well sorted, lithic arenite.

Diagenesis has been accomplished mainly by mechanical compaction, cementation and replacement. Carbonate, silica (quartz and chert) and authigenic clays (especially kaolinite) cements are widespread and are the main porosity reducing agents in this sandstone. The carbonate (calcite) cement occurs as pore filling coarse mosaic of anhedral subequant crystals whereas the silica cement occurs mainly as quartz and chert overgrowths. The authigenic clays (kaolinite, mixed-layer smectite/illite, and chlorite) occur as pore linings and pore fillings, and are characterized by very small crystal size and submicroscopic porosity. Partial and complete replacement of some unstable detrital grains such as feldspars and rock fragments by calcite and a phyllosilicate are common.





The petrophysical properties of porosity and permeability have been measurably modified by diagenesis resulting in porosities of less than 5 to 23 percent as measured by Core Laboratory analysis, and less than 1 to 13 percent as measured by thin section point counting. The permeability values for the same samples range from less than 1 md to 680 md. Comparison of Core Laboratory analysis and thin section data shows that the authigenic clays are a major control on the reservoir quality of the basal Belly River sandstone. Adsorbed, interlayer and possibly OH lattice water contribute to the relatively high Core Laboratory analysis porosity and water saturation values, but do not yield production water.





## ACKNOWLEDGEMENTS

The author wishes to thank Dr. J. F. Lerbekmo for the suggestion of this topic, his friendly and untiring supervision of the research and constructive comments during the writing of this thesis. This work was made possible through initial financial support in the form of a scholarship from the Department of Petroleum Resources, Ministry of Petroleum and Energy, Nigeria. The work was completed with financial assistance in the form of a Graduate Teaching Assistantship from the Geology Department, University of Alberta and NRC Grant A2127 to Professor J. F. Lerbekmo.

I gratefully acknowledge the cooperation of Imperial Oil Company, Calgary for kindly making slabbed cores and production data available to me, and the Exploration Review Branch, Department of Energy and Natural Resources, Edmonton for granting access to its log files. I thank Dr. J. Shaw for the use of his automatic counter, F. Dimitrov and E. Ezeofor for their technical advice on drafting, and G. Braybrook for operating the scanning electron microscope.

I would also like to thank Rod Moore for his hospitality during the preparation and writing of this thesis. Finally, I thank my parents, brothers and sisters for their continuous kindness, help and encouragement throughout the duration of this project.





# TABLE OF CONTENTS

	Page
DEDICATION . . . . .	iv
ABSTRACT . . . . .	v
ACKNOWLEDGMENTS . . . . .	vii
CHAPTER	
I. INTRODUCTION . . . . .	1
Purpose and Scope of the Study . . . . .	1
Previous Work . . . . .	7
Methods of Study . . . . .	10
II. STRATIGRAPHY AND LITHOLOGY . . . . .	15
The Belly River Formation of West-Central Alberta and Its Correlation with Contiguous Formations . . . . .	15
Lithology of the Basal Belly River Sandstone in the Study Area . . . . .	17
Mechanical Log Characteristics of the Basal Belly River Sandstone . . . . .	19
III. MINERALOGICAL COMPOSITION AND CLASSIFICATION	27
Classification . . . . .	27
Essential Components . . . . .	27
Quartz . . . . .	27
Feldspars . . . . .	38
Rock Fragments . . . . .	38
Accessory Minerals . . . . .	48
IV. GRANULOMETRIC ANALYSIS . . . . .	52
Size Frequency Distribution . . . . .	52
Parameters . . . . .	52
Textural Maturity . . . . .	54
Other Textural Attributes . . . . .	57
V. DIAGENESIS . . . . .	59
Definition . . . . .	59
Compaction and Pressure Solution . . . . .	59
Cementation . . . . .	63



CHAPTER	Page
V. (Continued)	
Calcite Cementation . . . . .	64
Quartz Cementation . . . . .	64
"Chert" Cementation . . . . .	69
Iron Oxide Cementation . . . . .	69
Secondary Clay Cementation . . . . .	72
Paragenesis of the Cements . . . . .	72
Replacement . . . . .	75
Recrystallization . . . . .	81
Solution . . . . .	81
Evaluation of the Diagenetic Effects in the Basal Belly River Sandstone . . . . .	82
VI. AUTHIGENIC CLAY IN BASAL BELLY RIVER SANDSTONE . . . . .	87
X-Ray Diffraction Analysis . . . . .	87
Scanning Electron Microscopy . . . . .	93
VII. A COMPARISON OF PETROGRAPHIC AND CORE ANALYSIS DATA . . . . .	103
VIII. INTERRELATIONSHIPS OF AUTHIGENIC CLAY AND WATER SATURATION IN THE BASAL BELLY RIVER SANDSTONE . . . . .	118
Relatively High Core Analysis Porosity . . . . .	118
High Core Analysis Water Saturation . . . . .	130
IX. SUMMARY AND CONCLUSIONS . . . . .	141
BIBLIOGRAPHY . . . . .	143
APPENDIX A. MEGASCOPIC DESCRIPTIONS OF BASAL BELLY RIVER CORE . . . . .	148
APPENDIX B. DATA SHEET FOR THE GRAIN-SIZE ANALYSES . . . . .	157





## LIST OF TABLES

Table	Description	Page
1.	Production in Barrels for 1971 and 1978, and Oil/Water Ratio Data	5
2.	Studied Wells in Townships 47 and 48 Range 4W5th Meridian with Basal Belly River Core	11
3.	Table of Formations of Southern Alberta and Adjoining Areas	18
4.	Essential Components (Recalculated to 100 Percent)	29
5.	Quartz Types as Percentage of Total Essential Components	31
6.	Feldspar Types as Percentage of Total Essential Components	39
7.	Rock Fragments as Percentage of Total Essential Components	43
8.	Summary Statistics of the Granulometric Analyses ( $\phi$ Units)	55
9.	Packing Proximity	61
10.	Cement Types and Percentages	65
11.	Relative Effects of Diagenesis on the Sediment Properties of the Basal Belly River Sandstone	85
12.	A Comparison of Observed Thin Section and Core Analysis Porosity Values	104
13.	Grain Mean Diameter, Observed Thin Section Porosity and Cement Percentages	106
14.	Summary of Observed Thin Section Porosity, Submicroscopic Porosity, 'Edge Error' and Core Analysis Porosity	113
15.	Core Laboratory Analysis Data and Observed Porosity	127





## LIST OF FIGURES

Figure		Page
1.	Typical Relative Permeability Relations with Varying Saturations of Water and Oil	3
2.	Pre-water Injection Oil-Water Ratio Map for Basal Belly River Sandstone in the Study Area	4
3.	Index Map	8
4.	Map of the Study Area showing Locations of Wells	9
5.	Megascopic Description of Core Typical of Basal Belly River Sandstone in the Study Area	22
6.	Fence Diagram of the Basal Belly River Sandstone in the Study Area	24
7.	Electrical Log Responses to the Basal Belly River Sandstone Lithology	26
8.	Compositional Classification of Basal Belly River Sandstone from the Study Area	28
9.	Cumulative Frequency Curves for Samples Representative of Basal Belly River Sandstone in the Study Area	53
10.	X-Ray Diffractogram of Less Than 2 $\mu$ Fraction of Oriented Mount of Sample #51 (10-35-47-4W5)	89
11.	X-Ray Diffractogram of Less Than 2 $\mu$ Fraction of Oriented Mount of Sample #23 (4-36-47-4W5)	90
12.	X-Ray Diffractogram of Less Than 2 $\mu$ Fraction of Oriented Mount of Sample #20 (10-35-47-4W5)	91
13.	X-Ray Diffractogram of Less Than 2 $\mu$ Fraction of Unoriented Mount of Sample #23 (4-36-47-4W5)	91
14.	Diagrammatic Sketch of Kaolinite Booklets and Plates Showing Submicroscopic Pores	99
15.	Grain Mean Diameter vs. Observed Thin Section Porosity Plot	108
16.	Core Analysis Porosity vs. Observed Thin Section Porosity Plot	110



Figure		Page
17.	Core Analysis Porosity vs. Observed Thin Section Porosity Plus 0.5 Kaolinite Cement Plot	115
18.	Edge Error as Percent of Total Obscured Porosity Plotted as a Function of Grain Size for Cubic-Packed Spheres	117
19.	Idealized Dehydration Curve for Kaolinite	124
20.	Dehydration Curve for Kaolinite, Ione, California	124
21.	Dehydration Curves (from Ross and Hendricks)	125
22.	Dehydration Curves (from Grim, Bray, and Bradley)	126
23.	Dehydration Curves (after Nutting)	126
24.	Core Laboratory Analysis Porosity vs. Permeability Plot	131
25.	Observed Thin Section Porosity vs. Permeability Plot	132
26.	Kaolinite Cement vs. Core Analysis Water Saturation Plot	136
27.	Permeability vs. Water Saturation Plot	137
28.	Permeability vs. Kaolinite Cement Plot	138





# LIST OF PLATES

Plate	Description	Page
1.	Photograph of top part of core slab typical of basal Belly River sandstone (Well: 4-36-47-4W5)	21
2.	Photomicrographs of thin sections of basal Belly River sandstone	35
3.	Photomicrographs of thin sections of basal Belly River sandstone	37
4.	Photomicrographs of thin sections of basal Belly River sandstone	42
5.	Photomicrographs of thin sections of basal Belly River sandstone	47
6.	Photomicrographs of thin sections of basal Belly River sandstone	50
7.	Photomicrographs of thin sections of basal Belly River sandstone	68
8.	Scanning electron micrographs of basal Belly River sandstone	71
9.	Photomicrographs of thin sections of basal Belly River sandstone	74
10.	Photomicrographs of thin sections of basal Belly River sandstone	77
11.	Photomicrographs of thin sections of basal Belly River sandstone	80
12.	Scanning electron micrographs of basal Belly River sandstone	95
13.	Scanning electron micrographs of basal Belly River sandstone	97
14.	Scanning electron micrographs of basal Belly River sandstone	101





## CHAPTER I. INTRODUCTION

### Purpose and Scope of the Study

The purpose of this study was twofold:

- 1) To study the diagenesis of the basal Belly River sandstone in the Keystone area of the Pembina field, and
- 2) To relate the petrography of this sandstone to its reservoir characteristics in the Pembina Keystone Belly River "B" pool.

The basal Belly River sandstone, which produces oil in the Pembina field area, is characterized by relatively high water saturations as measured by both electrical logs and laboratory core analyses. In the commercial Core Laboratory, water content of a formation is determined from sidewall and conventional cores by atmospheric distillation of the core in a retort at controlled temperatures, followed by the collection and measurement of the volume of the released water. The water content determination in whole cores is by vacuum distillation of the core. The water saturation,  $S_w$ , as percent of the pore space, in both cases, is arrived at by dividing the water content by the pore volume and multiplying by 100.

$$S_w = \frac{\text{Water content}}{\text{Pore volume}} \times 100 \quad (\text{Fundamentals of Core Analysis, Mod II})$$

Core Laboratory water saturation measurements in the Pembina Keystone Belly River "B" pool range from 30 to 67 percent with an average of 48 percent. When one



considers these water saturation values and their usual effect on relative permeabilities of a reservoir to immiscible fluids (for example, oil and water), one would expect high water/oil production from the basal Belly River sandstone because the relative permeabilities of a reservoir to two or more immiscible fluids depend directly upon their individual saturations in the pores. The relative permeabilities in turn determine the water/oil production from a reservoir. Figure 1, a typical relative permeability versus saturation curve, illustrates the above point. This curve shows that at a saturation of 56 percent for water and 44 percent for oil, the permeability of the rock is the same for both fluids and both flow equally well (Levorsen, 1967). In other words, the water and oil productions at these saturations are approximately equal. In view of the fact that (i) average Core Laboratory water and oil saturation values for three of the studied wells are approximately 53 and 8 percent, respectively; and (ii) during production this water/oil ratio (saturation) changes continually resulting in higher water saturation, one would normally anticipate an early 1:1 (or even greater) water/oil production ratio from the basal Belly River sandstone reservoir. However, reference to the oil-water ratio map for the pre-water injection production in 1971 (Figure 2) and Table 1 show a very low water recovery.





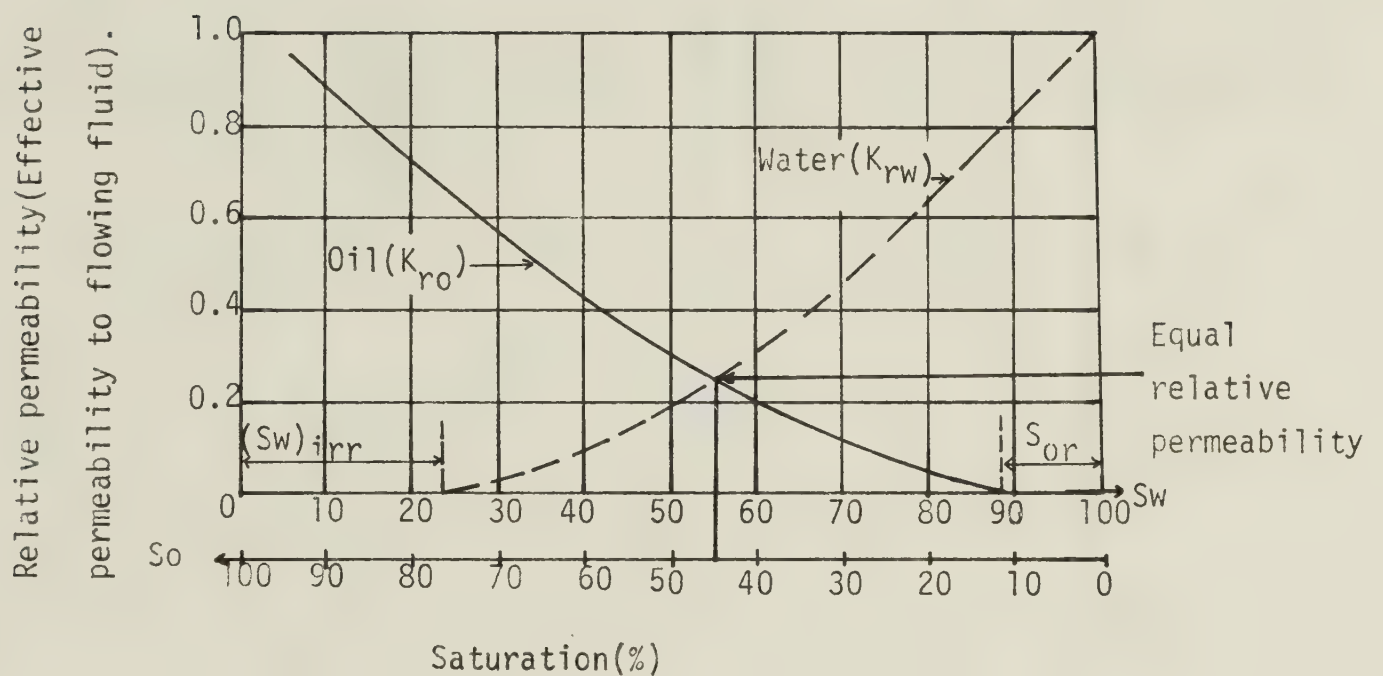


FIGURE 1. Typical relative permeability relations with varying saturations of water and oil.  $K_{ro}$  = Relative permeability to oil,  $K_{rw}$  = Relative permeability to water,  $S_{or}$  = Residual oil saturation,  $(S_w)_{irr}$  = Irreducible water saturation. (Modified after Levorsen, 1967; Schlumberger Log Interpretation, 1972).



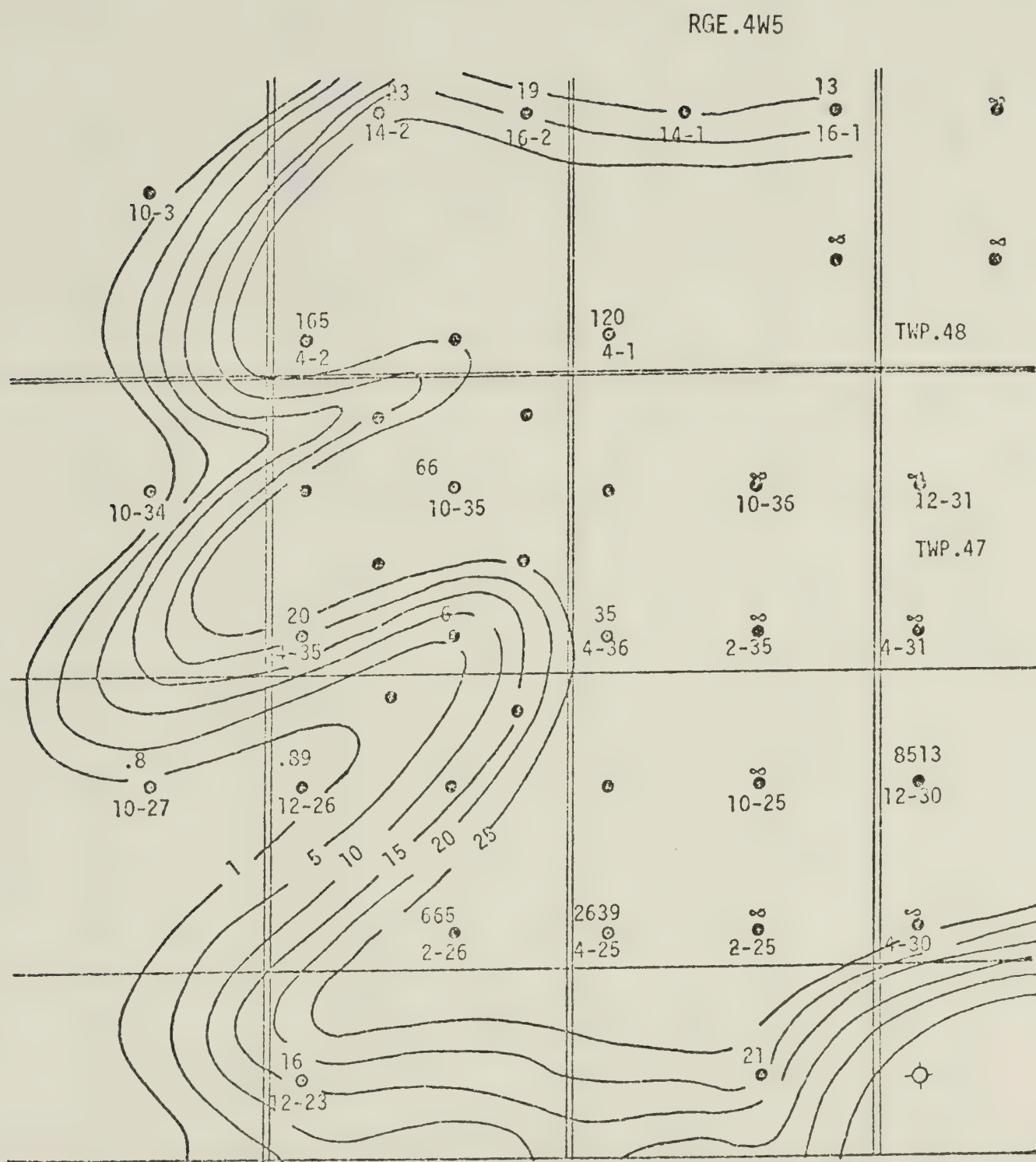


FIGURE 2. Pre-water injection Oil-water ratio map for basal Belly River Sandstone in the study area. (C.I.=5 Barrels of oil to 1 water).





TABLE 1.  
Production in Barrels for 1971 and 1978, and Oil/Water Ratio Data

Serial No.	Well Name	Location	Cumulative Production							
			For 1971 (Pre-water injection)				For 1978 (During water injection)			
			Oil Prod.	Gas Prod.	Water Prod.	Oil/ Water	Oil Prod.	Gas Prod.	Water Prod.	Oil/ Water
1.	IOE CDN- SUP PEMBINA	12-23-47 -4W5					44,529	51,106	8,815	5.1
2.	IOE CDN- SUP PEMBINA	4-25-47 -4W5	73,885	35,321	-		253,993	132,525	50,126	5.1
3.	IOE CDN- SUP PEMBINA	10-27-47 -4W5	17,858	8,096	18,829	0.95	19,463	10,363	20,499	0.95
4.	IOE CDN- SUP PEMBINA	10-34-47 -4W5	29,814	8,038	51,921	0.6	35,186	10,273	57,068	0.62
5.	IOE CDN- SUP PEMBINA	4-35-47 -4W5	82,449	30,269	4,720	17.5	255,059	92,406	31,858	8.0
6.	IOE CDN- SUP PEMBINA	10-35-47 -4W5	272,614	95,708	4,126	66.1	573,495	197,485	47,733	12.0

.../Continued



TABLE 1. - Continued

Serial No.	Well Name	Location	Cumulative Production							
			For 1971 (Pre-water injection)				For 1978 (During water injection)			
			Oil Prod.	Gas Prod.	Water Prod.	Oil/ Water	Oil Prod.	Gas Prod.	Water Prod.	Oil/ Water
7.	IOE CDN- SUP PEMBINA	4-36-47 -4W5	184,638	39,649	5,332	34.6	529,988	132,142	58,963	9.0
8.	IOE CDN- SUP PEMBINA	4-1-48 -4W5	78,196	41,171	653	119.7	212,065	105,966	10,663	20.0
9.	IOE CDN- SUP PEMBINA	4-2-48 -4W5	68,451	18,649	416	164.5	375,528	133,313	68,642	5.5



Also the production data by the end of 1975 showed an oil/water ratio of 15.3 (Trollope, 1976, Personal Communication). This production evidence tends to negate the Core Laboratory and electrical log predictions and to make their formation fluid saturation values (water and hydrocarbon saturations) suspect. The problem then was to ascertain the reason or reasons for the questionable saturations obtained from electrical log responses and laboratory core analysis.

The area chosen for this study is located in the eastern portion of the Pembina field (Keystone area) in townships 47 and 48, range 4 west of 5th meridian and is shown in Figures 3 and 4. This area was selected because of the availability of necessary cores. The cores from a group of wells owned by Imperial Oil Company were kindly loaned by the company for study.

### Previous Work

A number of geologists have addressed themselves to the study of the Belly River Group, or part of it, in various geographic areas. Such geologists include Dawson (1883), Dowling (1917), Williams and Dyer (1930), Russell and Landes (1940), Hildenbrand (1960), Lerbekmo (1961, 1963), Khamesra (1963), McLean (1971), Shawa and Lee (1975), Nelson and Glaister (1975), Ogunyomi and Hills (1977).

The work has been spread across many aspects of this lithostratigraphic unit with most emphasis on







FIGURE 3. Index Map



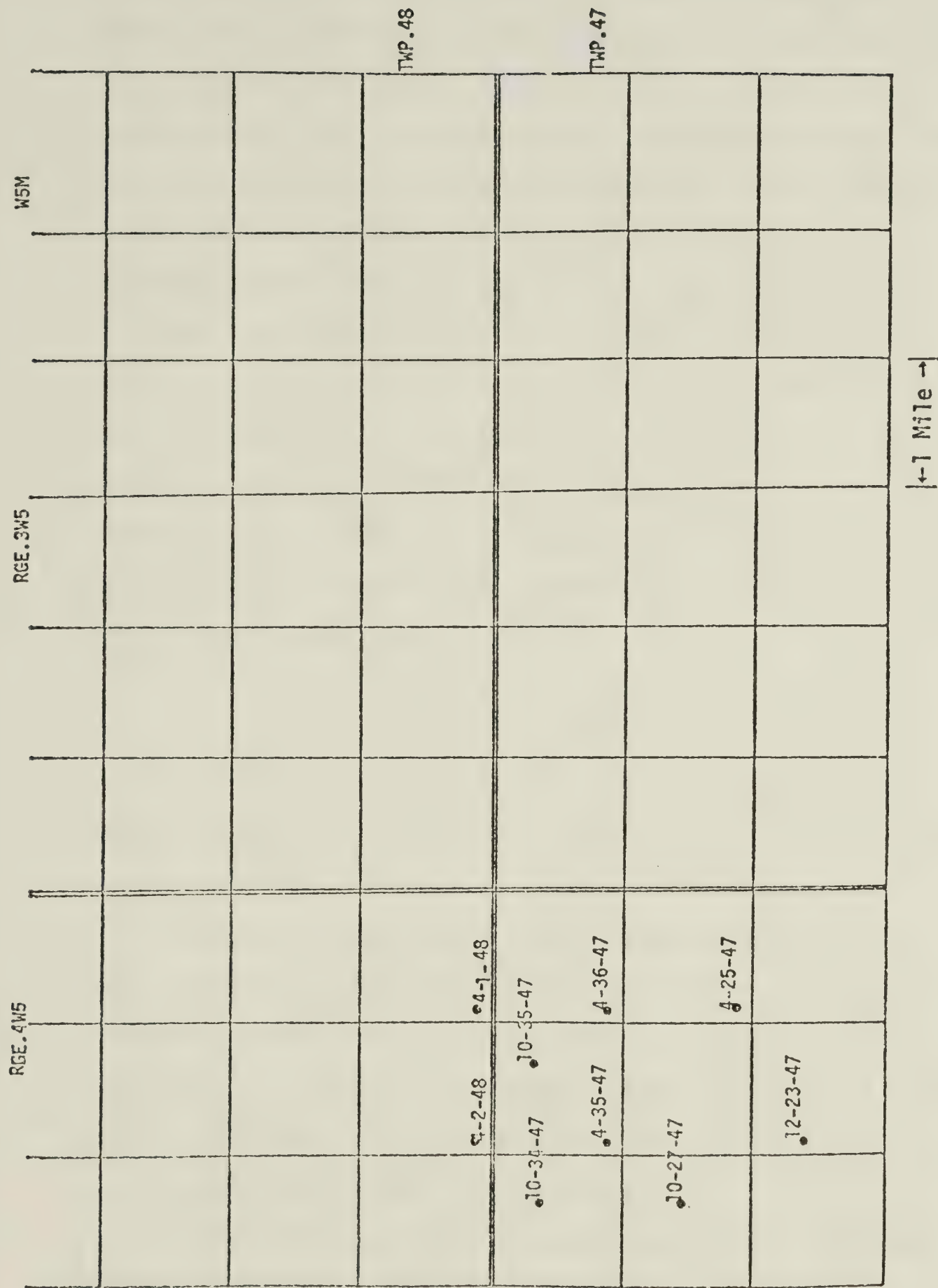


FIGURE 4. Map of the study area showing location of wells.





stratigraphy and depositional environments. The petrography and, in particular, the diagenesis of this unit had, in most cases, been given only cursory attention. The exceptions to this are the detailed study by Lerbekmo (1963) which focused on the petrology of the Belly River Formation in the Southern Alberta Foothills, and his earlier study (Lerbekmo, 1961) which showed the presence of authigenic clays and their possible effects in the Cretaceous sandstones of Alberta, of which the Belly River Formation is one. The presence of authigenic chlorite and illite cements in the basal Belly River sandstone of the Foothills region was also noted by Carrigy and Mellon (1964) in their study of the authigenic clay mineral cements in Cretaceous and Tertiary sandstones of Alberta.

#### Methods of Study

Techniques involving stereoscopic examination, thin sections, and scanning electron microscopy were used, as well as x-ray diffraction. Cores of the basal Belly River sandstone from Imperial Oil Company wells in townships 47 and 48, range 4 west of 5th meridian were examined (Table 2). Mechanical logs (spontaneous-potential, resistivity, conductivity, gamma, caliper and acoustic (one well only)) were primarily used for local correlation from well to well within the area of study.

Thirty-eight samples were selected for detailed analyses and study. Special attention was given to the



TABLE 2.

Studied Wells in Townships 47 and 48 Range 4 W5th Meridian with Basal Belly River Core

Serial No.	Well Name	Location	Cored Interval	Recovered Core Footage	Top of Lea Park*	Top of Basal Belly River*	Thickness of Basal Belly River
1.	IOE CDN-SUP PEMBINA	12-23-47 -4W5	3319-3398	78.0	3395.0 FT	335.0 FT	60.0 FT
2.	IOE CDN-SUP PEMBINA	4-25-47 -4W5	3137-3197 -3222	85.0	3223.0 FT	3158.0 FT+	65.0 FT
3.	IOE CDN-SUP PEMBINA	10-27-47 -4W5	3185-3244	59.0x	3256.0 FT	3205.0 FT	51.0 FT
4.	IOE CDN-SUP PEMBINA	10-34-47 -4W5	3142-3227	85.0x	3215.0 FT	3153.0 FT	62.0 FT
5.	IOE CDN-SUP PEMBINA	4-35-47 -4W5	3136-3196	113.0	3231.0 FT	3175.0 FT	56.0 FT
6.	IOE CDN-SUP PEMBINA	10-35-47 -4W5	3229-3306	77.0x	3300.0 FT	3240.0 FT+	60.0 FT
7.	IOE CDN-SUP PEMBINA	4-36-47 -4W5	3217-3307	90.0x	3300.0 FT	3247.0 FT	53.0 FT

.../Continued



TABLE 2. - Continued

Serial No.	Well Name	Location	Cored Interval	Recovered Core Footage	Top of Lea Park*	Top of Basal Belly River*	Thickness of Basal Belly River
8.	IOE CDN-SUP PEMBINA	4-1-48 -4W5	3232-3302	70.0	3297.0 FT	3239.0 FT	58.0 FT
9.	IOE CDN-SUP PEMBINA	4-2-48 -4W5	3165-3239	74.0x	3236.0 FT	3165.0 FT	71.0 FT

\* Data from Schedule of Wells drilled for oil and gas, Province of Alberta, 1965 and 1966.

+ Picked from ES-log.

x Wells from which thin-sections were prepared.





preparation of thin sections to ensure preservation of the delicate authigenic clay mineral cements. Most of the thin sections were made by Fred Roberts, Monterey Park, California and were impregnated with blue epoxy to preserve the original texture of the samples and to facilitate the identification of microscopic pores.

Compositional analysis of the thin sections was achieved by recording 600 points within a 6 sq. cm grid utilizing an automatic point-count mechanical stage. A check made after counting 300 points in thin section revealed that counting more than 600 points was unnecessary.

Because the samples selected for detailed examination are lithified, the necessary data for granulometric analyses were also obtained from the thin sections, utilizing a Humphries' micrometer eyepiece. Four hundred grains were measured in each thin section. A comparison with the data obtained from the first 200 grains, showed that measuring more than 400 grains was not justified.

For the mineralogical analysis of the authigenic clay mineral cement, x-ray diffraction was employed in addition to SEM examination. To obtain a relatively pure clay fraction uncontaminated by allogenic clays and nonclay grains produced by disaggregation, a modification of the method of separation recommended by Wilson and Pittman (1977) was adopted. The samples were gently crushed using mortar and pestle. The gentle treatment liberated the authigenic clays without pulverizing the argillaceous rock



fragments. The sample was then sieved and the less than 2 micron fraction (equivalent settling diameter) was collected and dispersed in a cylinder of water. Two oriented specimens of the clay per sample were collected on glass slides utilizing the settling characteristics of the clay in water. One specimen of each pair was x-rayed after air drying (i.e. drying to room temperature and humidity), and again after glycolation (i.e. saturation with ethylene glycol vapor) to help detect expandable clays. The other specimen was x-rayed after heating to 550° C for two hours to differentiate between kaolinite and dickite. X-ray diffraction patterns were obtained using a diffractometer with geiger counter pick-up and strip-chart recorder. To understand the exact morphology of the authigenic clay mineral cement, which is not usually determinable from thin sections, and to supplement the x-ray diffraction identifications, scanning electron microscopy was also carried out using a Cambridge Stereoscan 150. The samples were scanned at various magnifications and micrographs taken. Thus, the mineralogical identification and habit of the authigenic clays are based on a combination of thin section petrography, x-ray diffraction analysis, and scanning electron microscopy.





## CHAPTER II. STRATIGRAPHY AND LITHOLOGY

### The Belly River Formation of West-Central Alberta and its Correlation with Contiguous Formations

The Belly River Formation in the area of study represents part of an eastward thinning clastic wedge that records the progradation of continental conditions associated with the eastward withdrawal of the Lea Park sea during the Upper Cretaceous (Campanian) time. It attains a thickness of about 1200 to 1400 feet (370-430 meters) in the Plains of Southern Alberta and increases westwards to about 2300 feet (700 meters) in the Southern Foothills (Lerbekmo, 1961), but in the area of study its thickness is about 850 feet (260 meters) (Schedule of Wells, 1965, 1966).

Nomenclature - A literature review of the term "Belly River" shows ambiguity and inconsistency in its usage since its inception in 1883. The author of the term, Dawson, in 1883 designated a series of beds underlying the Pierre shales in Southern Alberta as the Belly River series. Williams and Dyer (1930) restricted the term Belly River to the Foremost beds and the Pale beds. Russell and Landes (1940) raised the Foremost and the Oldman beds to formation status in the belief that the term "Belly River series" is ambiguous. Hildenbrand (1960) stated that the term "Belly River" as now used includes the Foremost and Oldman formations of Southern Alberta and should be given group status. McLean (1971) has recently argued for dropping of the term Belly River for the



American term Judith River for reasons of priority of usage. In the west-central Alberta Plains and Foothills this unit is undivided and called the Belly River Formation.

In the present study, the following definitions are used:

1. the term "Belly River Formation" in west-central Alberta includes only the stratigraphic interval between the top of Lea Park Formation and the bottom of the Bearpaw Shale,
2. the term "basal Belly River sandstone" refers to the lowermost sandstone unit of the Belly River Formation; it ranges from 50 feet to 71 feet (17-21.5 meters) in thickness (Schedule of Wells, Province of Alberta, 1965 and 1966).

The sediments of the Belly River Group (Foremost and Oldman formations) consist of sandstone, siltstone, mudstone, shale and coal, and are characterized by both vertical and lateral rapid facies changes. This reflects the changing nature of the depositional processes and environments, which ranged from continental through deltaic and littoral to marine. In southeastern Alberta and southwestern Saskatchewan, these facies changes result in much intertonguing of the Belly River Group with the underlying marine Lea Park Formation (McLean, 1971).

The Belly River Group is conformable with both the underlying marine shale (Pakowki, Lea Park or Wapiabi) and with the overlying Bearpaw Shale. Despite its conformable contacts with both the subjacent and superjacent formations, the Belly River Group is not a time-stratigraphic unit. It



is time-transgressive (diachronous), becoming younger to the east. It is the lateral equivalent and continuation of the Two Medicine Formation and Virgelle Sandstone of northern Montana, and of the Judith River Formation of north-central Montana (Hildenbrand, 1960; McLean, 1971). Table 3 shows the regional correlation of the Belly River "Formation".

The basal Belly River sandstone is the correlative of Allan's (1919) Brosseau member exposed along the North Saskatchewan River valley in the east-central Alberta plains and Slipper and Hunter's (1931) Verdigris Sandstone farther south. Slipper and Hunter believed that the Verdigris Sandstone was the beach deposit of the retreating Montana Sea. In the subsurface, Shaw and Harding (1954) also recognized the Brosseau member in the east-central Alberta plains.

#### Lithology of the Basal Belly River Sandstone in the Study Area

In the area of study in west-central Alberta, the basal Belly River sandstone is the lowermost sandstone unit of the Belly River Formation and ranges from 50 feet to 71 feet (17-21.5 meters) in thickness. It consists of horizontal-bedded and cross-stratified, light grey to grey, "salt and pepper", fine to medium grained, poorly to moderately sorted, occasionally pebbly sandstones, and minor amounts of dark grey mudstones, siltstones, and carbonaceous and bentonitic shales. It has a gradational contact with the underlying Lea Park Shale, grading from very fine and





Table 3. Table of Formations of Southern Alberta and adjoining areas.  
(From Energy Resources Conservation Board, 1966).



shaly sandstone through siltstone and mudstone into the Lea Park shale. This lower contact is also time-transgressive (diachronous) becoming younger to the east. The upper contact appears to be sharper and is in many places marked by thin shale and mudstone beds followed by coal; in other places the coal beds directly overlies the sandstone. Internally the basal Belly River sandstone shows some heterogeneities in the form of mudstone and siltstone lenses and shaly partings. The basal Belly River sandstone represents near-shore, progradational deposition beginning with marine shale followed by shoreline sands and terminated by deltaic deposits (coal beds). Some of the above mentioned features of this sandstone unit can be readily observed in the photographs of core slabs (Plate 1). Figure 5 shows a detailed megascopic description of core typical of the basal Belly River sandstone in the area of study. (See Appendix A for more core descriptions.)

#### Mechanical Log Characteristics of the Basal Belly River Sandstone

All available electrical and radiation logs (spontaneous-potential, resistivity, conductivity, gamma and acoustic) for the Imperial Oil Company wells in the area of study (townships 47 and 48, range 4 west of 5th meridian) were examined. They show that the basal Belly River sandstone and some marker horizons can be easily identified on the logs. Several markers such as a prominent bentonitic







PLATE 1. PHOTOGRAPH OF TOP PART OF CORE SLAB TYPICAL OF  
BASAL BELLY RIVER SANDSTONE (WELL: 4-36-47-  
4W5M)

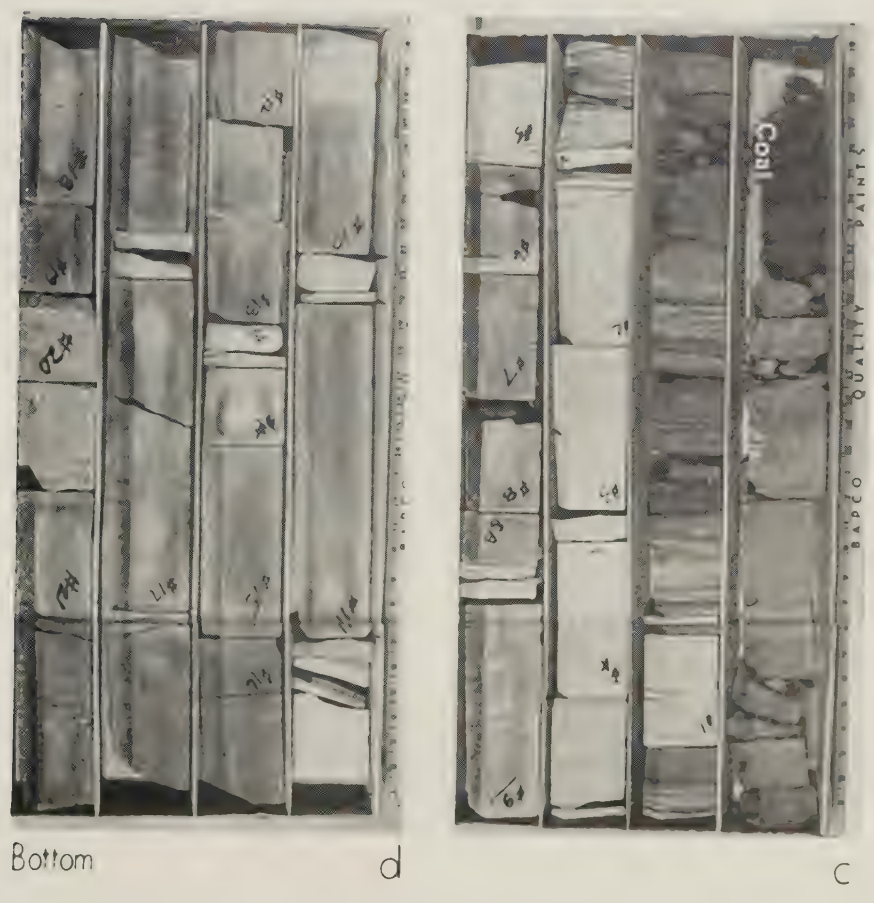
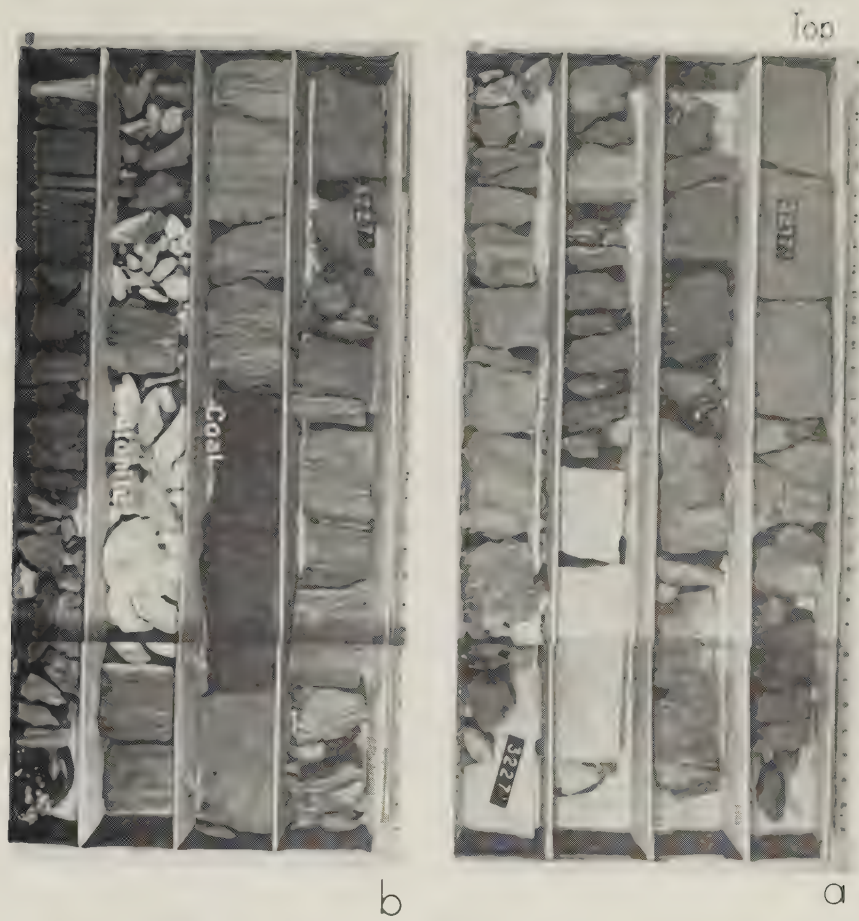
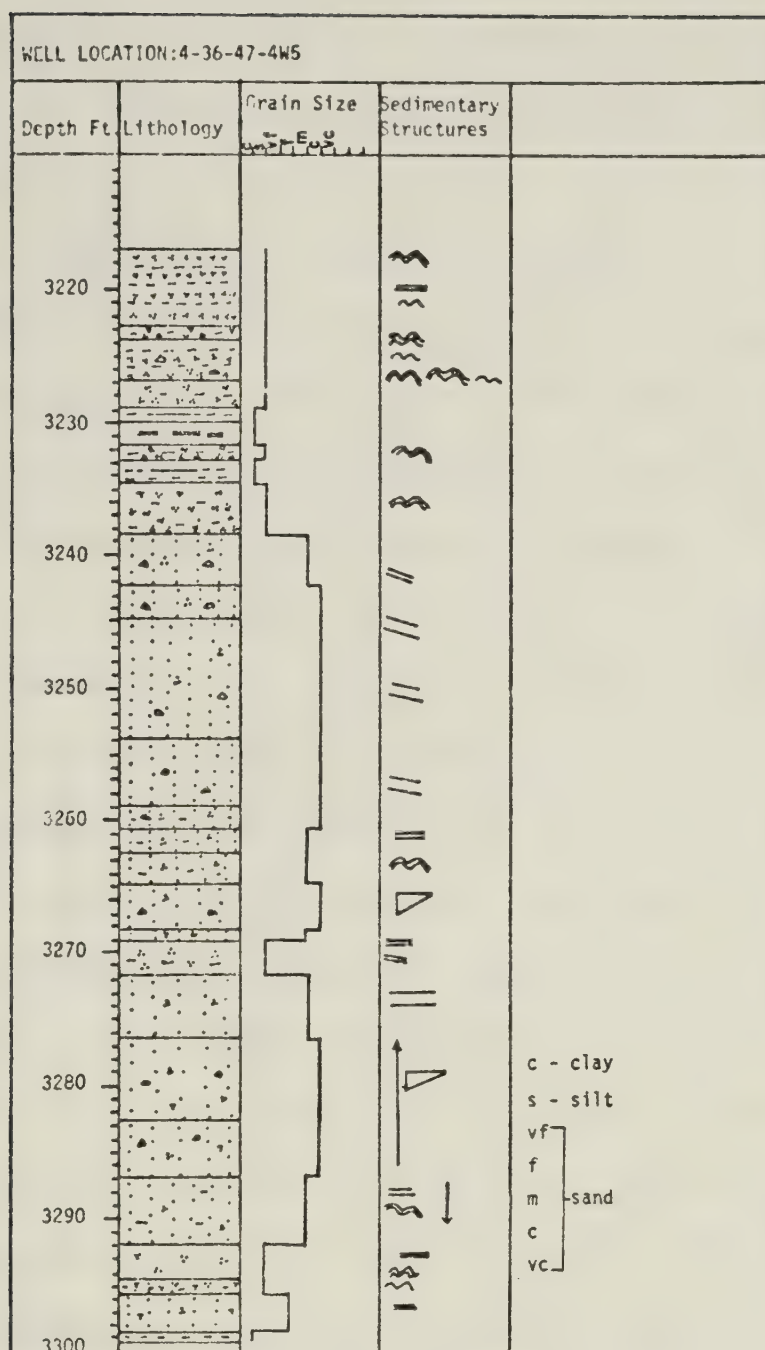


PLATE 1.





## LEGEND:

- Sandstone
- Shaly Sandstone
- Shale
- Sandy Shale
- Siltstone
- Mudstone
- Coal Bed
- Bentonitic Bed
- Pebbly

- Horizontal Bedding
- Thick Bedding
- Cross Stratification
- Parallel Lamination
- Cross Lamination
- Irregular Lamination
- Slump Structure
- Bioturbation(Churning)
- Rootlets
- Fining Upward
- Coarsening Upward

FIGURE 5. Megascopic description of core typical of basal Belly River sandstone in the study area.



layer near the top of this basal sandstone unit, and some coal beds, proved valuable for local correlation from well to well (Figure 6).

On the spontaneous potential curve, the gross basal Belly River sandstone ideally shows as a negative deflection from the shale base-line. The amount of deflection is dependent on such factors as borehole conditions, depth of mudfiltrate invasion, formation fluid chemistry and the petrography of the beds. In some places, such as where the sandstone contains calcite-cemented zones, mudstone and siltstone lenses or shaly partings, the spontaneous potential curve shows some reduction in deflection. Khamesra (1963) observed that spontaneous potential deflection is poorly developed in wells drilled with high conductivity (low resistivity) "calcium chloride-starch" mud, and that in some cases reversal of the spontaneous potential was noted. This was also observed in the present study and well 4-35-47-4W5 is a good example. This may be a result of either the use of low resistivity mud, as suggested by Khamesra, or the presence of fresh formation water in the sandstone. However, in most cases the basal Belly River sandstone responds to the spontaneous potential logging tool as a negative deflection.

The resistivity logs are generally characterized by relatively higher resistivities opposite the sandstone than the subjacent and superjacent shales and mudstones. This may be in part a reflection of the sandstone's





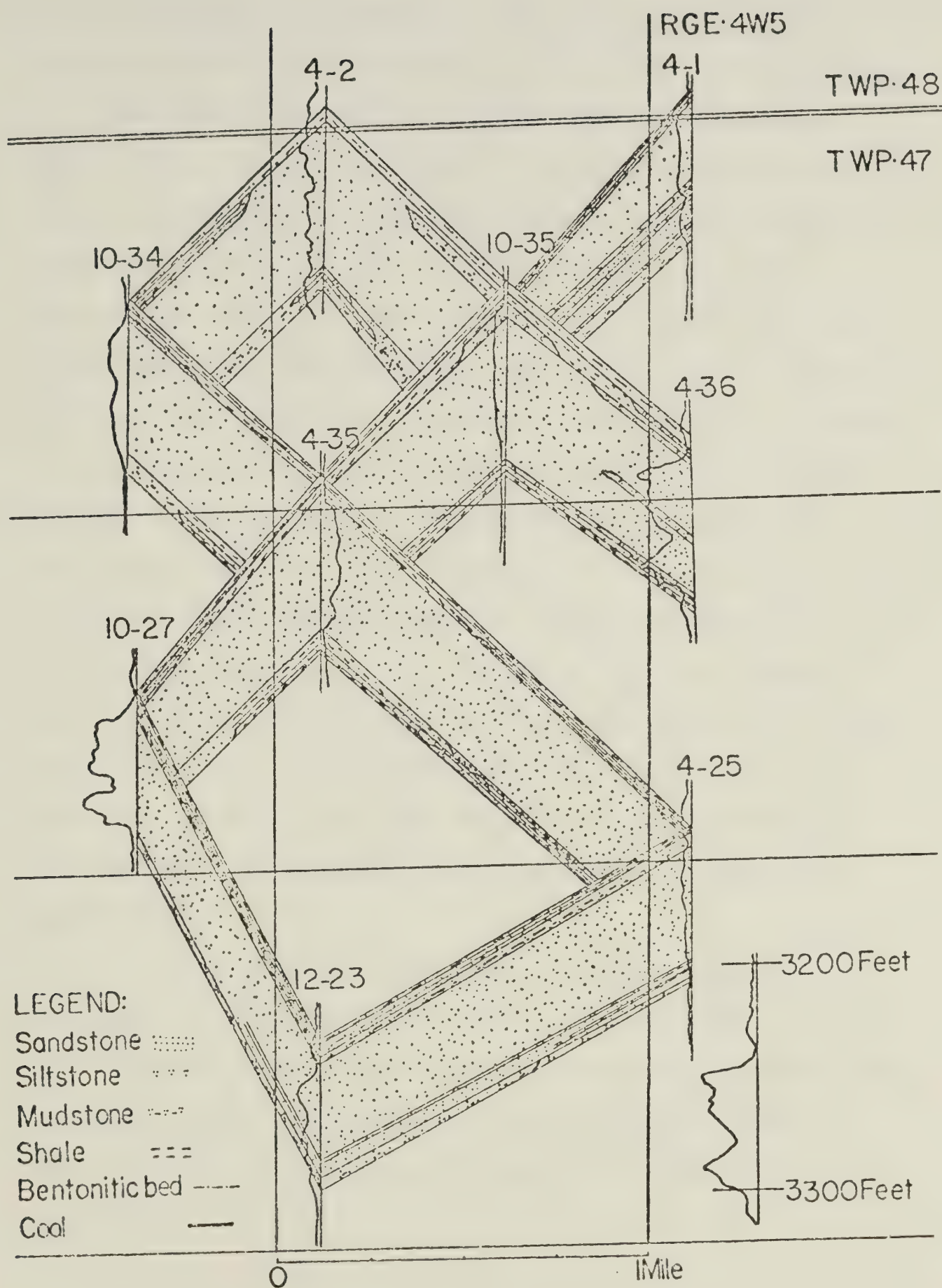


FIGURE 6. Fence diagram of the basal Belly River sandstone in the study area.



contained fluid-hydrocarbons. But even in these cases of relatively high resistivities, it may be that the readings are lower than they would be if it were not for the resistivity reduction due to the presence of authigenic clays. In cases where there are tight, calcite-cemented sandstone streaks within the porous sandstone, the resistivity readings are abnormally high, while the sandwiched mudstone and siltstone lenses and shaly partings are shown as low resistivity readings. The coal beds responded to the resistivity logging tool as highly resistive beds similar to the tight, calcite-cemented sandstone zones. On the conductivity log, the bentonitic bed which was used as a local time-stratigraphic marker, showed prominently as a very highly conductive bed. Figure 7 shows an example of the electrical log responses to the basal Belly River sandstone lithology. Only minor depth adjustments were made to match the lithology with the electrical log responses in both the above lithologic plot (Figure 5) and those in Appendix A.

The gamma-ray log shows the basal Belly River sandstone as a low gamma-ray reading unit relative to both the underlying marine shale and the overlying mudstones and bentonitic beds. Intercalated siltstones, mudstones and shaly partings show as minor deflections within the sandstone unit.









### CHAPTER III.

#### MINERALOGICAL COMPOSITION AND CLASSIFICATION

##### Classification.

The classification scheme adopted in the present study at the microscopic level is that of Lerbekmo (1963) which incorporates the essentials of Gilbert's (1954), Travis (1955) and Crook's (1960) classification schemes. Figure 8 illustrates this classification scheme and shows the plots of the analysed samples of the basal Belly River sandstone on the ternary diagram. All thirty-eight samples plot as lithic arenite (sandstone) in this classification scheme.

##### Essential Components.

The essential components, which are those used in the classification of the sandstones, are quartz, feldspars and rock fragments. The basal Belly River sandstone in the "B" pool of the Pembina field is composed mainly of rock fragments (50 to 79 percent), quartz (16 to 34 percent), and feldspars (1 to 17 percent) averaging 63.6, 25.7 and 10.6 percent respectively (Table 4).

##### Quartz.

On the bases of the type and amount of inclusions, crystal outline (faces) and extinction character, four quasi-genetic types of quartz as defined by Lerbekmo (1963) plus quartzite (polycrystalline quartz) grains were identified (Table 5). The most abundant type in the samples



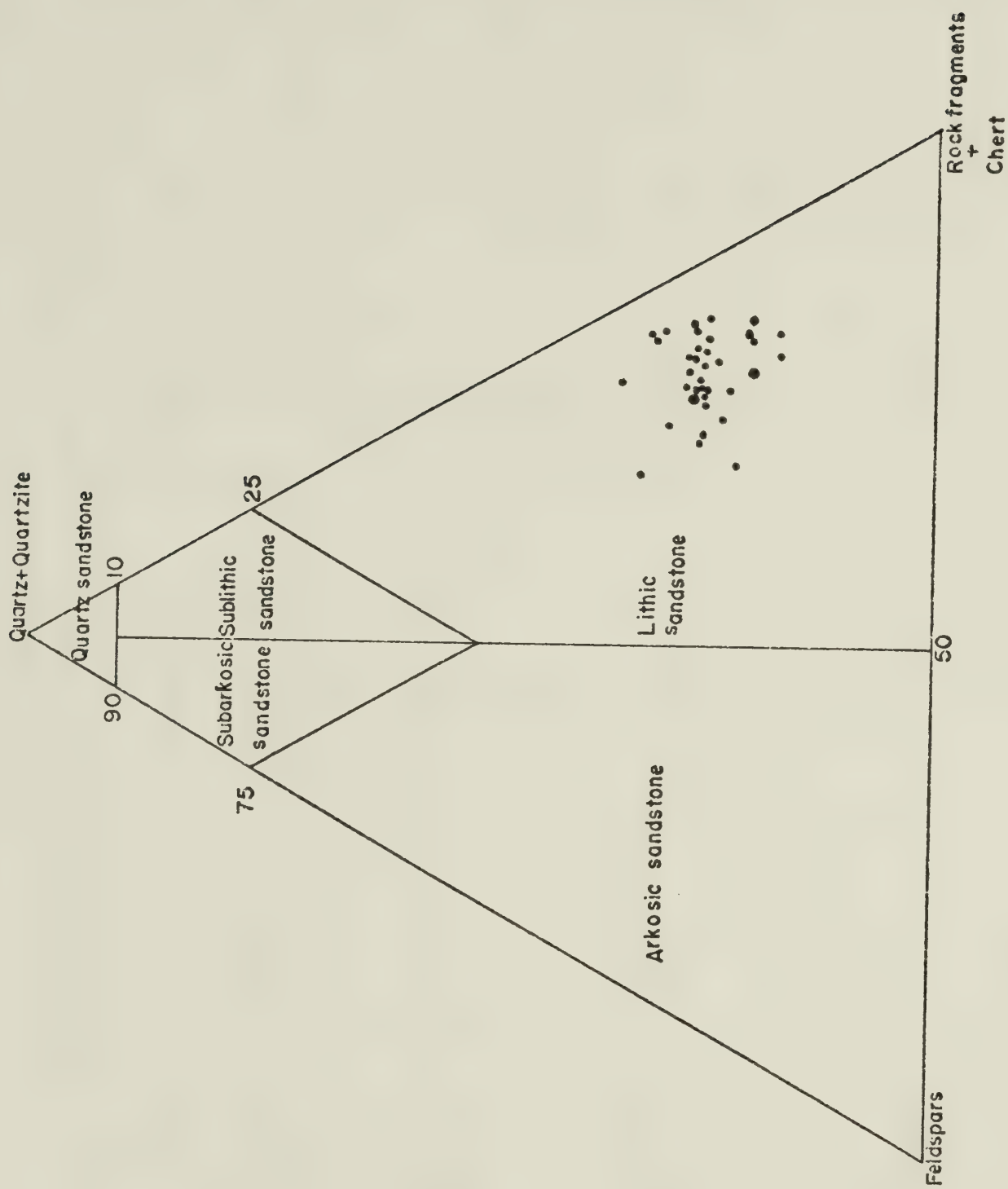


FIGURE 8. Compositional classification of basal Belly River sandstone from the study area. (After Lerbekmo, 1963).



TABLE 4.  
Essential Components (Recalculated to 100 Percent)

Serial No.	Well Name	Location	Sample No.	Quartz (%)	Feldspars (%)	Rock Fragments (%)
1.1	IOE CDN-SUP PEMBINA	10-27-47 -4W5	At 3212.8 ft	17.3	13.6	69.1
1.2			At 3215.4 ft (A)	20.9	7.3	71.8
1.3			At 3215.4 ft (B)	16.8	6.9	76.3
1.4			At 3219.1 ft	25.7	17.0	57.3
1.5			At 3233.8 ft	29.3	14.0	56.6
2.6	IOE CDN-SUP PEMBINA	10-34-47 -4W5	At 2186.3 ft (A)	19.1	1.1	79.8
2.7			At 2186.3 ft (B)	18.3	3.1	78.6
2.8			40	25.4	7.0	67.6
2.9			41	24.9	12.6	62.5
2.10			50	25.6	13.2	61.2
2.11	IOE CDN-SUP PEMBINA	10-35-47 -4W5	52	26.0	17.3	56.7
2.12			53	22.6	13.9	63.5
3.13			6	25.1	14.1	60.8
3.14			18	17.6	10.8	71.6
3.15			20	25.0	7.9	67.1
3.16	IOE CDN-SUP PEMBINA	4-36-47 -4W5	23	27.4	11.3	61.3
3.17			25	27.2	8.8	64.0
3.18			39	26.6	5.8	67.6
3.19			46	25.2	9.0	65.8
4.20			12	26.9	8.8	64.2
4.21	IOE CDN-SUP PEMBINA		16	29.4	4.9	65.7
4.22			18	31.3	4.2	64.5
4.23			19	34.4	7.4	58.2
4.24			23	20.7	10.0	69.4

.../Continued





TABLE 4. - Continued

Serial No.	Well Name	Location	Sample No.	Quartz (%)	Feldspars (%)	Rock Fragments (%)
4.25	IOE CDN-SUP PEMBINA	4-36-47 -4W5	25	26.0	12.5	61.5
4.26			35	28.7	11.6	59.8
4.27			37	26.4	12.7	60.9
5.28	IOE CDN-SUP PEMBINA	4-2-48 -4W5	12	23.8	16.0	60.2
5.29			13	31.0	5.0	64.0
5.30			16	26.4	6.2	67.4
5.31			23	20.7	7.3	72.1
5.32			23	29.8	14.5	55.7
5.33			33	25.2	5.3	69.5
5.34			33	18.2	11.4	70.5
5.35			42	32.3	17.3	50.4
5.36			46	27.6	10.0	62.3
5.37			47	20.4	10.4	69.2
5.38			51	25.1	8.9	66.0
			Average	25.7	10.6	63.6

NB: A = Coarse part of slide (thin section)  
 B = Fine part of slide (thin section)



TABLE 5.

Quartz Types as Percentage of Total Essential Components

Serial No.	Well Name	Location	Sample No.	"Common" Quartz	Metamorphic Quartz	Volcanic Quartz	Sedimentary Quartz	Quartzite Rock Fragments
1.1	IOE CDN-SUP	10-27-47	At 3212.8 ft	14.8	2.1	-	-	0.4
1.2	PEMBINA	-4W5	At 3215.4 ft	19.0	-	0.9	0.4	0.6
1.3			At 3215.4 ft	12.2	0.6	4.0	-	-
1.4			At 3219.1 ft	19.0	4.3	-	-	2.4
1.5			At 3233.8 ft	20.7	4.1	-	-	4.5
2.6	IOE CDN-SUP	10-34-47	At 2186.3 ft	15.8	0.7	0.6	0.7	1.3
2.7	PEMBINA	-4W5	At 2186.3 ft	15.6	1.2	1.0	0.6	-
2.8			40	14.1	4.3	1.6	0.4	5.1
2.9			41	17.8	4.5	-	-	2.6
2.10			50	19.6	3.6	0.4	-	2.0
2.11			52	21.7	3.1	-	-	1.2
2.12			53	15.8	4.5	-	-	2.3
3.13	IOE CDN-SUP	10-35-47	6	19.0	3.4	-	1.1	1.5
3.14	PEMBINA	-4W5	18	9.1	4.5	0.6	0.6	2.8
3.15			20	11.6	5.1	0.5	0.5	7.4
3.16			23	16.0	6.1	0.5	-	4.7
3.17			25	4.8	7.5	1.3	6.6	7.0
3.18			39	6.2	8.1	1.5	5.4	5.4
3.19			46	6.8	2.1	3.0	8.1	5.1
4.20	IOE CDN-SUP	4-36-47	12	16.9	6.5	0.8	1.2	1.5
4.21	PEMBINA	-4W5	16	18.9	6.4	0.4	1.1	2.6
4.22			18	16.6	7.9	1.5	0.4	4.9
4.23			19	20.7	7.0	1.6	-	6.1
4.24			23	14.8	4.1	0.7	-	1.1

.../Continued



TABLE 5. - Continued

Serial No.	Well Name	Location	Sample No.	"Common" Quartz	Metamorphic Quartz	Volcanic Quartz	Sedimentary Quartz	Quartzite Rock Fragments
4.25	IOE CDN-SUP PEMBINA	4-36-47-4W5	25	20.0	3.4	0.4	0.4	1.9
4.26			35	19.5	6.4	0.4	-	2.4
4.27			37	14.1	6.5	0.7	1.1	4.0
5.28	IOE CDN-SUP PEMBINA	4-2-48-4W5	12	20.9	1.9	0.5	-	0.5
5.29			13	25.6	4.3	0.4	-	0.8
5.30			16	22.5	1.9	-	-	1.9
5.31			23	10.1	4.0	-	0.4	6.1
5.32			23	23.4	3.2	-	-	3.2
5.33			33	15.9	4.5	0.4	-	4.5
5.34			33	12.5	3.0	1.9	-	0.8
5.35			42	23.7	5.6	-	1.1	1.9
5.36			46	18.0	4.6	0.8	0.4	3.8
5.37			47	16.9	1.5	-	-	1.9
5.38			51	17.4	3.5	-	1.2	3.1
			Average	16.6	4.5	0.6	0.9	3.1

NB: A = Coarse part of slide  
B = Fine part of slide





studied is "common" quartz which ranges from 5 to 25 percent of the rock and averages 16.6 percent. It is characterized by irregular outline, a few inclusions in the form of bubbles, and moderate undulose extinction (Plate 2A, B). These characteristics are suggestive of plutonic origin but the possibility of alternative origins such as metamorphic and vein cannot be ruled out (Folk, 1974).

The second most abundant quartz type is the metamorphic variety. It makes up from 1 to more than 8 percent of the samples and averages 4.5 percent. Strong undulose extinction, and inclusions of metamorphic minerals such as micas characterize these quartz grains (Plate 2C, D).

Sedimentary quartz (up to 6 percent) is next in abundance, averaging 0.9 percent. Quartz grains included in this variety are characterized by appreciable rounding (Plate 2E, F). But as Thiel (1940) pointed out, quartz grains of medium sand size require much transport to produce noticeable rounding and, therefore, it is likely that many first cycle sedimentary quartz grains have been mistakenly included with other varieties; hence, the low apparent count.

Identifiable volcanic quartz is the least abundant of the quartz types (up to 3 percent). Quartz grains identified as volcanic are characterized by one or more well-developed crystal faces and the lack of inclusions (Plate 3A, B). In the case of fragmented volcanic quartz grains without preserved crystal faces, the absence of inclusions





PLATE 2. PHOTOMICROGRAPHS OF THIN SECTIONS OF BASAL BELLY  
RIVER SANDSTONE

- A. "Common" quartz (a) coated by dark brown iron oxide (hematite?) cement (arrow). Authigenic clay (b) plugs a pore between detrital quartz grains. (Well: 10-35-47-4W5. Sample no. 20. Plane light. X40)
- B. Same as A, but between crossed nicols. Iron oxide cement (arrow) followed by quartz overgrowth which is in turn followed and partially replaced by authigenic kaolinite. Note the low birefringence of authigenic kaolinite. X40.
- C. Metamorphic quartz grain (a) characterized by inclusions of muscovite. Mudrock fragment (b) with recrystallized crystals of muscovite. Chert rock fragment (c) made up of cryptocrystalline quartz. (Well: 10-34-47-4W5. Sample no. 52. Plane light. X40)
- D. Same as C, but between crossed nicols. X40.
- E. Rounded sedimentary quartz (a) is surrounded by dark brown siderite 'blebs' of cement (arrow). Plagioclase feldspar (b) has been partially replaced along twinning planes by calcite cement (c). (Well: 10-35-47-4W5. Sample no. 18. Plane light. X40)
- F. Same as E, but between crossed nicols. X40.



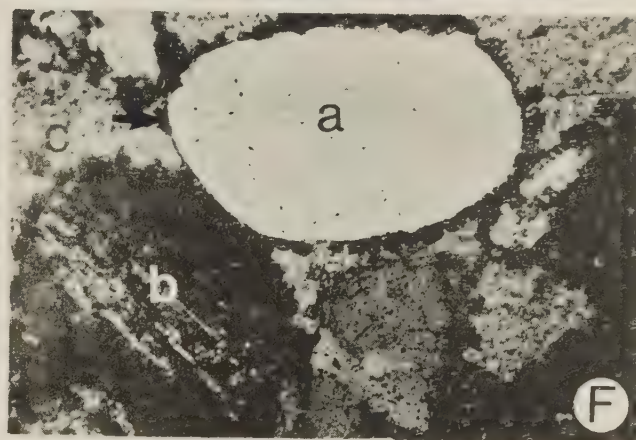
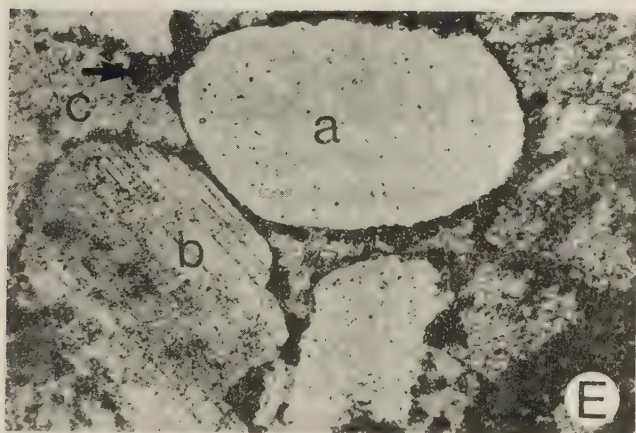
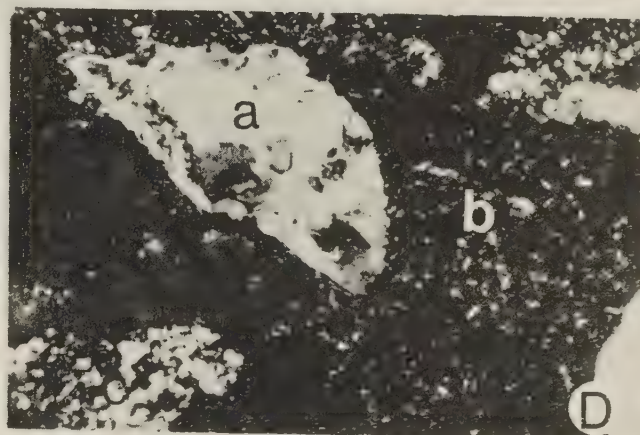
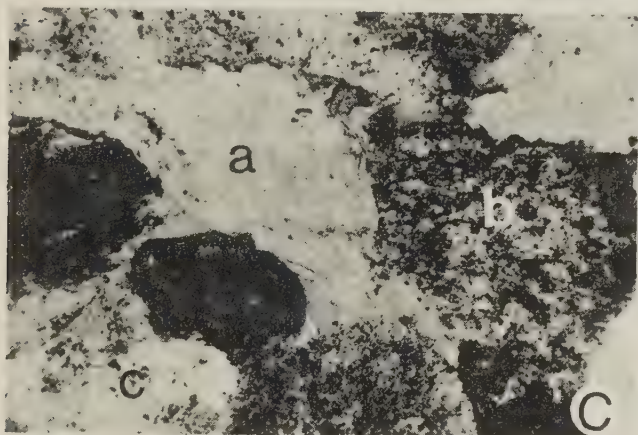
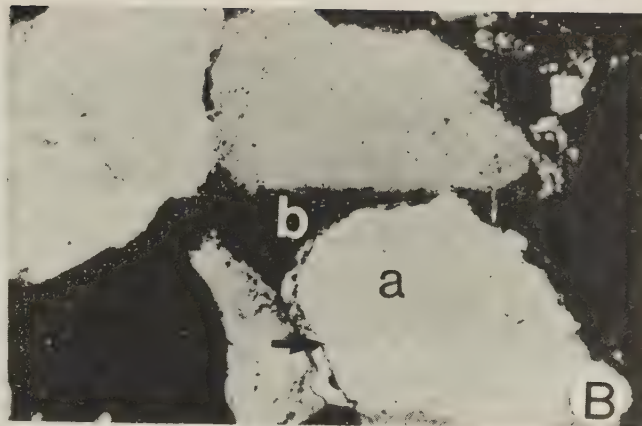
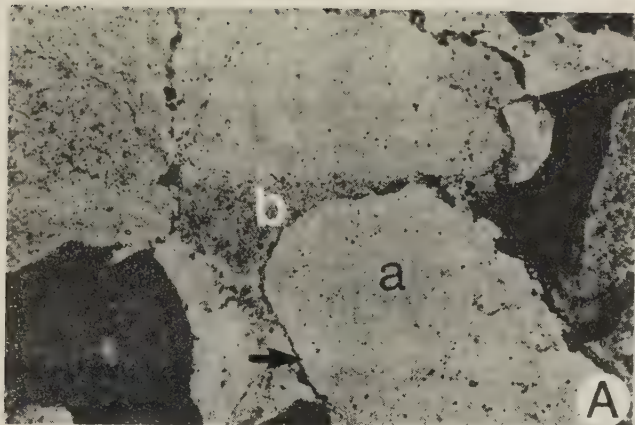


PLATE 2







PLATE 3. PHOTOMICROGRAPHS OF THIN SECTIONS OF BASAL BELLY  
RIVER SANDSTONE

- A. Volcanic quartz (a) exhibiting well developed crystal faces and very few inclusions, surrounded by authigenic clay cement (b). (Well: 10-35-47-4W5. Sample no. 39. Plane light. X40)
- B. Same as A, but between crossed nicols. X40.
- C. Quartzite fragment (polycrystalline quartz) (a) consisting of metamorphic quartz crystals characterized by inclusions of muscovite. (Well: 10-34-47-4W5. At 2186.3 feet. Plane light. X40)
- D. Same as C, but between crossed nicols; note size and shape of individual quartz crystals in quartzite fragment (a).
- E. Potassic feldspar grain (a) (volcanic sanidine?) exhibiting well preserved crystal outline, and fresh, clear appearance. Chert rock fragment (b) and authigenic kaolinite cement (c) have similar appearance and relief. (Well: 10-35-47-4W5. Sample no. 39. Plane light. X40)
- F. Same as E, but between crossed nicols; authigenic clay cement (c) shows lower birefringence than chert rock fragment (b). X40.

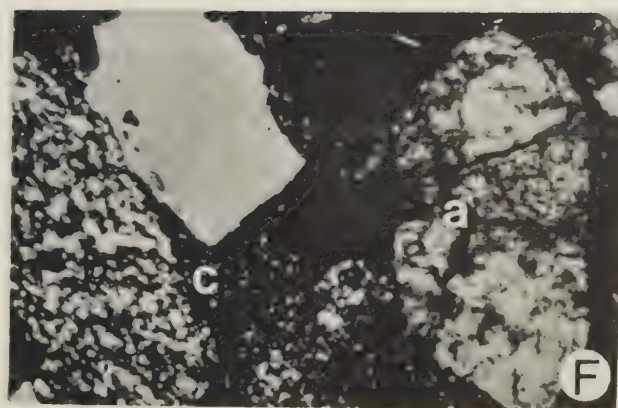
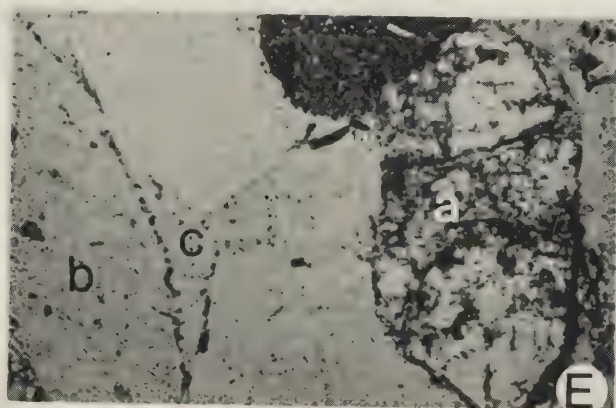
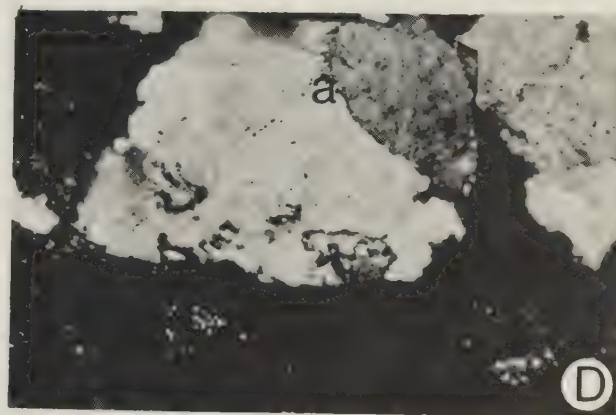
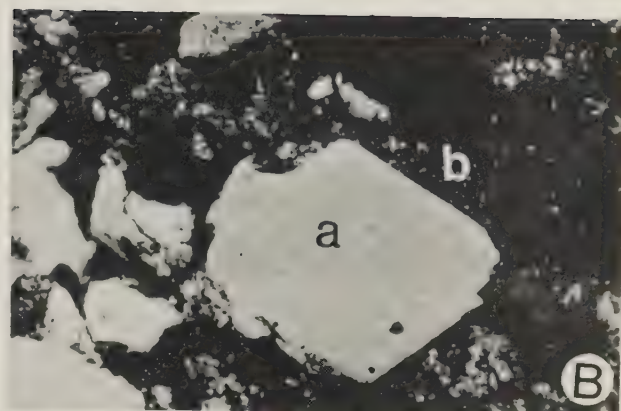
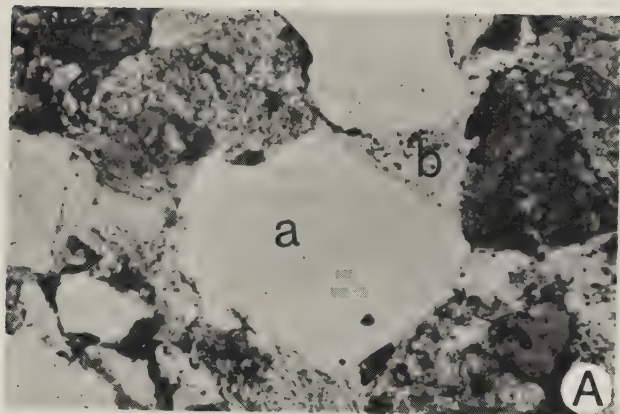


PLATE 3



alone was used as a basis for their identification, though it is realized that such identifications are less reliable than those that utilized both properties.

Quartzite rock fragments (composite quartz grains) form up to 7 percent of the sandstones and average 3.1 percent. The individual quartz crystals within the composite grain show strong undulose extinction characteristic of metamorphic quartz. The presence of metamorphic minerals such as muscovite is common (Plate 3C, D).

#### Feldspars.

The feldspars were simply classified into potassic and plagioclase types (Table 6). To facilitate the identification of the k-feldspars in thin section, they were selectively stained yellow with sodium cobaltinitrite. The potassic feldspar grains were commonly fresh and clear in appearance (Plate 3E, F) and constitute 1 to 6 percent of the detrital grains averaging 2.8 percent. The plagioclase feldspars form 1 to 14 percent (7.8 percent average) of the sandstones and, in contrast to the k-feldspars, are mostly altered (Plate 4A, B, C, D).

#### Rock Fragments.

Table 7 summarizes the rock fragment composition of the sandstones. Genetically, they belong to three groups, namely: sedimentary, volcanic and metamorphic.

The sedimentary group is the most abundant and is classified into mudstone, chert and carbonate. The mudstone





TABLE 6.  
Feldspar Types as Percentage of Total Essential Components

Serial No.	Well Name	Location	Sample No.	K-Feldspar	Plagioclase Feldspar
1.1	IOE CDN-SUP PEMBINA	10-27-47 -4W5	At 3212.8 ft (A)	6.6	7.0
1.2			At 3215.4 ft (B)	2.1	5.2
1.3			At 3215.4 ft (B)	4.4	2.5
1.4			At 3219.1 ft	3.2	13.8
1.5			At 3233.8 ft	2.9	11.2
2.6	IOE CDN-SUP PEMBINA	10-34-47 -4W5	At 2186.3 ft (A)	0.7	0.4
2.7			At 2186.3 ft (B)	1.0	2.1
2.8			40	1.2	5.9
2.9			41	1.5	11.2
2.10			50	3.2	10.0
2.11	IOE CDN-SUP PEMBINA	10-35-47 -4W5	52	3.5	13.8
2.12			53	2.6	11.3
3.13			6	3.0	11.0
3.14			18	5.7	5.1
3.15			20	2.8	5.1
3.16	IOE CDN-SUP PEMBINA	4-36-47 -4W5	23	5.7	5.7
3.17			25	4.8	3.9
3.18			39	3.5	2.3
3.19			46	3.0	6.0
4.20			12	2.7	6.2
4.21	IOE CDN-SUP PEMBINA		16	1.1	3.8
4.22			18	1.5	2.6
4.23			19	1.6	5.9
4.24			23	3.0	7.0
4.25			25	3.8	8.7
4.26			35	3.2	8.4
4.27			37	2.2	10.5

.../Continued



TABLE 6. - Continued

Serial No.	Well Name	Location	Sample No.	K-Feldspar	Plagioclase Feldspar
5.28	IOE CDN-SUP PEMBINA	4-2-48 -4W5	12	2.9	13.1
5.29			13	0.4	4.7
5.30			16	1.2	5.0
5.31			(A)	2.0	5.3
5.32			(B)	3.2	11.3
5.33			(A)	1.6	3.7
5.34			(B)	0.8	10.6
5.35			33	4.5	12.8
5.36			42	2.9	7.1
5.37			46	1.5	8.8
5.38			47	2.3	6.6
			51		
			Average	2.8	7.8

NB: A = Coarse part of slide  
B = Fine part of slide



THESE DOCUMENTS SONT  
 DEPOSES A LA BIBLIOTHEQUE  
 NATIONALE

LE 10/01/1971  
 A 14 H 00

PAR  
 M. [illegible]

LE 10/01/1971  
 A 14 H 00

PAR  
 M. [illegible]



PLATE 4. PHOTOMICROGRAPHS OF THIN SECTIONS OF BASAL BELLY  
RIVER SANDSTONE

- A. Partially albitized plagioclase feldspar (a) partially replaced by calcite cement (b). (Well: 4-2-48-4W5. Sample no. 12. Plane light. X100)
- B. Same as A, but between crossed nicols; the plagioclase feldspar grain shows anomalously high birefringence due to calcite replacement. X100.
- C. Partially calcite replaced and altered plagioclase feldspar grain (a) with intragranular pore (p) as opposed to intergranular pore (b). (Well: 10-34-47-4W5. Sample no. 52. Plane light. X100)
- D. Same as C, but between crossed nicols. Replacement of the plagioclase feldspar grain by calcite (high birefringence) is more obvious. X100.
- E. Argillite rock fragment (a) showing recrystallization of the phyllosilicates to sericite. Note also the presence of reddish brown siderite (b), and chert (c) and mudrock (d) fragments. (Well: 4-2-48-4W5. Sample no. 12. Plane light. X40)
- F. Same as E, but between crossed nicols. X40.

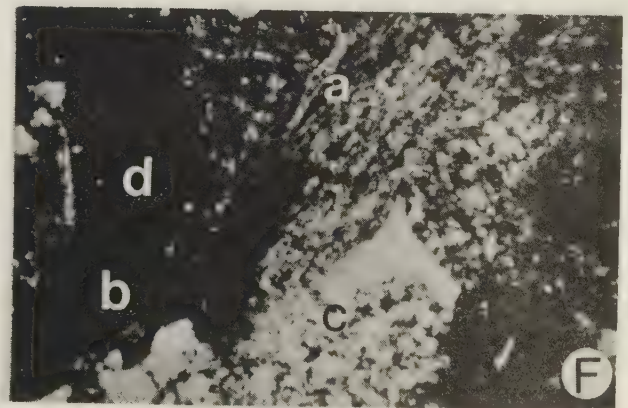
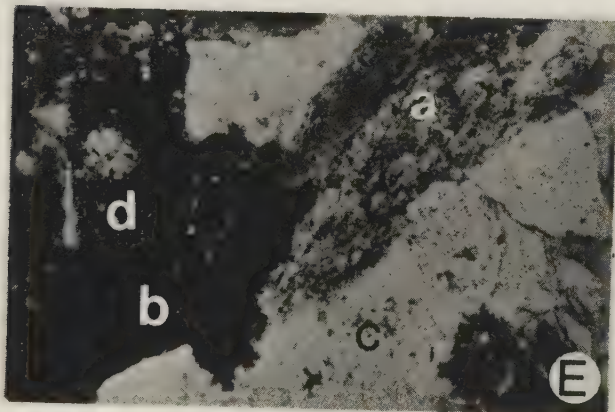
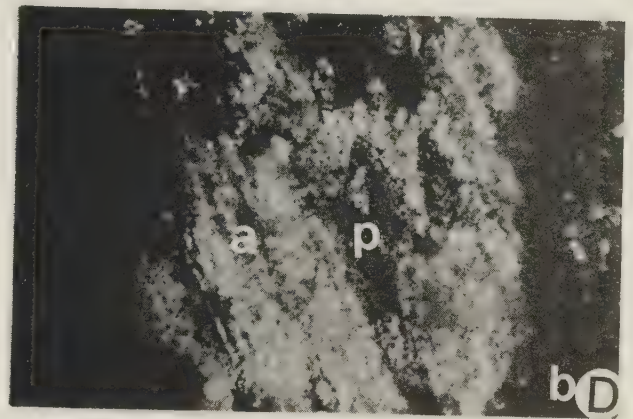
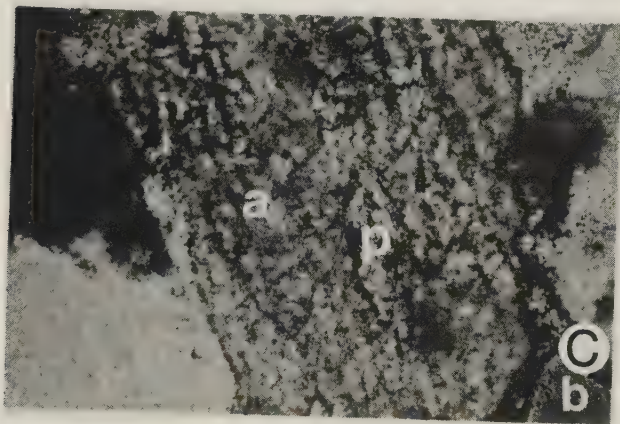


PLATE 4



TABLE 7.  
Rock Fragments as Percentage of Total Essential Components

Serial No.	Well Name	Location	Sample No.	Carbo- nate	Chert	Mud- stone	Meta- morphitic	Volcanic	Opaque + Carbo- naceous Material
1.1	IOE CDN- SUP PEMBINA	10-27-47 -4W5	At 3212.8 ft	-	4.5	30.9	14.8	18.1	0.8
1.2			At 3215.4 ft (A)	-	3.5	22.9	2.2	43.1	-
1.3			At 3215.4 ft (B)	-	3.6	27.0	2.7	43.0	-
1.4			At 3219.1 ft	0.8	8.3	16.6	9.1	22.5	-
1.5			At 3233.8 ft	-	10.7	15.7	6.2	23.1	0.8
2.6	IOE CDN- SUP PEMBINA	10-34-47 -4W5	At 2186.3 ft (A)	-	4.4	51.6	1.1	22.4	0.4
2.7			At 2186.3 ft (B)	-	1.5	24.1	3.3	49.5	0.2
2.8			40	-	25.4	20.3	5.1	13.7	3.1
2.9			41	-	11.5	26.0	8.9	15.6	0.4
2.10			50	-	16.0	17.6	10.0	14.4	3.2
2.11	IOE CDN- SUP PEMBINA	10-35-47 -4W5	52	-	13.4	20.5	10.6	12.2	-
2.12			53	-	6.4	20.3	17.3	19.2	0.4
3.13			6	-	9.1	17.5	8.7	24.7	0.8
3.14			18	3.4	19.9	19.3	22.2	6.3	0.6
3.15			20	2.8	17.6	24.5	14.8	7.4	3.2
3.16	IOE CDN- SUP PEMBINA	4-36-47 -4W5	23	2.4	20.8	14.6	20.3	3.3	1.4
3.17			25	0.9	15.8	16.7	27.6	3.1	-
3.18			39	1.9	15.1	20.5	25.9	4.2	-
3.19			46	0.9	9.4	23.1	27.4	5.1	-
4.20			12	0.4	13.5	22.7	13.5	13.1	1.2
4.21	IOE CDN- SUP PEMBINA		16	0.4	20.8	27.2	9.8	4.5	3.0
4.22			18	-	19.2	21.5	17.7	6.0	-
4.23			19	-	15.6	18.8	16.4	6.3	1.2

.../Continued





TABLE 7. - Continued

Serial No.	Well Name	Location	Sample No.	Carbo- nate	Chert	Mud- stone	Meta- morphie	Volcanic	Opaque + Carbo- naceous Material
4.24	IOE CDN- SUP PEMBINA	4-36-47 -4W5	23	-	19.2	28.4	12.5	7.7	1.5
4.25			25	0.4	10.9	20.0	17.0	8.3	4.9
4.26			35	-	19.5	24.3	9.2	5.6	1.2
4.27			37	-	15.2	18.5	12.3	9.8	5.1
5.28	IOE CDN- SUP PEMBINA	4-2-48 -4W5	12	0.5	11.7	19.4	10.2	18.4	-
5.29			13	-	17.4	21.7	8.1	15.9	0.8
5.30			16	-	21.3	17.4	6.2	22.1	0.4
5.31			23	0.8	32.4	20.2	7.3	8.9	2.4
5.32			23	0.4	12.5	17.7	11.7	12.5	0.8
5.33			33	1.2	19.1	15.4	10.6	23.2	-
5.34			33	-	6.4	12.5	12.1	39.0	0.4
5.35			42	-	7.5	15.0	8.3	18.4	1.1
5.36			46	0.4	6.3	24.3	7.5	21.3	2.5
5.37			47	0.4	7.7	25.4	5.8	26.5	3.5
5.38			51	0.4	10.4	25.5	4.2	24.7	0.8
			Average	0.5	14.4	20.6	12.6	14.3	1.3

NB: A = Coarse part of slide  
B = Fine part of slide





rock fragments, which are essentially fine, detrital silicate rocks of silt and clay sizes, are the most plentiful of the sedimentary rock fragments and constitute an average of 20.6 percent of the sandstones (Plates 2C, D; 4E, F). Chert fragments (cryptocrystalline siliceous rock fragments) are the second most abundant of the sedimentary rock fragments and average more than 14 percent of the sandstone. Both colorless and pale brown varieties are common (Plates 2C, D; 4E, F). Carbonate rock fragments occur in some of the samples, but in most cases constitute less than 4 percent. They occur in the form of fine-grained limestone and a few sideritic fragments (Plate 4E, F).

Fine-grained volcanic rock fragments average about 14 percent of the sandstones. Most are characterized by the presence of plagioclase feldspar microlites and can therefore be differentiated from other similar fine-grained fragments such as argillite and chert (Plate 5A, B).

Metamorphic rock fragments in the form of argillite and metasiltstone are abundant in all the samples and average 12.6 percent of the sandstone. Argillite, which is the metamorphic equivalent of mudrock, is characterized by the recrystallization of the phyllosilicates into metamorphic minerals such as sericite, and has a fairly homogeneous texture (Plate 4E, F), while metasiltstone is the metamorphic equivalent of siltstone and consists essentially of silt-size quartz grains (Plate 5C, D). Both are the





PLATE 5. PHOTOMICROGRAPHS OF THIN SECTIONS OF BASAL BELLY  
RIVER SANDSTONE

- A. Volcanic rock fragment (a) showing slightly higher relief than chert (c). Arrow points to sutured contact between two chert rock fragments (c) and (d). Note also intergranular pore (b). (Well: 10-35-47-4W5. Sample no. 20. Plane light. X40)
- B. Same as A, but between crossed nicols. Volcanic rock fragment (a) is characterized by small laths of feldspar. X40.
- C. Metasiltstone (a) is essentially made up of silt sized quartz grains. Note also intergranular pore (b) and straight contact (arrow) between two quartz grains (c) and (d). (Well: 10-34-47-4W5. Sample no. 40. Plane light. X25)
- D. Same as C, but between crossed nicols. X25.
- E. Photomicrograph shows specimen with moderate packing. Black opaque material (a) of uncertain origin (probably organic) partially fills a pore. (Well: 10-34-47-4W5. Sample no. 40. Plane light. X10)
- F. Same as E, but between crossed nicols. X10.



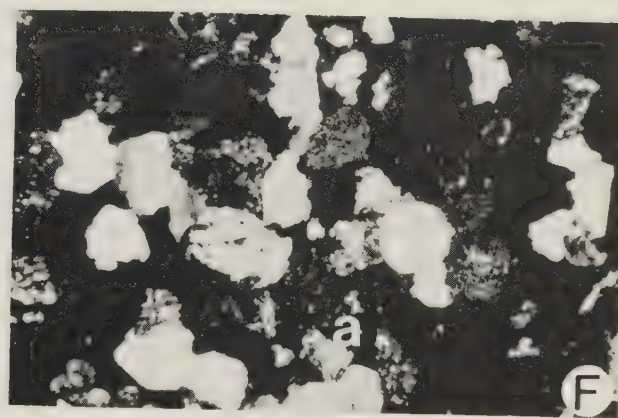
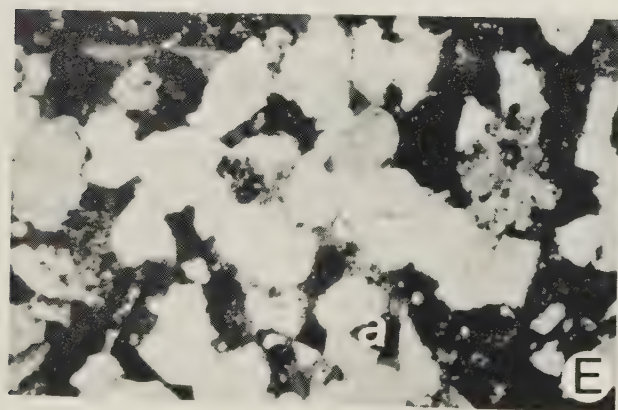
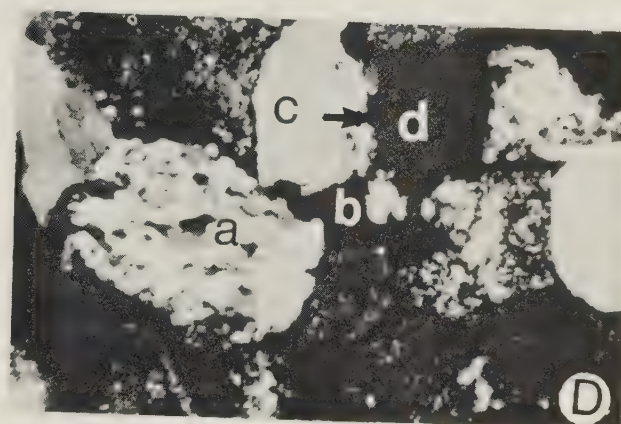
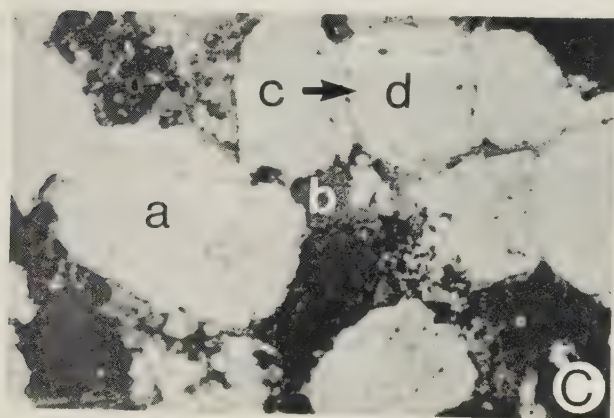
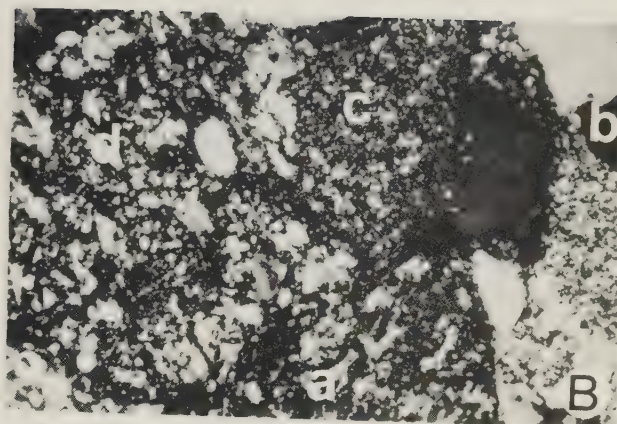
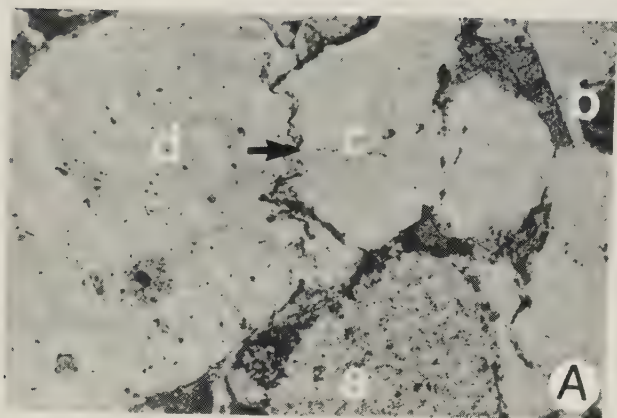


PLATE 5





product of low grade metamorphism.

Opaque and carbonaceous materials of uncertain affinity (Plate 5E, F) are common in most of the samples, but do not constitute a significant proportion of the sandstone (less than 1.5 percent average). Probably they are either badly altered inorganic material, or organic remains such as plant debris and petroleum residue.

#### Accessory Minerals.

Biotite, muscovite, glauconite and chlorite form the accessory mineral suite identified in the samples. In most cases, these minerals constitute less than 1 percent of the detrital components. Biotite is the most prevalent and in a few samples amounts to 1 percent. It is brown to reddish brown in color (Plate 6A, B). Muscovite occurs in nearly all samples but unlike biotite rarely constitutes 1 percent of the sandstone. Glauconite occurs in some of the samples in the form of greenish pellets consisting of microcrystalline aggregates, and may be an alteration product of detrital phyllosilicates, or fecal pellets, or a product of interstitial processes. Greenish, micaceous flakes were sparingly encountered in some of the samples (Plate 6C, D). These are probably a variety of the chlorite group of minerals.

In general, the distribution of these accessory minerals is not uniform and is either a reflection of changes of provenance of the detritus or of the hydraulic





PLATE 6. PHOTOMICROGRAPHS OF THIN SECTIONS OF BASAL BELLY  
RIVER SANDSTONE

- A. Reddish brown biotite grain (a) and recrystallized mudrock fragment (b). (Well: 4-2-48-4W5. Sample no. 12. Plane light. X40)
- B. Same as A, but between crossed nicols. The mudrock fragment (b) shows higher than normal birefringence due to recrystallization of the phyllosilicates to sericite. X40.
- C. Arrow shows concavoconvex contact between chlorite grain (a) and quartz grain (b). (Well: 10-35-47-4W5. Sample no. 20. Plane light. X40)
- D. Same as C, but between crossed nicols. X40.
- E. Photomicrograph shows a specimen with zero packing proximity. Detrital grains are "floating" in a ground-mass of calcite cement (a). Arrow shows siderite 'blebs' outlining the boundary of a calcite replaced detrital grain. (Well: 10-35-47-4W5. Sample no. 18. Plane light. X10)
- F. Same as E, but between crossed nicols. X10.

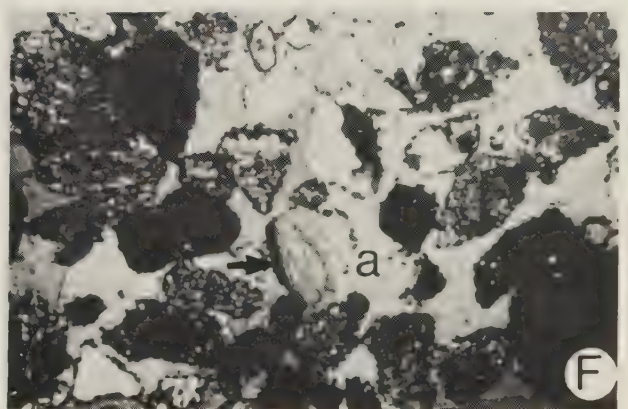
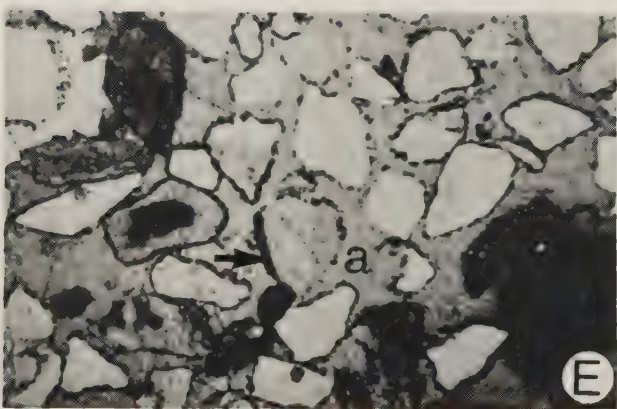
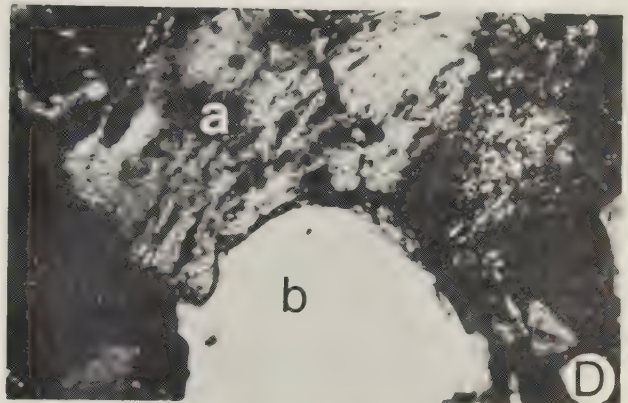
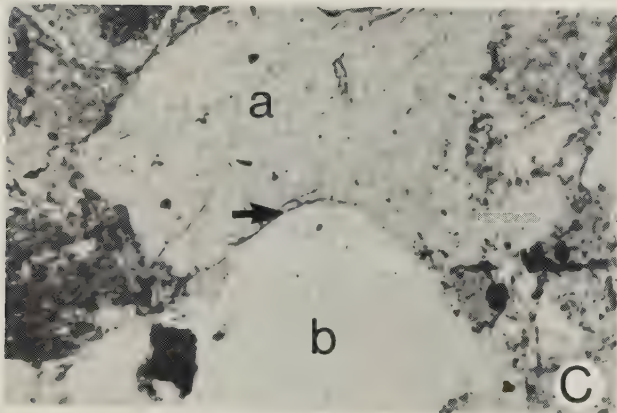
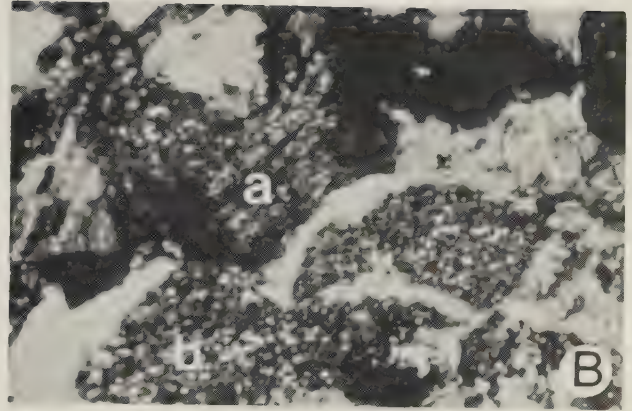
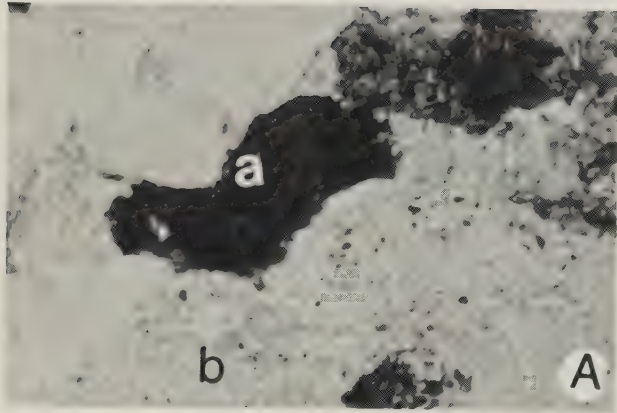


PLATE 6





sorting of the sediments.



## CHAPTER IV. GRANULOMETRIC ANALYSIS

## Size Frequency Distribution

The raw data obtained from the grain size analyses using thin sections and a Humphries' micrometer eyepiece are presented in Appendix B. The results of these thin section grain size analyses were plotted as cumulative curves using a probability scale ordinate to show the size frequency distribution of the samples (Figure 9). This facilitates visual comparison of the samples and indicates that most of them show bimodality.

Parameters.

From these cumulative curves, some descriptive statistical measures of average size (mode, median, graphic mean) and sorting or uniformity (inclusive graphic standard deviation) were obtained. Folk's (1974) formulae were used for the computation of these graphic statistics as follows:

1. Graphic Mean ( $M_Z$ ) =  $\frac{\phi_{16} + \phi_{50} + \phi_{84}}{3}$

## 2. Inclusive Graphic Standard Deviation ( $\sigma_T$ )

$$= \frac{\phi_{84} - \phi_{16}}{4} + \frac{\phi_{95} - \phi_5}{6.6}$$

Arithmetic means and standard deviations were also computed by the method of moments using the following equations:

1.  $M_a = \frac{\sum fm\phi}{\sum f}$       where

	$M_a$ = arithmetic mean,
	$f$ = number frequency in each class,
	$m\phi$ = midpoint of each size class in phi values,
	$\sum f$ = total count.



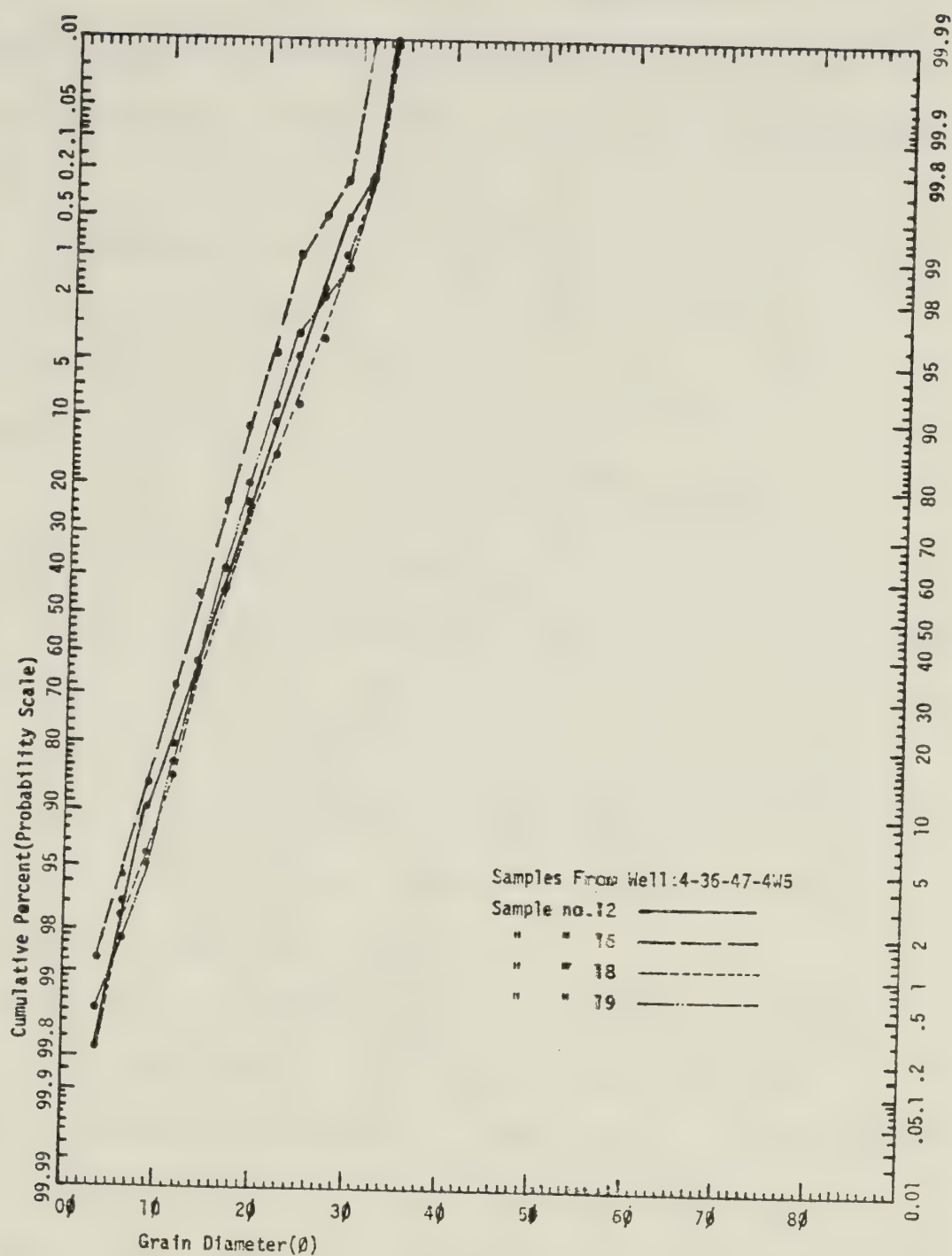


FIGURE 9. Cumulative frequency curves for samples representative of basal Belly River sandstone in the study area.









TABLE 8.  
Summary Statistics of the Granulometric Analyses ( $\phi$  Units)

Serial No.	Well Name	Location	Sample No.	F.S. Mode (Frequency Peak)	F.S. Median (50 Percentile)	Sieve Median	F.S. Graphic Mean	Sieve Graphic Mean	F.S. Arithmetic Mean	Sieve Arithmetic Mean	F.S. Inclusive Graphic Std. Deviation	Sieve Inclusive Graphic Std. Deviation	Arithmetic Std. Deviation
1.1	IOE CDN-SUP	10-27-47	At 3212.8 ft	2.88	2.5	2.94	2.49	2.88	2.60	2.99	0.64	0.49	0.63
1.2	PEMBINA	-4W5	At 3215.4 ft	2.38	2.33	2.76	2.34	2.72	2.45	2.82	0.50	0.37	0.50
1.3			At 3215.4 ft	2.63	2.55	3.0	2.57	2.97	2.70	3.09	0.48	0.35	0.50
1.4			At 3219.1 ft	1.88	1.95	2.35	2.04	2.4	2.16	2.51	0.54	0.40	0.55
1.5			At 3233.8 ft	1.88	1.61	1.98	1.62	1.95	1.75	2.07	0.43	0.31	0.46
2.6	IOE CDN-SUP	10-34-47	At 2186.3 ft	1.63	1.65	2.02	1.74	2.08	1.87	2.20	0.62	0.48	0.62
2.7	PEMBINA	-4W5	At 2186.3 ft	2.38	2.35	2.78	2.35	2.73	2.47	2.85	0.53	0.39	0.54
2.8			40	1.38	1.31	1.65	1.38	1.69	1.49	1.79	0.58	0.44	0.58
2.9			41	1.88	1.70	2.07	1.70	2.03	1.82	2.15	0.50	0.37	0.52
2.10			50	1.63	1.61	1.98	1.65	1.98	1.78	2.11	0.45	0.32	0.47
2.11			52	1.88	1.63	2.00	1.65	1.98	1.78	2.11	0.49	0.36	0.50
2.12			53	2.13	1.88	2.27	1.88	2.23	1.99	2.33	0.55	0.41	0.55
3.13	IOE CDN-SUP	10-35-47	6	1.63	1.63	2.00	1.65	1.98	1.76	2.08	0.48	0.35	0.49
3.14	PEMBINA	-4W5	18	1.13	1.06	1.38	1.18	1.47	1.29	1.58	0.63	0.48	0.64
3.15			20	1.38	1.45	1.80	1.50	1.82	1.63	1.94	0.54	0.40	0.55
3.16			23	1.38	1.30	1.64	1.34	1.64	1.47	1.77	0.56	0.42	0.57
3.17			25	1.38	1.33	1.67	1.35	1.66	1.47	1.77	0.49	0.36	0.50
3.18			39	1.38	1.48	1.84	1.52	1.84	1.65	1.97	0.57	0.43	0.57
3.19			46	1.63	1.55	1.91	1.55	1.87	1.71	2.03	0.52	0.39	0.54

.../Continued



TABLE 8. - Continued

Serial No.	Well Name	Location	Sample No.	F.S. Mode (Frequency Peak)	F.S. Median (50 Percentile)	Sieve Median	F.S. Graphic Mean	Sieve Graphic Mean	F.S. Arithmetic Mean	Sieve Arithmetic Mean	F.S. Inclusive Graphic Std. Deviation	Sieve Inclusive Graphic Std. Deviation	Arithmetic Std. Deviation
4.20	IOE CDN-SUP PEMBINA	4-36-47-4W5	12	1.63	1.58	1.94	1.54	1.86	1.67	1.99	0.49	0.36	0.49
4.21			16	1.38	1.35	1.69	1.35	1.66	1.46	1.76	0.43	0.31	0.44
4.22			18	1.63	1.58	1.94	1.63	1.96	1.73	2.05	0.50	0.37	0.51
4.23			19	1.63	1.52	1.88	1.54	1.86	1.66	1.98	0.42	0.30	0.45
4.24			23	1.88	1.68	2.05	1.68	2.01	1.82	2.15	0.45	0.32	0.48
4.25			25	1.62	1.70	2.07	1.69	2.02	1.81	2.14	0.59	0.45	0.59
4.26			35	1.38	1.31	1.65	1.34	1.64	1.49	1.79	0.54	0.40	0.56
4.27			37	1.63	1.60	1.97	1.64	1.97	1.75	2.07	0.48	0.35	0.50
5.28	IOE CDN-SUP PEMBINA	4-2-48-4W5	12	2.13	2.00	2.4	2.00	2.36	2.14	2.49	0.46	0.33	0.48
5.29			13	1.63	1.50	1.86	1.55	1.87	1.65	1.97	0.50	0.37	0.53
5.30			16	1.38	1.35	1.69	1.36	1.67	1.51	1.82	0.47	0.34	0.49
5.31			23	1.13	1.20	1.53	1.22	1.32	1.37	1.67	0.58	0.44	0.59
5.32			23	1.88	1.75	2.13	1.76	2.1	1.90	2.23	0.54	0.40	0.54
5.33			33	1.65	1.5	1.86	1.54	1.86	1.65	1.97	0.54	0.40	0.53
5.34			33	2.13	2.01	2.41	2.00	2.36	2.16	2.51	0.49	0.36	0.51
5.35			42	1.63	1.61	1.98	1.67	2.00	1.83	2.16	0.44	0.31	0.46
5.36			46	1.88	1.67	2.04	1.66	1.99	1.79	2.12	0.47	0.34	0.47
5.37			47	1.63	1.63	2.00	1.62	1.95	1.73	2.05	0.46	0.33	0.49
5.38			51	2.13	1.75	2.13	1.73	2.06	1.85	2.18	0.50	0.37	0.52

NB: A = Coarse part of slide  
B = Fine part of slide





samples, this sandstone unit is classified as texturally mature since all the standard deviations ( $\sigma_I$ ) are under 0.50 and the detrital grains are still not rounded (Folk, 1974).

It is pertinent to note that size frequency distribution and sorting are dependent on various factors whose individual effects are difficult to assess, and that the above analyses are no exceptions. Such factors include size range of available particles, current characteristics, type of deposition and rate of supply of detritus compared with efficiency of the sorting agent (Folk, 1974).

#### Other Textural Attributes

The textural attributes of shape and fabric were also studied in the course of this granulometric analysis. Roundness, an element of shape was studied by visual comparison of grains with standard images of grains of known roundness, and according to Power's (1953) scale of roundness, most of the grains are angular to subangular which correspond to Folk's (1955) rho values of 1 to 3. Scanning electron microscopy reveals some surface textures in the form of irregular "scars" and "markings" on some of the detrital grains. Plate 8A illustrates such surface textures on a quartz grain. These surface textures are similar to those reported by Le Ribault (1975) and interpreted as post-depositional solution effects in a deltaic environment. The discussion of the fabric of these samples is deferred till



Chapter V, while the entire granulometric data is used purely for descriptive purposes in the present study.



## CHAPTER V. DIAGENESIS

Definition: Diagenesis is the postdepositional alteration (excluding weathering) of sediments under normal surface or outer part of the crust conditions of temperature and pressure. It may affect mineralogical and chemical composition, interstitial fluids (formation waters) and the texture of the sediments. The important factors in diagenesis are particle size, water content, organic content and mineralogical composition of the sediments, plus the temperature, pressure, and chemical conditions of the environment (Krumbein, 1942). Because of these factors, a wide variety of diagenetic changes is possible, inasmuch as variations in the end-product may occur either with different sediments in the same environment, or with the same kind of sediment in different environments. Diagenesis involves the broad phenomena of dissolution and precipitation of minerals from interstitial fluids, and has been accomplished in the basal Belly River sandstone by the diagenetic processes of compaction and pressure solution, cementation, replacement, recrystallization and simple solution.

Compaction and Pressure Solution: Krumbein (1942) defined compaction as the reduction of the bulk volume of a sediment expressed as a percentage of the original voids present, effected by the overburden pressure that acts normal to the surface of the sediment body. He also pointed out that the magnitude of the effect of compaction is a function of the





porosity and water content of the original sediment, the size and shape of its particles, the rate of deposition and thickness of the overburden, and time. It has both mechanical and chemical components with the mechanical component predominating in the early stages of the process while the chemical component (pressure solution) occurs at a later stage in the presence of extreme overburden pressure on unyielding detrital grains (Füchtbauer, 1967). Mechanical compaction, the rearrangement of the detrital grains under vertical pressure resulting in closer packing, appears to be the main type of compaction that affected the basal Belly River sandstone. A study of the fabric of this rock unit shows no preferred grain orientation (crystallographic or dimensional) at the microscopic level. An evaluation of the packing, the spacing or density pattern of the detrital grains in a rock, of the samples using Kahn's (1956) packing proximity gave values that ranged from less than 1 percent to 71 percent but with most of the values in the 30 to 50 percent range (Plates 5E, F; 6E, F; Table 9). Packing proximity, the ratio of the number of grain-to-grain contacts (encountered in a traverse across the thin section) to the total number of contacts of all kinds encountered in the same traverse, is a numerical measure of packing (Blatt et al. 1972). The low packing proximity values obtained for the samples of the basal Belly River sandstone are due to the presence of matrix and early cement before the accomplishment of considerable compaction. Most of the contacts



TABLE 9.  
Packing Proximity

Serial No.	Well Name	Location	Sample No.	Packing Proximity (%)
1.1	IOE CDN-SUP PEMBINA	10-27-47-4W5	At 3212.8 ft	55.55
1.2			At 3215.4 ft (A)	5.07
1.3			At 3215.4 ft (B)	28.5
1.4			At 3219.1 ft	42.42
1.5			At 3233.8 ft	30.0
2.6	IOE CDN-SUP PEMBINA	10-34-47-4W5	At 2186.3 ft (A)	29.86
2.7			At 2186.3 ft (B)	33.4
2.8			40	31.57
2.9			41	41.66
2.10			50	33.33
2.11	IOE CDN-SUP PEMBINA	10-35-47-4W5	52	55.55
2.12			53	70.96
3.13			6	50.0
3.14			18	0
3.15			20	54.54
3.16	IOE CDN-SUP PEMBINA	4-36-47-4W5	23	44.44
3.17			25	28.57
3.18			39	37.5
3.19			46	35.0
4.20			12	54.54
4.21	IOE CDN-SUP PEMBINA		16	38.88
4.22			18	45.0
4.23			19	47.05
4.24			23	55.55
4.25			25	50.0

.../Continued



TABLE 9. - Continued

Serial No.	Well Name	Location	Sample No.	Packing Proximity (%)
4.26	IOE CDN-SUP PEMBINA	4-36-47-4W5	35	50.0
4.27			37	45.45
5.28	IOE CDN-SUP PEMBINA	4-2-48-4W5	12	33.33
5.29			13	21.05
5.30			16	17.64
5.31			23	40.7
5.32			23	52.9
5.33			33	41.06
5.34			33	49.5
5.35			42	57.14
5.36			46	33.33
5.37			47	40.9
5.38			51	36.36

NB: A = Coarse part of slide  
 B = Fine part of slide





between the detrital grains are long i.e. straight, using Taylor's (1950) terminology (Plate 5C, D); but there are also a few concavoconvex (Plate 6C, D), sutured (Plate 5A, B) and tangential contacts. The predominance of long contacts is a reflection of the shape of the detrital grains (angular to subangular) while the concavoconvex contacts are due to juxtaposing of grains of unequal strength; for example, detrital quartz and chlorite grains (Plate 6C, D). The scarcity of tangential contacts is due to lack of adequate shapes (round and spherical) to generate such effect (point contacts), and lack of juxtaposition of grains of equal strength; while the paucity of sutured contacts is an indication of the existence of insufficient overburden pressure and presence of large amount of cement before appreciable compaction was accomplished. The absence of appreciable number of pressure solution (sutured or stylolitic) contacts shows that the compaction of the basal Belly River sandstone was essentially mechanical and that this rock unit did not suffer appreciable chemical compaction (pressure solution).

Cementation: The precipitation of mineral cements (binding materials) within the pore spaces of a sediment is one of the main diagenetic processes that affected the basal Belly River sandstone. Five types of cement were observed in the samples examined and include the following: calcium carbonate (calcite), quartz, chert overgrowth, iron oxide and authigenic clay. The samples show variations in the type



and amount of cements (Table 10).

Calcite Cementation: Calcite is the most abundant cement in the basal Belly River sandstone and ranges from less than 1 percent to about 40 percent in some samples. It occurs as a coarse mosaic of anhedral subequant crystals. In some of the samples with abundant calcite cement, the packing proximity of the grains is almost zero and one gets the impression of "floating grains" in a groundmass of calcite cement (Plate 6E, F). Although there is some obvious partial and complete calcite replacement of detrital grains in these very calcareous samples, most of the calcite was precipitated from the formation waters early in this rock unit's diagenetic history.

Quartz Cementation: Quartz is a common but quantitatively insignificant cement in this rock unit. Volumetrically it ranges from less than 1 percent to just more than 1 percent and occurs both as overgrowths and pore fillings, but mainly as overgrowths. The quartz overgrowths are normally delimited from the detrital quartz nuclei by dark brown to opaque "dust lines" but are still in crystallographic and optical continuity (Plate 7A, B). The presence of such a line facilitates the identification of the overgrowth, but in some cases this boundary mark is lacking, indicating a clean surface before the precipitation of the overgrowth. In such cases, recourse was made to judgements based upon the amount of inclusions (normally more abundant in the nuclei than in the overgrowths), degree of straining of the



TABLE 10.  
Cement Types and Percentages

Serial No.	Well Name	Location	Sample No.	Grain Mean Dia. (mm)	Other Cements (%)	Other Cement Types (%)	Clay Cement (%)
1.1	IOE CDN-SUP PEMBINA	10-27-47 -4W5	At 3212.8 ft	0.17	17.5	C=17.5	0.5
1.2			At 3215.4 ft (A)	0.18	1.2	C=1.2	7.7
1.3			At 3215.4 ft (B)	0.16	19.8	C=19.7, Q=0.2	0.5
1.4			At 3219.1 ft	0.23	3.8	C=3.8	8.0
1.5			At 3233.8 ft	0.30	12.8	C=12.5, Q=0.3	6.8
2.6	IOE CDN-SUP PEMBINA	10-34-47 -4W5	At 2186.3 ft (A)	0.27	0.3	Q=0.3	7.8
2.7			At 2186.3 ft (B)	0.18	0.7	I=0.5, C=0.2	10.0
2.8			40	0.36	0.8	Q=0.7, C=0.1	2.5
2.9			41	0.29	0	0	6.2
2.10			50	0.29	7.2	C=7.0, Q=0.2	7.8
2.11	IOE CDN-SUP PEMBINA	10-35-47 -4W5	52	0.29	0.5	C=0.2, Q=0.3	8.3
2.12			53	0.25	0.2	Q=0.2	6.6
3.13			6	0.30	1.8	C=1.5, Q=0.3	8.8
3.14			18	0.41	39.7	C=39.7	1.3
3.15			20	0.33	0.7	I=0.3, Q=0.3	4.8
3.16	IOE CDN-SUP PEMBINA	4-36-47 -4W5	23	0.36	23.8	C=23.8	7.4
3.17			25	0.36	2.0	C=0.2, I=0.2	4.5
3.18			39	0.32	0.7	Q=1.3, H=0.3	6.3
3.19			46	0.31	4.5	Q=0.7, C=4.3, Q=0.2	8.3
4.20			12	0.31	0.5	Q=0.5	7.5
4.21	IOE CDN-SUP PEMBINA		16	0.36	1.0	Q=1.0	5.8
4.22			18	0.30	1.3	C=0.2, I=0.5	6.5
4.23			19	0.32	1.3	Q=0.7, I=0.2, Q=1.2	4.7

.../Continued





TABLE 10. - Continued

Serial No.	Well Name	Location	Sample No.	Grain Mean Dia. (mm)	Other Cements (%)	Other Cement Types (%)	Clay Cement (%)
4.24	IOE CDN-SUP PEMBINA	4-36-47 -4W5	23	0.29	1.0	I = 0.5, Q = 0.5	6.7
4.25			25	0.29	0.2	C = 0.2	8.7
4.26			35	0.36	8.2	C = 7.2, I = 0.5	5.5
4.27			37	0.30	1.8	Q = 0.5 I = 1.7, Q = 0.7	9.8
5.28	IOE CDN-SUP PEMBINA	4-2-48 -4W5	12	0.23	17.0	C = 17.0	6.5
5.29			13	0.32	0.3	Q = 0.3	5.3
5.30			16	0.35	0.7	Q = 0.7	5.0
5.31			23	0.39	0	0	5.2
5.32			23	0.27	0.3	C = 0.2, I = 0.2	4.5
5.33			33	0.32	0.2	Q = 0.2	7.0
5.34			33	0.22	0.3	C = 0.2, Q = 0.2	5.3
5.35			42	0.28	1.5	C = 0.2, I = 1.0 Q = 0.2	10.3
5.36			46	0.29	1.0	C = 0.6, I = 0.2 Q = 0.2	9.7
5.37			47	0.30	0.3	C = 0.2, I = 0.2	9.3
5.38			51	0.28	0.5	H = 0.2, Q = 0.3	9.7

NB: C = Calcite  
I = Iron Oxide  
H = Chert Overgrowth  
Q = Quartz Overgrowth  
A = Coarse part of slide  
B = Fine part of slide





PLATE 7. PHOTOMICROGRAPHS OF THIN SECTIONS OF BASAL BELLY  
RIVER SANDSTONE

- A. Detrital quartz nucleus (a) delimited from the quartz overgrowth (b) by dark brown "dust line" (arrow). Note also good crystal faces on the overgrowth (b) and an intergranular pore (c). (Well: 10-35-47-4W5. Sample no. 25. Plane light. X40)
- B. Same as A, but between crossed nicols. X40.
- C. Detrital quartz nucleus (a) not delimited from the overgrowth (b) by a "dust line", but overgrowth (b) identified by presence of crystal faces. (Well: 10-35-47-4W5. Sample no. 25. Plane light. X40)
- D. Same as C, but between crossed nicols. X40.
- E. "Cleaner" chert overgrowth (a) on a detrital chert grain (c). Authigenic kaolinite cement (b), characterized by small crystal size, even color and texture. (Well: 4-2-48-4W5. Sample no. 16. Plane light. X100)
- F. Same as E, but between crossed nicols. Chert overgrowth shows up as coarser chert aggregate surrounding the detrital chert grain (c). Note also the low birefringence of the pore-filling authigenic kaolinite (b). X100.

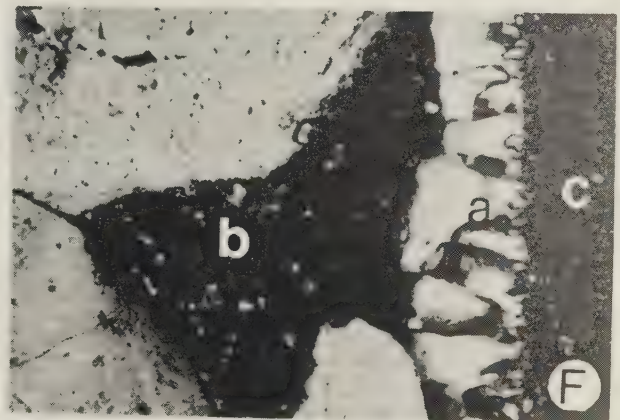
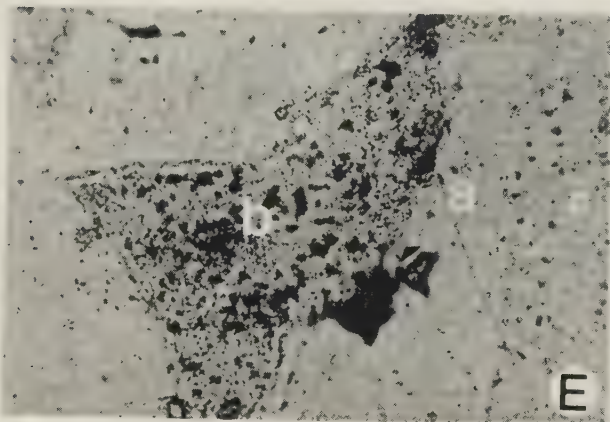
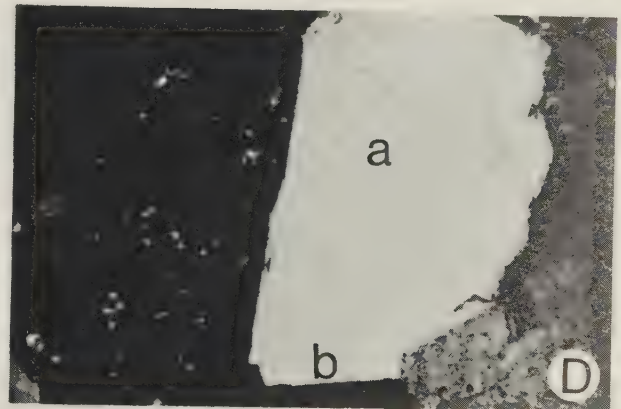
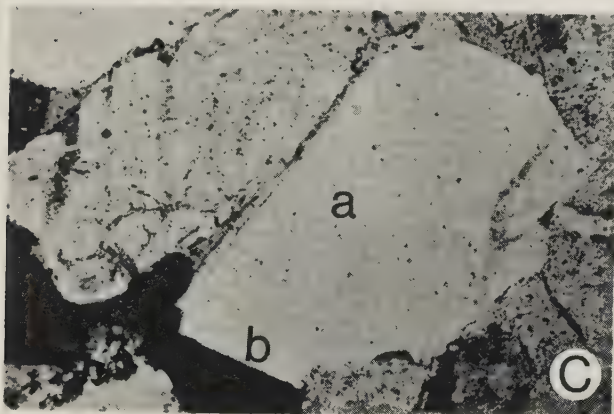
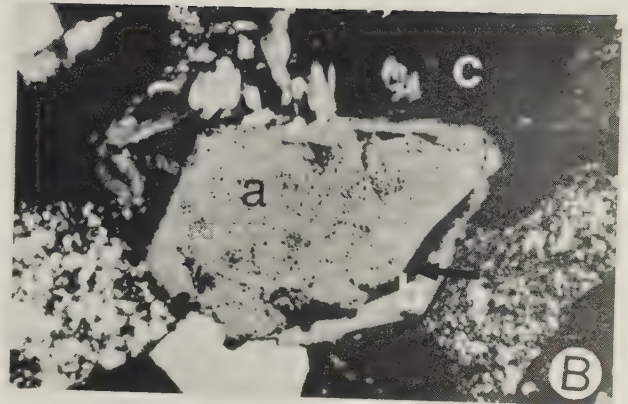
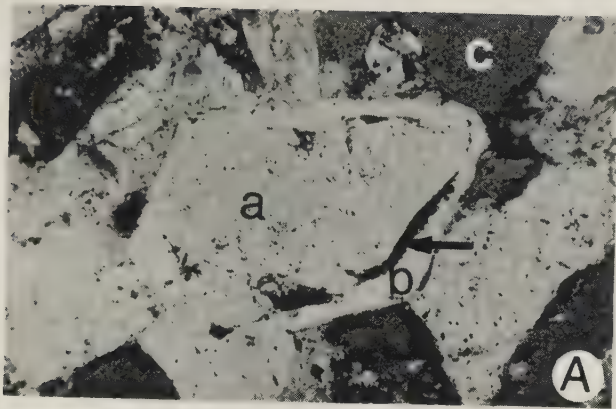


PLATE 7





nuclei as indicated by its undulose extinction, and the presence of crystal faces on the overgrowths, for their identification (Plates 7C, D; 8B, C). The authigenic pore filling quartz characterized by small crystal size and well developed hexagonal crystal faces is more obvious under the scanning electron microscope (Plate 8D).

"Chert" Cementation: Another form of silica cement present in this rock unit is chert overgrowth. It is not as common as quartz overgrowth and was observed only in a few samples. In all instances, it is less than 0.5 percent by volume. Lerbekmo (1961) attributed the paucity of chert overgrowths to the various orientations of the individual silica units of the chert grain, which is not very conducive to the growth of a single quartz structure. In the few instances of chert overgrowth, it is seen under the petrographic microscope as a coarser and cleaner chert aggregate surrounding the detrital chert nucleus (Plate 7E, F). It is better revealed by scanning electron microscope as an aggregate of fine hexagonal quartz crystals on a detrital chert grain (Plate 8E, F).

Iron Oxide Cementation: Reddish brown to dark brown iron oxide (hematite?) binding material is present in amounts ranging from less than 0.2 percent to about 2 percent in some of the samples. It occurs as a coating on most of the larger detrital quartz and chert grains (Plate 2A and B). Although there is some controversy about the origin of such hematite binding material (detrital, Van Houten, 1968;





PLATE 8. SCANNING ELECTRON MICROGRAPHS OF BASAL BELLY RIVER  
SANDSTONE

- A. Irregular surface texture (a) on a detrital quartz grain, probably etching feature (?). (Well: 4-36-47-4W5. Sample no. 12. X600)
- B. Quartz overgrowth (a) with well developed crystal faces. Note also intergranular pore (b) reduced by quartz overgrowths on surrounding detrital quartz grains. (Well: 4-36-47-4W5. Sample no. 16. X60)
- C. Closeup of B. Quartz overgrowth (a) followed by authigenic chlorite (b). (Well: 4-36-47-4W5. Sample no. 16. X180)
- D. Authigenic pore filling quartz (?) (a) with well developed hexagonal crystal faces and fan-shaped clusters of chlorite (c) partially occluding submicroscopic pore (b). (Well: 4-36-47-4W5. Sample no. 37. X2500)
- E. Chert overgrowth (a) as an aggregate of fine hexagonal quartz crystals on a detrital chert grain (b). (Well: 4-36-47-4W5. Sample no. 19. X120)
- F. Closeup of E. (Well: 4-36-47-4W5. Sample no. 19. X300)



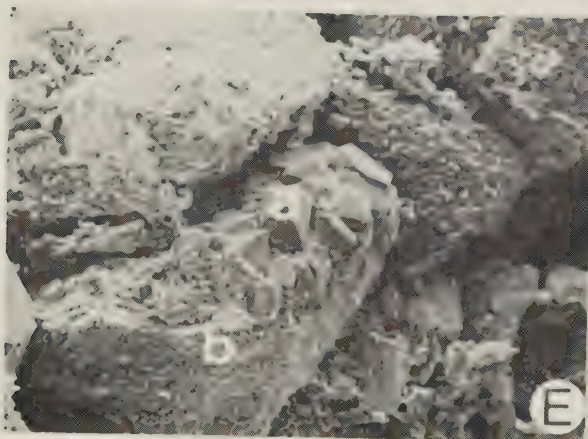
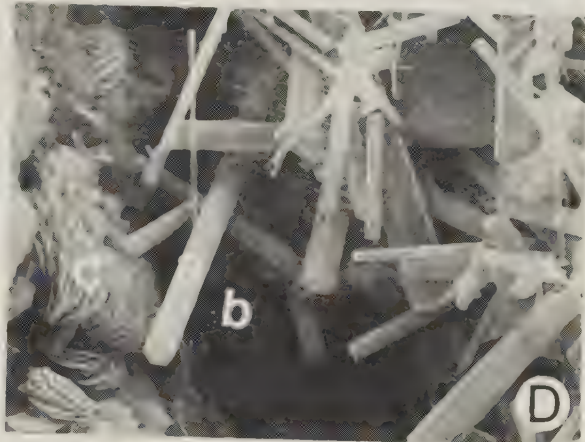
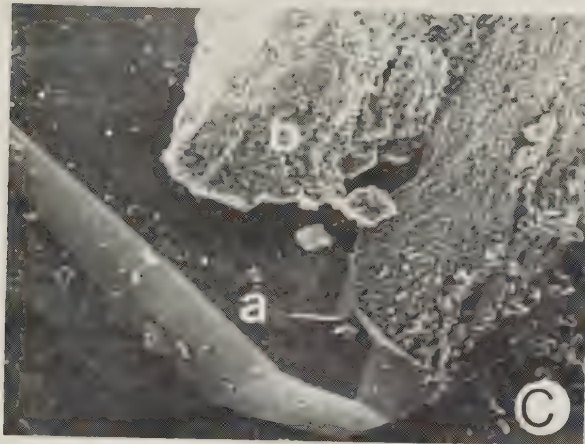
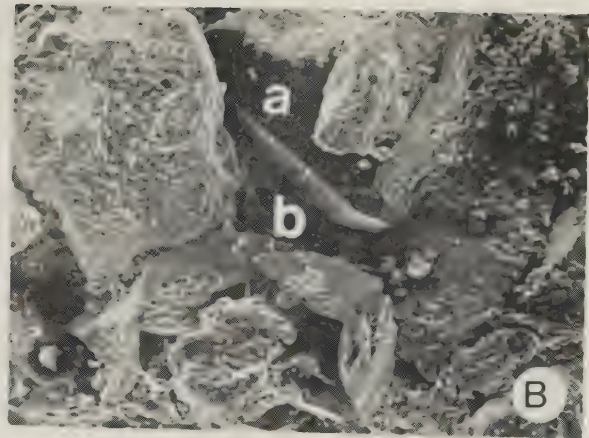
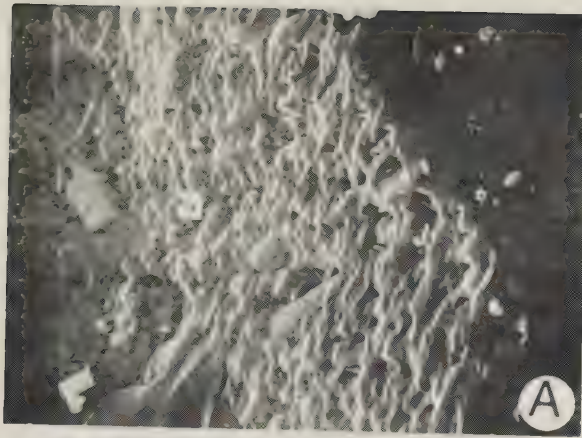


PLATE 8





diagenetic, Walker, 1967), the hematite in the basal Belly River sandstone appears to be of diagenetic origin because of the delicate nature of these hematite coatings which could not have survived transportation.

Secondary Clay Cementation: Authigenic clay cement is next in abundance to calcite in the basal Belly River sandstone. It is the most prevalent of all the cements, being present in almost all samples and ranging from less than 1 percent to over 10 percent by volume. There is an inverse relationship between authigenic clay and the other cement types taken together in most of the samples (Table 10). The authigenic clay is characterized by an even color, texture and composition, low birefringence (gray interference color) and submicroporosity (Plates 7E, F; 9A, B, C, D). It occurs both as a thin coating on the detrital grains (pore lining) and as a filling of the pore spaces (pore filling). For a better understanding of the texture and composition of this authigenic clay cement, scanning electron microscopy and X-ray diffraction techniques were employed. The discussion of these observations is deferred until Chapter VI.

Paragenesis of the Cements: The paragenesis of the cementing materials in the basal Belly River sandstone is not easily discernible. This is further complicated by the fact that the cementation pattern of the samples as seen today may be only the end-product of a series of sequences of cementations, decementations and replacements, and therefore may not give the actual paragenesis of the cements. Therefore from petro-





PLATE 9. PHOTOMICROGRAPHS OF THIN SECTIONS OF BASAL BELLY  
RIVER SANDSTONE

- A. Metamorphic quartz grain (a). Pore filling authigenic kaolinite (b) follows chert overgrowth (c). (Well: 4-2-48-4W5. Sample no. 16. Plane light. X40)
- B. Same as A, but between crossed nicols. X40.
- C. Detrital quartz nucleus (a) delimited from quartz overgrowth (b) by "dust line". Authigenic kaolinite (c) follows quartz overgrowth as the last pore filler and partly replaces the quartz overgrowth. Note the absence of quartz overgrowth on lower part of detrital quartz grain (a) which may be due to the presence of authigenic kaolinite (d) which prevented the formation of quartz overgrowth. (Well: 10-34-47-4W5. Sample at 2186.3 feet. Plane light. X40)
- D. Same as C, but between crossed nicols. Authigenic kaolinite (c, d) has lower birefringence than the detrital chert grain (e). X40.
- E. Detrital quartz (a) delimited from overgrowth (b) by "dust line". Quartz overgrowth (b) with well developed crystal faces is followed by calcite cement (c) (last pore filler). (Well: 4-2-48-4W5. Sample no. 13. Plane light. X40)
- F. Same as E, but between crossed nicols. X40.



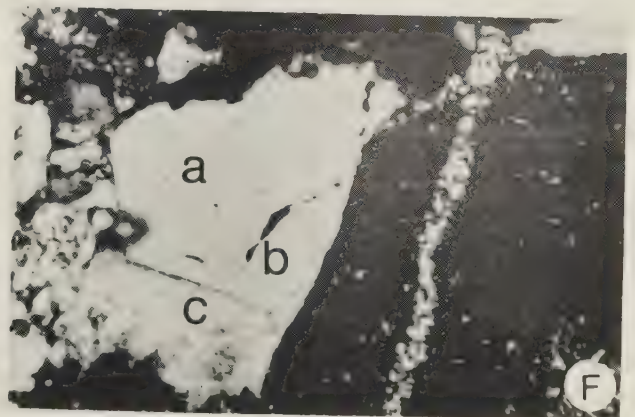
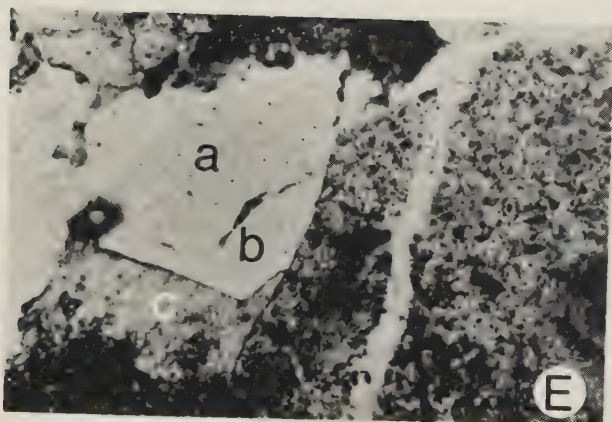
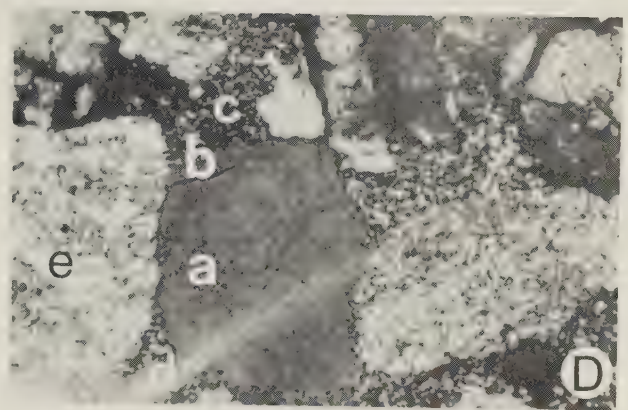
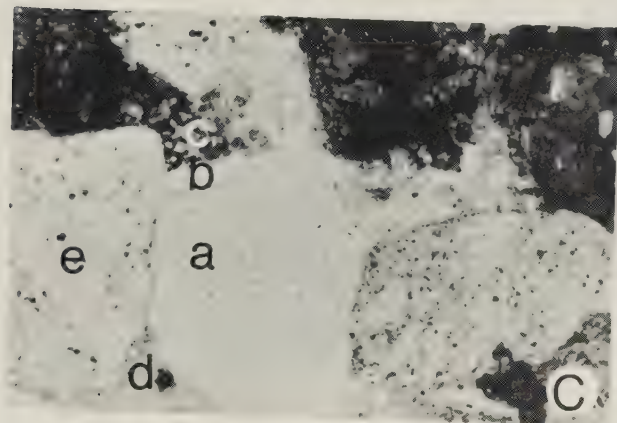
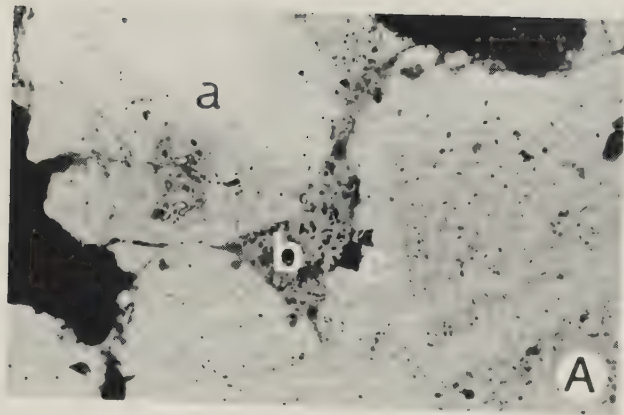


PLATE 9





graphic observation no infallible sequence of cementation can be inferred for this rock unit, but the following observations appear to be generally applicable:

1. The presence of authigenic clay cement in the form of pore linings and fillings, and carbonate cement, tend to forestall the formation of quartz overgrowths. No quartz overgrowth was observed to follow any authigenic clay or calcite cement (Plate 9C, D).
2. Calcite or authigenic clay cement may follow quartz overgrowth (Plates 2A, B; 9C, D, E, F).
3. Iron oxide cement is usually followed by authigenic clay cement or quartz overgrowth (Plate 10A, B).
4. Incomplete coating of a detrital quartz grain by iron oxide cement does not hinder the formation of quartz overgrowths.
5. Calcite and/or authigenic clay cements are the last pore fillings.
6. Most of the samples show "patchy" cementation with most or all of the five cement types present in a single thin section, and in some cases two to three cement types occur side by side (Plates 10C, D; 12F).

Replacement: The simultaneous solution of one mineral and precipitation of another, or the growth of a new mineral in place of another mineral or mineral aggregate without changing the external form, affected both the primary detrital grains and the secondary precipitated cements of the basal Belly River sandstone to varying degrees. In some





PLATE 10. PHOTOMICROGRAPHS OF THIN SECTIONS OF BASAL BELLY  
RIVER SANDSTONE

- A. Dark brown iron oxide (hematite?) (arrow) coating detrital quartz grain (a) is followed by quartz overgrowth (b). Note well developed crystal faces of overgrowth facing intergranular pore (c). (Well: 10-35-47-4W5. Sample no. 20. Plane light. X40)
- B. Same as A, but between crossed nicols. X40.
- C. Photomicrograph illustrating "patchy" cementation. Two cement types - calcite (a) and kaolinite (b) are present in same thin section. Note altered fine grained volcanic rock fragment (c) showing higher relief. (Well: 10-35-47-4W5. Sample no. 46. Plane light. X40)
- D. Same as C, but between crossed nicols. X40.
- E. Former detrital grain (a) has been completely replaced by authigenic calcite (b). Irregular fringes of dark brown siderite cement (arrow) marks the outline of the original grain. (Well: 10-35-47-4W5. Sample no. 18. Plane light. X25)
- F. Same as E, but between crossed nicols. Two calcite crystals are seen to have replaced the detrital grain. X25.



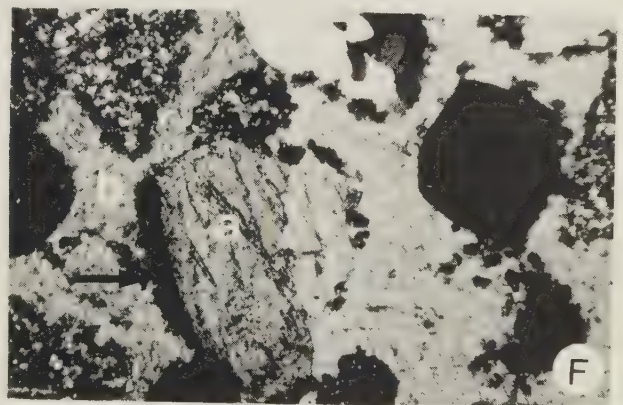
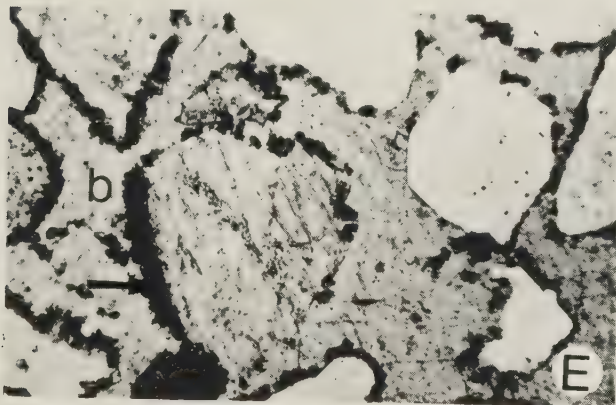
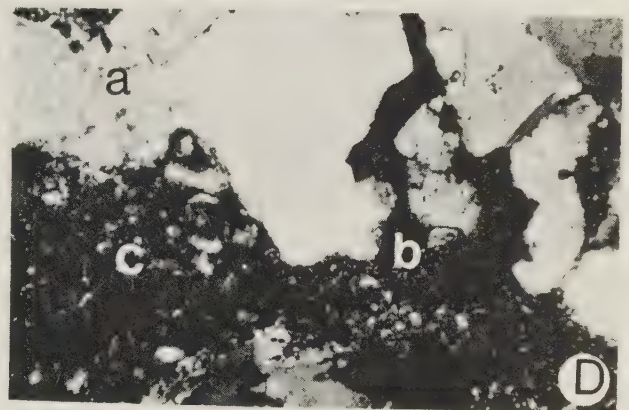
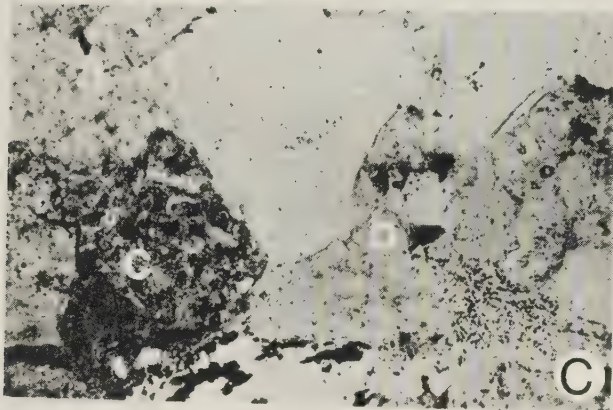
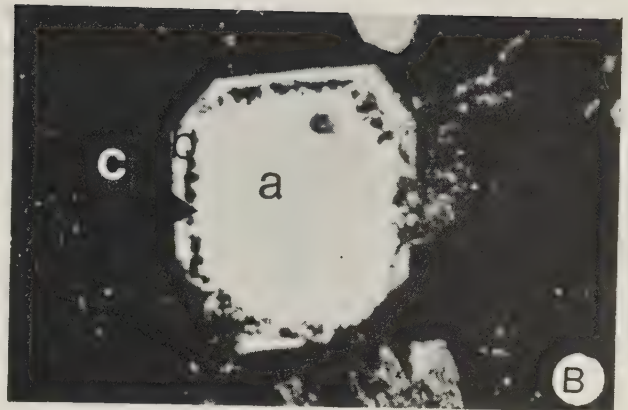
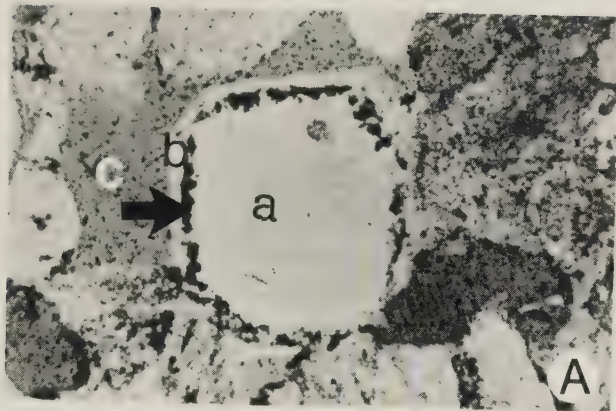


PLATE 10





of the very calcareous samples, the calcite cement has completely replaced some of the detrital grains, probably rock fragments and feldspars, and the outline of the original grain appears as a telltale boundary between the calcite replaced grain and the true pore filling calcite cement (Plate 10E, F). Normally the outline of the original grain is marked by dark brown siderite blebs and the grain is discernible as a "ghost", especially under crossed-nicols (Plate 10F). However, in some cases the replacement of the detrital grain is less complete and the calcite mineral veins or ramifies them, giving the grains a "worm-eaten" appearance (Plate 11A, B). In the case of rock fragments, the more resistant minerals such as quartz and mica persist while the less resistant minerals, e.g.; feldspars, are replaced. Albitization of the calcic plagioclase feldspars is common in this rock unit. The albitized plagioclase has a cloudy and mottled appearance which is dependent upon the degree of the replacement (Plate 4A, B, C, D). Replacement of plagioclase feldspars by calcite is also common (Plate 2E, F). Lerbekmo (1963) made similar observations in his study of the Belly River Formation in the Southern Alberta Foothills, and stated that the diagenetic alteration was within the realm of the zeolite facies, and that the principal mineral transformation was the replacement of intermediate plagioclase by albite, a slightly birefringent phyllosilicate and calcite. Although quartz replacement of both the calcite cement and the detrital grains is not a





PLATE 11. PHOTOMICROGRAMS OF THIN SECTIONS OF BASAL BELLY  
RIVER SANDSTONE

- A. Detrital potassic feldspar grain (a) partially replaced by authigenic calcite (b) giving the grain a "worm-eaten" appearance. Arrow points to dark brown 'blebs' of siderite cement. (Well: 10-35-47-4W5. Sample no. 18. Plane light. X40)
- B. Same as A, but between crossed nicols. X40.
- C. Volcanic rock fragment (a) with intragranular pores (lighter colored spots). Relatively clear argillite rock fragment (b) shows recrystallization of the phyllosilicates to sericite. (Well: 4-2-48-4W5. Sample no. 12. Plane light. X40)
- D. Same as C, but between crossed nicols. X40.
- E. Volcanic rock fragment (a) with intragranular solution pore (b); (c) is an intergranular pore. (Well: 4-2-48-4W5. Sample no. 46. Plane light. X40)
- F. Same as E, but between crossed nicols. X40.



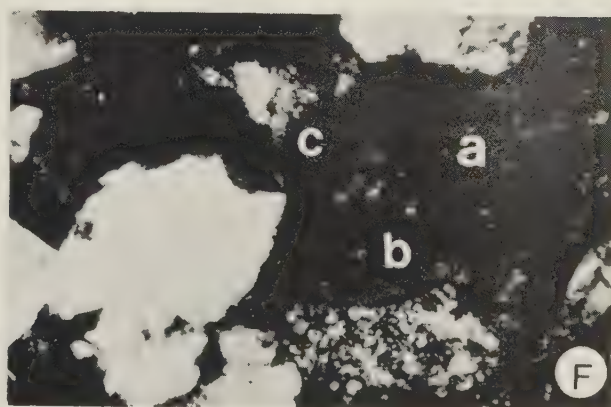
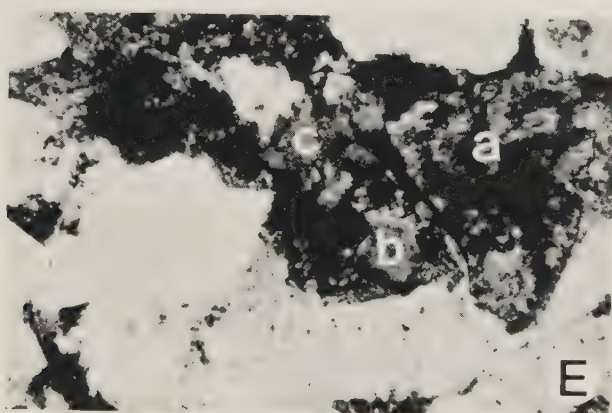
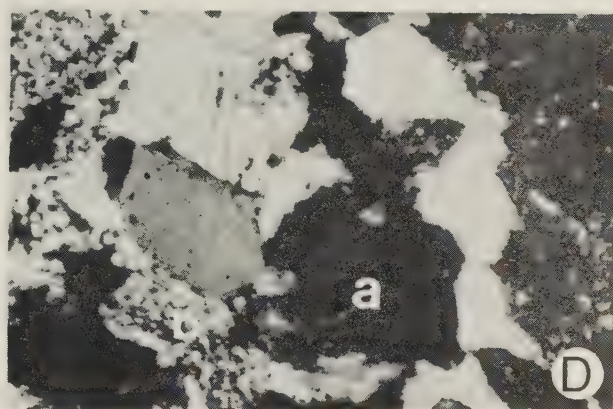
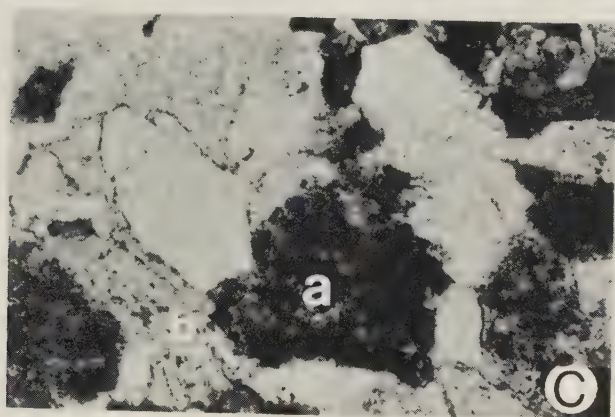
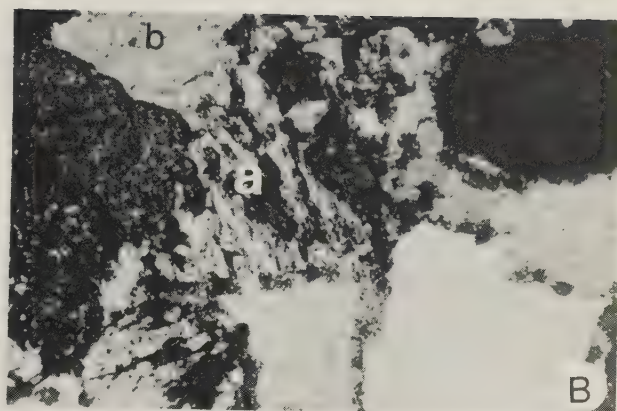
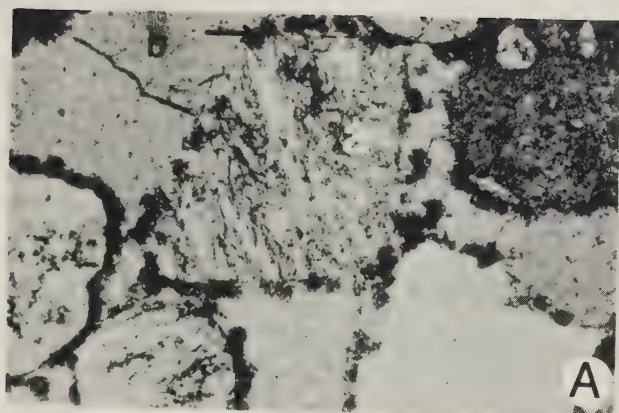


PLATE 11





common and obvious phenomenon, it is a possibility. Some of the authigenic pore filling quartz might have originated in this way. Also, in some cases, some of the quartz overgrowth has been partially replaced by authigenic clay cement (Plate 2A, B).

Recrystallization: Krumbein's (1942) definition of recrystallization, "changes in crystalline texture caused by a growth of small crystals and fragments into an aggregate of coarser crystals" is the one adopted in this discussion. It is highly probable that the detrital mudrock fragments and the clay matrix have recrystallized following their deposition and burial. This conclusion is based on the following facts:

1. Some of the mudrock fragments tend to have cleaner, larger crystals of minerals e.g. micas, and more even texture (Plate 2C, D).
2. Some of the samples lack easily and positively identifiable clay matrix; though this second quality may be due to good sorting.

Solution: This is the change of matter from the solid or gaseous into the liquid state by its combination with a liquid, and may be accompanied by chemical or physical change. Solution plays a major role during the diagenesis of sediments and is involved in the processes of replacement, recrystallization, cementation, decementation and intrastatal or differential solution. Most of the very fine grained volcanic and mudstone rock fragments and feldspars



have intraparticle (intragranular) pore spaces which are evidences of differential solution of the less resistant minerals (Plates 11C, D, E, F). This has resulted in what may be called intraparticle moldic porosity. It is plausible that some of the less resistant detrital grains such as feldspars have suffered complete intrastratal solution resulting in interparticle moldic porosity. The process of decementation, the removal of earlier precipitated cements, might also have occurred in the basal Belly River sandstone. The solution of one cement, e.g., calcite, may be followed by the precipitation of another cement, e.g., quartz, but in the absence of subsequent cementation, decementation results in the restoration of porosity. In all cases, however, it is difficult to assess the degree of differential solution in a sediment since all that is seen as the effect is porosity (pore spaces) which is subject to different interpretations. In some cases the porosity could be either depositional or diagenetic in origin.

#### Evaluation of the Diagenetic Effects in the Basal Belly River Sandstone

From the foregoing observations and discussion, it is evident that a number of diagenetic processes have affected to varying degrees the primary textural and compositional properties of the basal Belly River sediment, and have resulted in many physical and chemical changes in the sediment. Fundamental properties of the grains (size, shape



and surface texture), fabric, and mineralogical composition of this rock unit have been modified to the extent that there is no simple relationship between the original sediment and the lithified sandstone. The particle sizes have been enlarged in some instances, e.g., quartz grains by cementation (quartz overgrowth), while others have been reduced, e.g., feldspars by intrastratal solution. Both particle shape and surface texture have changed during diagenesis by solution, recrystallization and cementation (overgrowths). The effect of the diagenetic processes on the fabric (orientation and packing) of this rock unit is obvious but variable. In some samples diagenesis has resulted in very close packing of the grains, mainly by compaction, while in others the grains are widely separated from one another by the authigenic mineral cements, giving the impression of "floating grains" in a groundmass of cement. The mineralogical composition of the detrital grains and even the bulk composition of the sediment also have greatly changed as a result of diagenetic processes such as replacement and cementation. In view of all these modifications of the properties of the particles during diagenesis it is very necessary to apply adequate corrections to these properties of the sediment when reconstructing the original conditions of deposition from these observed but modified properties (Krumbein, 1942).

The economically important bulk properties of the sediment (porosity and permeability) also have been modified





in this rock unit by the diagenetic processes of compaction, cementation, and to a certain extent by solution. Compaction and cementation have generally reduced the initial porosity of this sandstone body to petrographically observable porosity values of 13 to less than 1 percent, and core analysis porosity values of 23 to less than 10 percent (Table 12). Thus both observed and core analysis porosity values are far less than the estimated average initial porosity of 40 percent for sandstones. Not only is the bulk porosity of the samples reduced, the pore sizes and throats also have been reduced by cementation and compaction (Plate 14F). (See Chapter VII for a more detailed discussion of porosity.) Although there is no straightline relationship between porosity and permeability, a reference to Table 15 shows that the more porous samples are the most permeable ones, and that the less porous ones are the less permeable ones. The logical inference then is that, other things being equal (initial particle size, degree of sorting etc.), the samples that have suffered more diagenesis (mostly cementation and compaction) are the least permeable ones, and therefore diagenesis has reduced the initial permeability of this rock unit.

Table 11 shows the diagenetic processes and the magnitude to which they might have occurred in the basal Belly River sandstone as revealed by observed petrographic evidence. From this evidence one can safely conclude that:

1. The diagenesis of this rock unit has resulted in the



TABLE 11.  
Relative Effects of Diagenesis on the Sediment Properties  
of the Basal Belly River Sandstone

Sediment Properties	Diagenetic Processes					
	Compaction	Cementation	Recrystallization	Replacement	Differential Solution	Authigenesis
Particle Size	-	X	X	-	X	-
Particle Shape and Roundness	X	X	?	-	X	-
Particle Surface Texture	-	X	-	-	X	-
Particle Orientation	?	?	?	-	?	-
Packing Proximity	XX	X	-	-	X	-
Mineral Composition	-	XX	-	XX	XX	XX
Porosity	XX	XX	?	-	XXX	XX
Permeability	XXX	XXX	?	-	XX	XXX
Lithification	X	XX	?	-	X	X

Legend: ? = Unknown effect; - = negligible effect;  
X = Small to moderate effect; XX = moderate to large effect;  
XXX = Property most strongly affected by a given process.



reduction of its initial bulk properties of porosity and permeability.

2. The differences in the porosity and permeability values amongst the samples are not related to depth effect since all the samples are from within 100 feet (30.5 meters) depth interval, but are mainly due to clay authigenesis, calcite and quartz cementation and solution.





## CHAPTER VI.

### AUTHIGENIC CLAY IN BASAL BELLY RIVER SANDSTONE

The widespread occurrence of authigenic clay cements in Cretaceous and Tertiary sandstones of Alberta has been documented by Lerbekmo (1961), and Carrigy and Mellon (1964). Microscopic examination of basal Belly River sandstone samples revealed that authigenic clay is the most prevalent and second most abundant cement, making up to 10 percent of the bulk volume. It appears white in hand specimen and is characterized petrographically by low birefringence, uniform clean texture, small crystal size and submicroscopic porosity (Plates 7E, F; 9A, B, C, D). It occurs mainly as scattered pore fillings though thin coatings on detrital grains (pore linings) are frequently encountered.

#### X-Ray Diffraction Analysis.

X-ray examination of the less than 2 microns fraction of three samples was undertaken, using a wide-angle goniometer diffractometer and strip chart recorder, to ascertain the mineralogy of the authigenic clay cement. Oriented mounts were used to enhance the basal X-ray reflections. Auxilliary tests of glycolation and heat-treatment (550° C for two hours) were also performed on the specimens. Glycolation provides a method for recognition of expanding-lattice montmorillonoid minerals, while heat-treatment collapses the lattice and thereby helps identify



certain of the clay minerals, especially within the Kaolin group (Molloy and Kerr, 1961; Brindley, 1961; Carroll, 1974). Untreated, glycolated and heat-treated oriented mounts of the less than 2 microns fraction were X-rayed and their diffractograms measured (Figures 10, 11 and 12). Constant instrument settings (scale factor 8, multiplier 1, time constant 4 sec.) were maintained throughout the examination of all specimens to permit direct diffraction intensity comparison between the untreated, glycolated and heat-treated specimens. In all untreated oriented specimens, the (001) and (002) reflections at 7.15 and  $3.58 \text{ \AA}$  were recorded, together with lesser peaks at 2.38 and  $1.79 \text{ \AA}$  (Figures 10A, 11A and 12A). Glycolation yielded no significant shift in the spacing or intensity of the peaks observed in the untreated patterns (Figures 10B, 11B and 12B). Heat-treatment of the specimens resulted in a drastic reduction in the intensity of the reflections (Figures 10C and 11C). This reduction in intensity is due to destruction of the crystal structure of the clay mineral by dehydration of the type  $\text{OH} + \text{OH} \rightarrow \text{H}_2\text{O} + \text{O}$  leaving a poorly crystalline phase - metakaolin (Molloy and Kerr, 1961; Brindley, 1961; Richardson, 1961; Grim, 1968; Carroll, 1974). A non-oriented specimen of the less than 2 microns fraction was also X-rayed (Figure 13). It shows peaks at 7.15, 3.58, 2.34, 2.28, 2.12, 1.98 and  $1.81 \text{ \AA}$  which correspond to the (001), (002), (202), (113),  $(02\bar{3})$ ,  $(2\bar{0}3)$  and (133) kaolinite reflections respectively. The presence of  $7.15 \text{ \AA}$  reflection



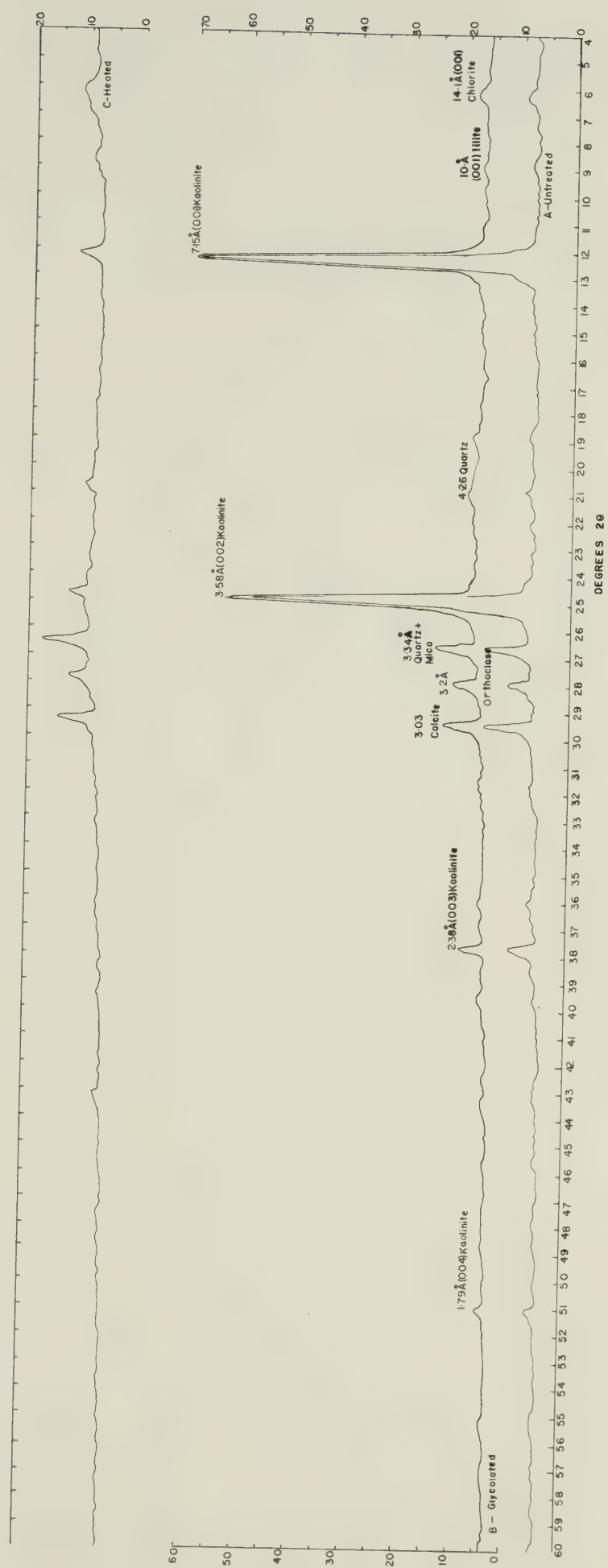


Figure 10-X-ray diffractogram of less than 2 $\mu$  fraction of oriented mount of sample #51(10-35-47-4W5)





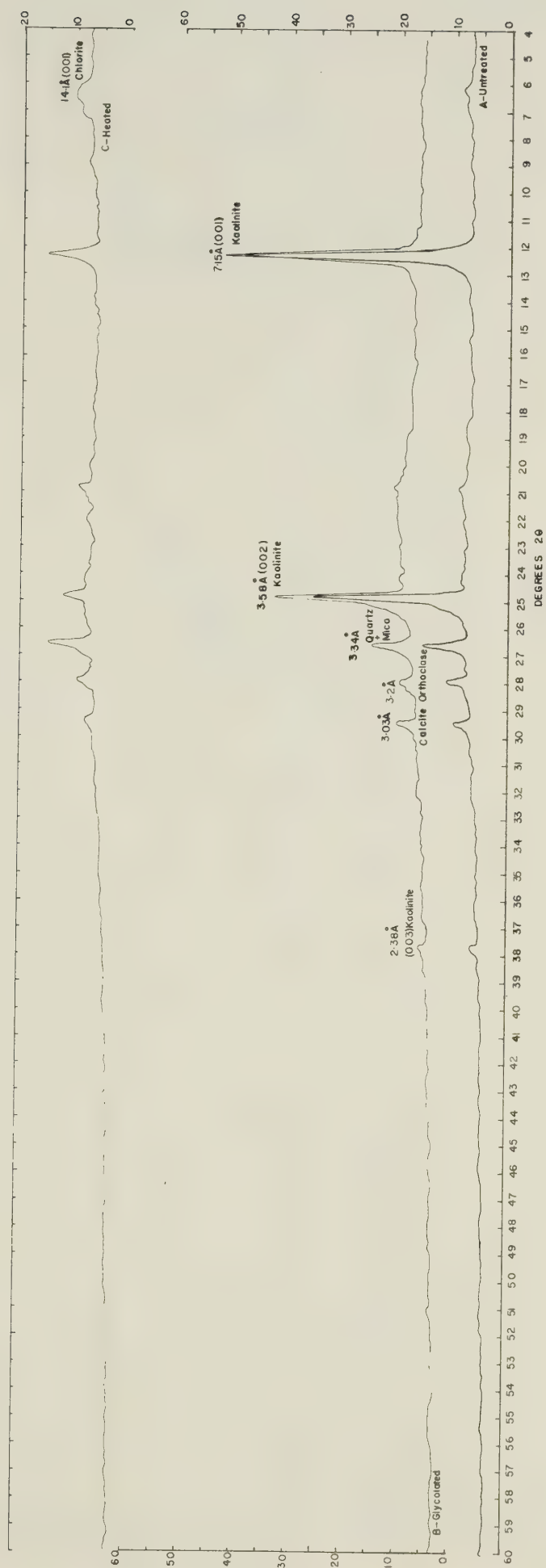


Figure 11. X-ray diffractogram of less than 2 $\mu$  fraction of oriented mount of sample #23(4-36-47-4W5)



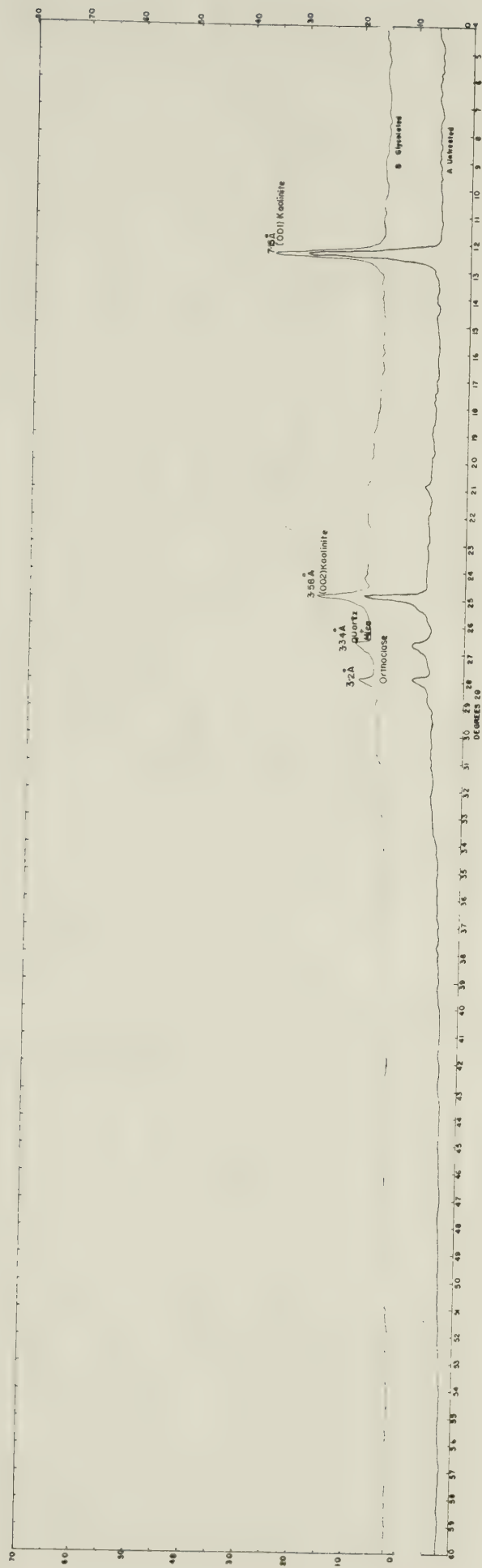


Figure 12. X-ray diffractogram of oriented mount of #20(10-35-47-4W5)

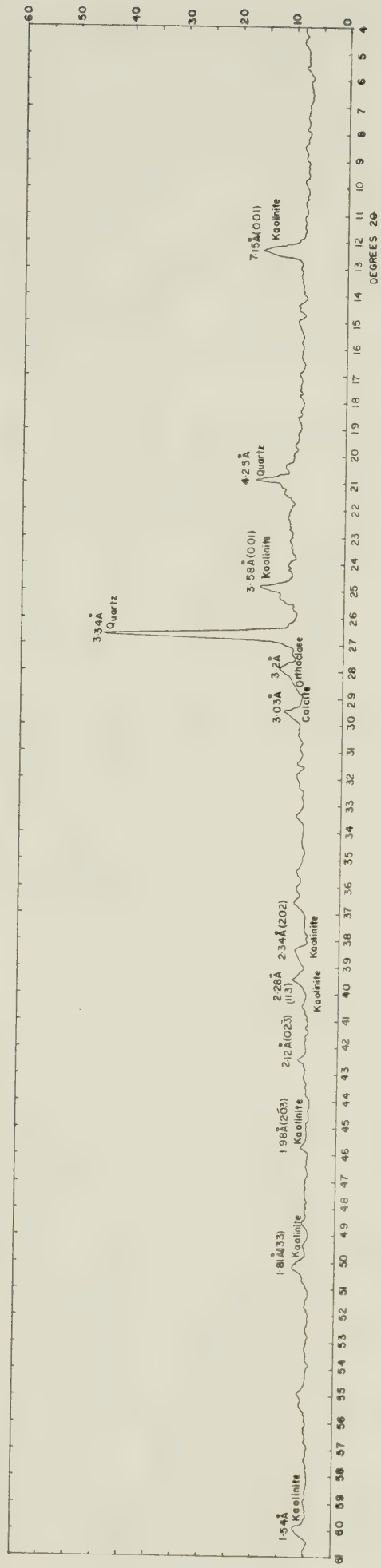


Figure 13. X-ray diffractogram of less than 2 $\mu$  fraction of unoriented mount of sample #23(4-36-47-4W5)  
(Quartz as an internal standard).



(001) and  $3.58 \text{ \AA}$  reflection (002) in oriented mounts, lack of appreciable difference on glycolation and collapse of the crystalline structure to a poorly crystalline phase (metakaolinite) upon heat-treatment at  $550^{\circ} \text{ C}$  for two hours show the authigenic clay to be kaolinite (Molloy and Kerr, 1961; Brindley, 1961; Richardson, 1961; Grim, 1968; Carroll, 1974).

A weak and diffuse peak at  $14.1 \text{ \AA}$  which showed no significant changes in its position and intensity on glycolation, but a slight increase in intensity on heat-treatment, was observed in the diffractogram of some of the oriented specimens (Figures 10 and 11) and interpreted as the (001) reflection of chlorite (Brindley, 1961; Carroll, 1974). The presence of authigenic chlorite growth habit (rosettes) under the SEM further corroborates the presence of chlorite in some of the studied samples. (See later part of this Chapter.)

A small broad peak at  $10.1 \text{ \AA}$  was also observed in the diffractogram of some of the oriented specimens (Figure 10A). It showed no appreciable changes in its position and intensity on glycolation and heat-treatment, and was interpreted as the (001) reflection of a 1M mica, illite (Bradley and Grim, 1961; Carroll, 1974). Characteristic illite growth habit of irregular flakes with short lath-like projections were also observed in the scanning electron micrographs. (See later part of this Chapter.) The examined specimens also contain some impurities (non-clay minerals)





which are indicated by small sharp peaks at 4.26, 3.34, 3.2 and 3.03 Å (Figures 10, 11 and 12). The impurities include quartz, feldspar (orthoclase) and calcite.

#### Scanning Electron Microscopy.

In an attempt to elucidate the detailed morphology and fabric of the authigenic clays in the studied samples, recourse was made to scanning electron microscopy. Scanning electron micrographs show that the authigenic clay cements are made up of well crystallized kaolinite (Plate 12A, B, C, D, E), rosette chlorite (Plate 13A, B) and irregular flakes of illite-montmorillonite(?) (Plate 13C, D, E, F). The well crystallized kaolinite occurs in the form of euhedral pseudohexagonal booklets (crystals) each of which is made up of a series of hexagonal plates. Individual plates range from 2 to 6 microns in width, 6 to 10 microns in length and 0.3 to 1.0 micron thick, and are stacked face-to-face, while some booklets (crystals) are up to 22 microns in thickness (Plate 12A, B). The booklets are randomly oriented with respect to each other and to the detrital grains, but in some cases the plates of booklets nearest a detrital grain appear to be preferentially arranged normal to the grain surface (Plate 12C). In most cases, the authigenic kaolinite plugs the whole pore and is characterized by intercrystalline sub-microscopic porosity with pore diameters of 5-10 microns (Plate 12A, B, C, D). On the average, the pores account for about 50 percent by volume of the bulk authigenic kaolinite, and are located between the booklets (Plate 12A, C; Figure





PLATE 12. SCANNING ELECTRON MICROGRAPHS OF BASAL BELLY  
RIVER SANDSTONE

- A. Scanning electron micrograph of well crystallized authigenic kaolinite booklets (b, c, and d) and associated submicroscopic pores (a) located between the booklets. Note hexagonal outline of kaolinite plates. (Well: 10-35-47-4W5. Sample no. 6. X600)
- B. Closeup of A showing face-to-face stacked plates (a, b, c, etc.) of a kaolinite booklet. Note the absence of space between the plates of the booklet. (Well: 10-35-47-4W5. Sample no. 6. X3000)
- C. Plates of a kaolinite booklet (a) nearest to a detrital quartz grain (b) arranged normal to the grain surface. Note submicroscopic pores, e.g., (c) between booklets. (Well: 4-36-47-4W5. Sample no. 23. X600)
- D. Microscopic pore (a) largely plugged by authigenic kaolinite cement which exhibits submicroscopic porosity. (Well: 10-35-47-4W5. Sample no. 6. X60)
- E. Well crystallized kaolinite plate (a) showing hexagonal outline, and submicroscopic pores (b), (c), (d) etc. (Well: 4-36-47-4W5. Sample no. 19. X3500)
- F. Chert overgrowth as an aggregate of small hexagonal quartz crystals, e.g., (a) on detrital chert grain and associated with authigenic chlorite (b). Submicroscopic pores (c) and (d) are located between fan-shaped chlorite clusters and between hexagonal quartz crystals, respectively. (Well: 4-36-47-4W5. Sample no. 37. X5000)



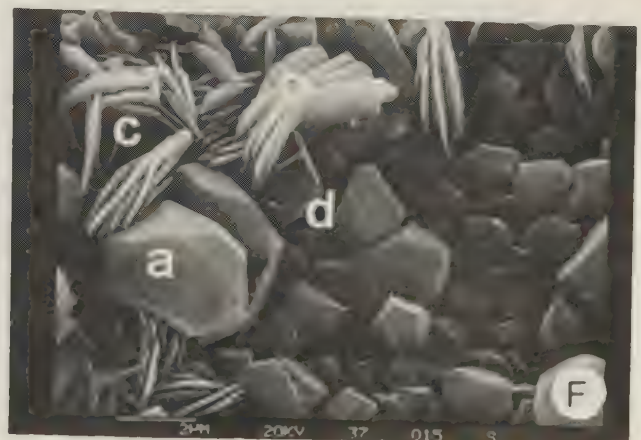
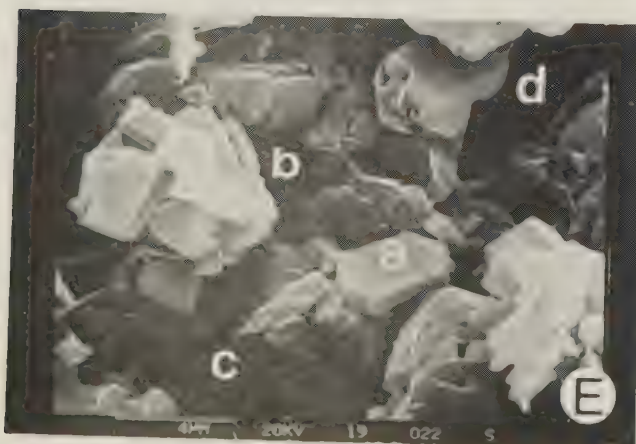
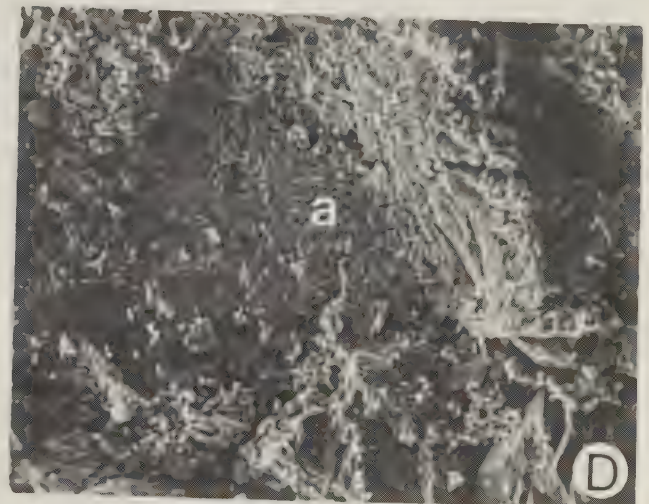
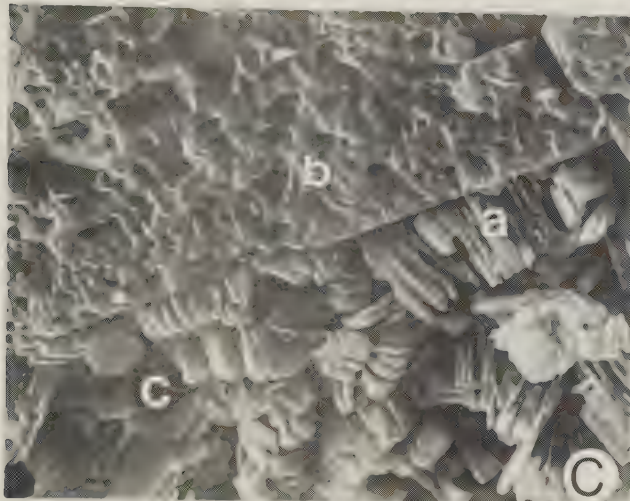
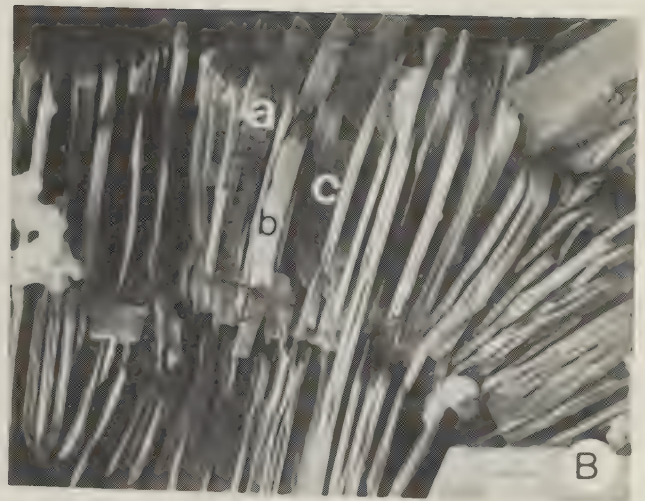
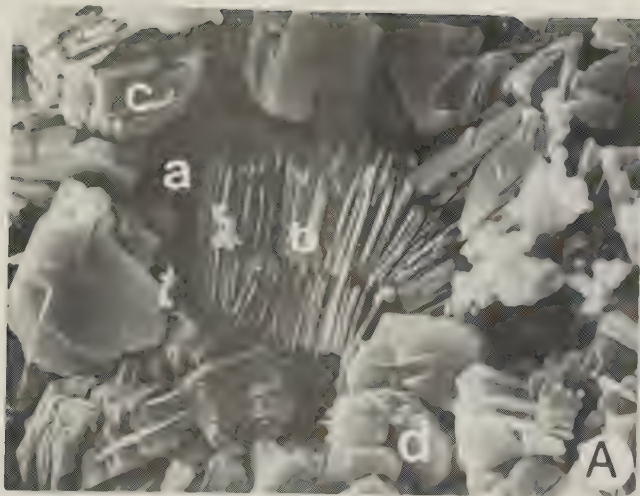


PLATE 12





<p>1. The first part of the paper discusses the importance of maintaining accurate records of all transactions.</p> <p>2. It then goes on to describe the various methods used to collect and analyze data.</p> <p>3. The results of the study are presented in the following table:</p>	<p>4. The data shows a clear trend of increasing sales over the period studied.</p> <p>5. This is due to a combination of factors, including improved marketing and better customer service.</p> <p>6. The overall conclusion is that the company is well-positioned for future growth.</p>
<p>7. The next section of the paper focuses on the challenges faced by the company.</p> <p>8. These include issues related to supply chain management and financial constraints.</p> <p>9. The author suggests several strategies to address these challenges.</p>	<p>10. The first strategy is to diversify the supply chain to reduce risk.</p> <p>11. The second is to implement cost-cutting measures without sacrificing quality.</p> <p>12. The third is to seek out new sources of financing.</p>
<p>13. The final part of the paper provides a summary of the findings and recommendations.</p> <p>14. It emphasizes the need for continuous monitoring and evaluation of the company's performance.</p> <p>15. The author concludes that with the right approach, the company can achieve its long-term goals.</p>	<p>16. The author also acknowledges the limitations of the study and suggests areas for further research.</p> <p>17. Finally, the paper includes a list of references and a list of figures.</p>

PLATE 13. SCANNING ELECTRON MICROGRAPHS OF BASAL BELLY  
RIVER SANDSTONE

- A. Authigenic hexagonal quartz crystal aggregate (a) and rosettes of chlorite, e.g., (b) and (d), with submicroscopic pores e.g., (c) between chlorite rosettes. (Well: 10-35-47-4W5. Sample no. 6. X600)
- B. Closeup of A showing rosettes of chlorite (b) and (d) partly plugging pore between authigenic quartz crystals (a) and (e). Note lobate edges of chlorite plates and submicroscopic pores, e.g., (c) located between rosettes of chlorite as well as between the plates of rosettes. (Well: 10-35-47-4W5. Sample no. 6. X1500)
- C. Interstratified illite-montmorillonite (?) pore lining (a) in the form of irregular shaped thin plates and flakes with short lath-like projections. Note also authigenic quartz (b) and pore (c). (Well: 4-36-47-4W5. Sample no. 12. X600)
- D. Closeup of C showing irregularly shaped thin plates of illite-montmorillonite (?) with short lath-like projections e.g., (a), and submicroscopic pores e.g., (b) and (c) located between the plates. (Well: 4-36-47-4W5. Sample no. 12. X3000)
- E. Authigenic illite-montmorillonite (?) (a) and associated submicroscopic porosity (b). Note the complex connections of the thin plates and flakes, and their large surface area. (Well: 4-36-47-4W5. Sample no. 16. X1800)
- F. Scaly, irregularly shaped illite-montmorillonite (?) plates (a) and associated submicroscopic porosity (b). (Well: 4-36-47-4W5. Sample no. 19. X12000)

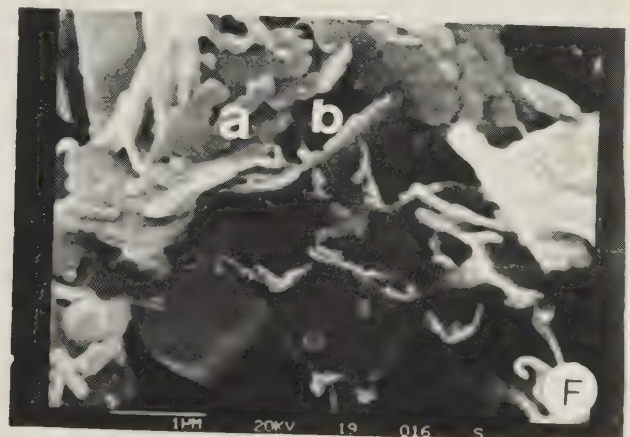
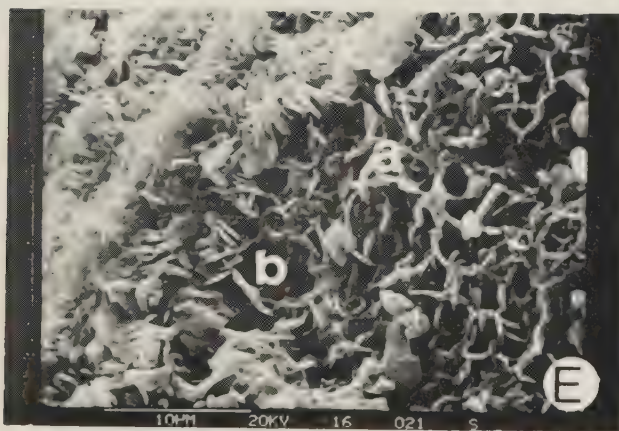
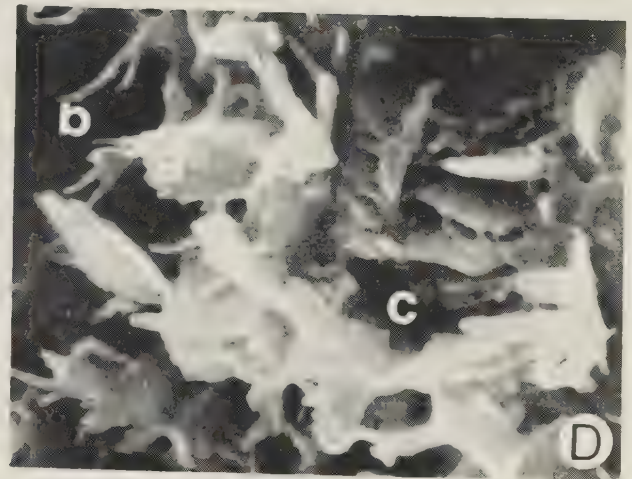
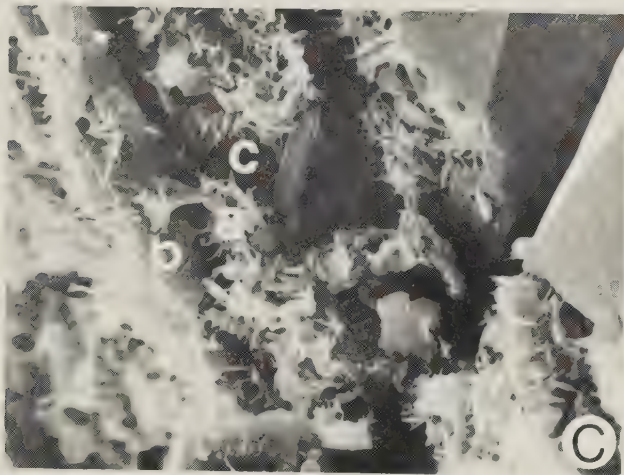
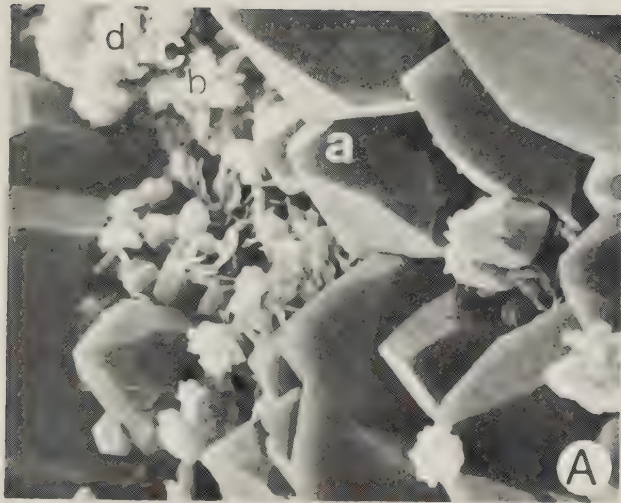


PLATE 13





14).

In addition to the authigenic kaolinite cement, some of the studied samples show the presence of chlorite in the form of rosettes and fan-shaped clusters (Plates 13A, B; 14A, B). In all cases these rosettes and fans are volumetrically insignificant and rarely completely fill up a pore. They generally occur in spaces amongst authigenic quartz crystals (Plate 14C, D). Individual rosettes or fans generally are 5 to 10 microns in diameter and are made up of randomly oriented, closely packed plates (crystals) that range from 2 to 10 microns across. The plates (crystals) have lobate edges; a characteristic which differentiates chlorite plates from superficially similar kaolinite plates (Wilson and Pittman, 1977). The chlorite rosettes are also characterized by submicroscopic porosity with pores located between the rosettes as in the case of kaolinite booklets, and also between the plates (Plates 13A, B; 14A, D).

A third and less common variety of authigenic clay cement texturally identified as interstratified illite-montmorillonite was observed in a few of the samples. It occurs in the form of pore linings and fillings (Plates 13C, D, E, F; 14E) and consists of irregular shaped thin plates and flakes with short lath-like projections (Plate 13D, F). The thin plates and flakes are bonded together in a complex manner that results in an open fabric producing submicroscopic porosity (Plate 13D, E, F). Similar morphology for poorly crystalline illite-rich interstratified illite-





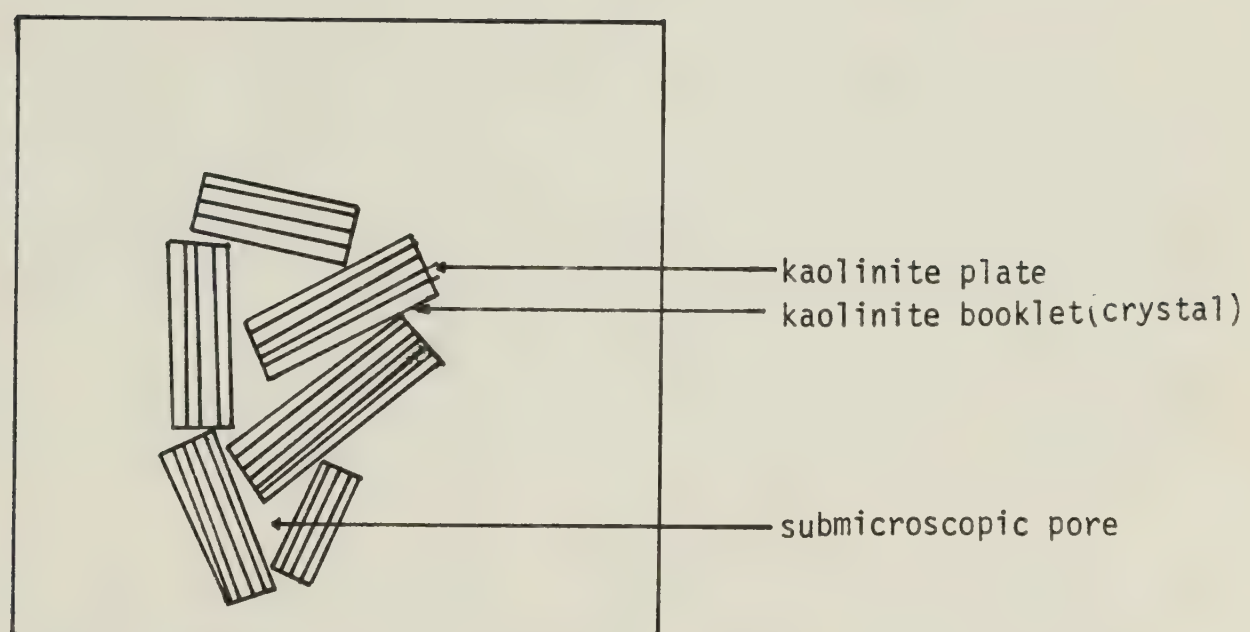


FIGURE 14. Diagrammatic sketch of kaolinite booklets and plates showing submicroscopic pores.





PLATE 14. SCANNING ELECTRON MICROGRAPHS OF BASAL BELLY  
RIVER SANDSTONE

- A. Rosettes and fan-shaped clusters of pore-filling chlorite made up of closely packed lobate-edged plates, e.g., (a), submicroscopic pores, e.g., (b) between fan-shaped clusters, e.g., (c), and between plates. (Well: 4-36-47-4W5. Sample no. 23. X4500)
- B. Closeup of A showing chlorite rosette (a) made up of randomly oriented, closely packed plates, and fan-shaped cluster of chlorite plates (b) plugging submicroscopic pore between authigenic quartz crystals (c) and (e). Note submicroscopic pores, e.g., (d). (Well: 4-36-47-4W5. Sample no. 23. X4750)
- C. Pore between authigenic quartz crystals (a) and (b) partially plugged by authigenic chlorite (c). (Well: 4-36-47-4W5. Sample no. 19. X600)
- D. Closeup of C. Authigenic chlorite (c) plugging pore between authigenic quartz crystals (a) and (b). Submicroscopic pores, e.g., (d) are still present. (Well: 4-36-47-4W5. Sample no. 19. X3500)
- E. Submicroscopic pore (c) enveloping a detrital quartz grain (d) in a seemingly tightly cemented specimen. Note that the very small individual plates and flakes of the authigenic clay (a) (illite-montmorillonite ?) still have submicroscopic pores, e.g., (b) between them. (Well: 4-36-47-4W5. Sample no. 23. X9000)
- F. Quartz overgrowth (a) and authigenic clay cement (b) have reduced the size and blocked the throat (d) of a former large pore (c). (Well: 4-36-47-4W5. Sample no. 12. X60)



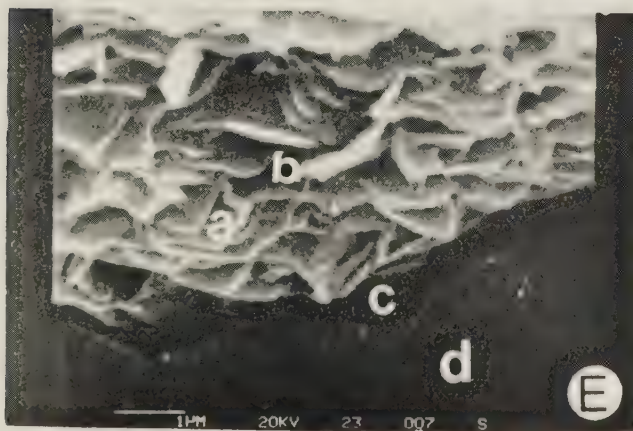
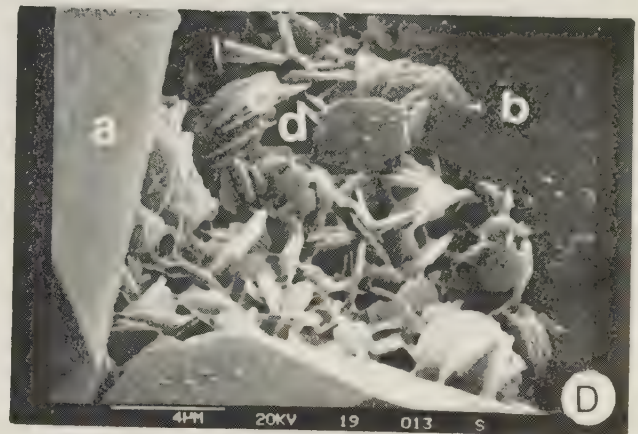
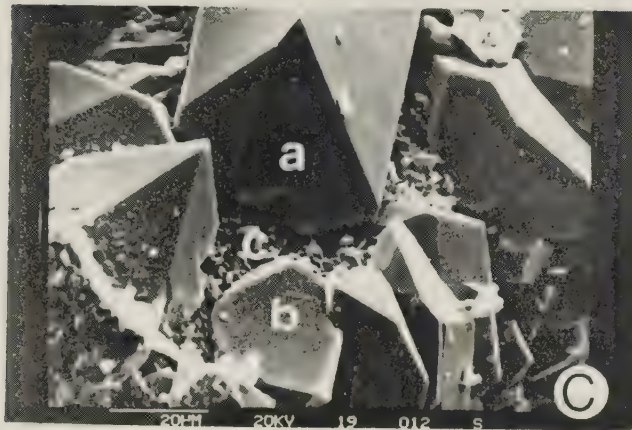
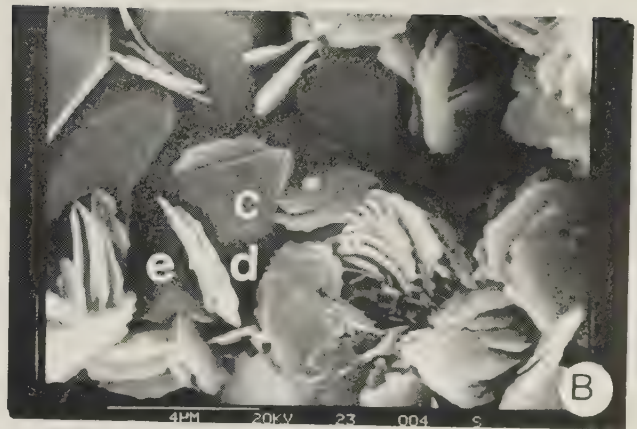
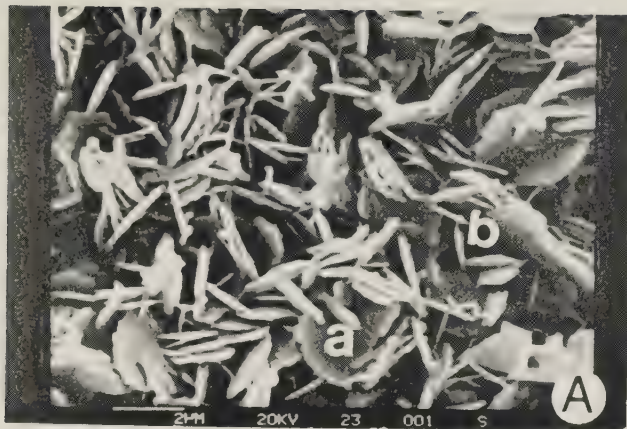


PLATE 14





montmorillonite has been documented by Wilson and Pittman (1977).

The pseudo-hexagonal habit of well crystallized kaolinite has been recognized through both electron microscopy (Bates, 1955) and scanning electron microscopy (Borst and Keller, 1969; Wilson and Pittman, 1977). Chlorite has been reported as occurring in rosette form (Wilson and Pittman, 1977). The crystal morphology and fabric (booklets of face-to-face hexagonal plates) of kaolinite, rosette growth habit of chlorite, and thin plates and flakes with short lath-like projections characteristic of illite-montmorillonite mixed-layer clay (Wilson and Pittman, 1977) revealed by the scanning electron microscope corroborate the petrographic and XRD evidence for the authigenic origin of kaolinite, chlorite and illite-montmorillonite cements in the studied samples of the basal Belly River sandstone. The delicacy and habit of the crystals preclude transport and attest to their insitu development in voids between detrital grains during diagenesis.



## CHAPTER VII.

### A COMPARISON OF PETROGRAPHIC AND CORE ANALYSIS DATA

Table 12 summarizes the observed thin section and core analysis porosity values for the samples of the basal Belly River sandstone studied. It reveals a significant difference in the porosity values determined by the two different methods. The observed thin section porosity values for this rock unit range from less than 1 percent to 13.3 percent while the core analysis porosity values range from 4.8 to 23.3 percent.

Table 13 shows the grain mean diameters, observed thin section porosity (microscopic, intergranular and intra-granular) values and the quantities of cements in the studied samples. The grain mean diameters and the observed thin section porosity values were graphed as a scatter diagram (Figure 15) and a correlation coefficient,  $r$ , and linear regression equation were calculated for the two variables. A regression line was fitted to the set of points (Figure 15). A fairly strong correlation exists between the two variables - thin section microporosity values and the grain mean diameters as shown by a correlation coefficient,  $r$ , of +0.52 and linear regression equation of  $y = 28.76X - 4.32$ . The coarser grained samples are also the more porous ones, though one has to realize that in some cases the initial porosity of the samples has been either greatly modified or eliminated by authigenic clay and calcite cementation.



TABLE 12.

A Comparison of Observed Thin Section and Core Analysis Porosity Values

Serial No.	Well Name	Location	Sample No.	Grain Mean Dia. (mm)	Observed T.S. Porosity	Core Analysis Porosity*
1.1	IOE CDN-SUP PEMBINA	10-27-47 -4W5	At 3212.8 ft	0.17	0	-
1.2			At 3215.4 ft (A)	0.18	1.5	-
1.3			At 3215.4 ft (B)	0.16	0.2	-
1.4			At 3219.1 ft	0.23	1.5	-
1.5			At 3233.8 ft	0.30	1.0	-
2.6	IOE CDN-SUP PEMBINA	10-34-47 -4W5	At 2186.3 ft (A)	0.27	0.7	-
2.7			At 2186.3 ft (B)	0.18	2.0	-
2.8			40	0.36	7.3	19.4
2.9			41	0.29	5.7	17.6
2.10			50	0.29	0.3	11.4
2.11	IOE CDN-SUP PEMBINA	10-35-47 -4W5	52	0.29	5.0	17.6
2.12			53	0.25	0.8	15.2
3.13			6	0.30	0.5	12.7
3.14			18	0.41	~1.0	4.8
3.15			20	0.33	11.7	19.7
3.16	IOE CDN-SUP PEMBINA	4-36-47 -4W5	23	0.36	2.5	10.8
3.17			25	0.36	13.3	23.3
3.18			39	0.32	5.2	18.0
3.19			46	0.31	3.3	16.6
4.20			12	0.31	5.8	16.8
4.21	IOE CDN-SUP PEMBINA		16	0.36	9.3	17.5
4.22			18	0.30	7.3	16.9
4.23			19	0.32	6.5	19.2

.../Continued





TABLE 12. - Continued

Serial No.	Well Name	Location	Sample No.	Grain Mean Dia. (mm)	Observed T.S. Porosity	Core Analysis Porosity*
4.24	IOE CDN-SUP PEMBINA	4-36-47 -4W5	23	0.29	3.3	17.8
4.25			25	0.29	3.8	15.0
4.26			35	0.36	0.8	15.5
4.27			37	0.30	2.2	14.8
5.28	IOE CDN-SUP PEMBINA	4-2-48 -4W5	12	0.23	2.7	9.4
5.29			13	0.32	6.7	19.6
5.30			16	0.35	10.3	22.4
5.31			23	0.39	6.2	16.5
5.32			23	0.27	5.0	16.5
5.33			33	0.32	4.5	20.3
5.34			33	0.22	1.7	20.3
5.35			42	0.28	2.5	17.9
5.36			46	0.29	5.5	20.2
5.37			47	0.30	3.8	19.9
5.38			51	0.28	4.7	20.4

NB: A = Coarse part of slide

B = Fine part of slide

\* = Data from Core Laboratory Analysis Sheet



TABLE 13.  
Grain Mean Diameter, Observed Thin Section Porosity and Cement Percentages

Serial No.	Well Name	Location	Sample No.	Grain Mean Dia. (mm)	Observed T.S. Porosity	Kaolinite Cement	Other Cements
1.1	IOE CDN-SUP PEMBINA	10-27-47-4W5	At 3212.8 ft	0.17	0	0.5	17.5
1.2			At 3215.4 ft (A)	0.18	1.5	7.7	1.2
1.3			At 3215.4 ft (B)	0.16	0.2	0.5	19.8
1.4			At 3219.1 ft	0.23	1.5	8.0	3.8
1.5			At 3233.8 ft	0.30	1.0	6.8	12.8
2.6	IOE CDN-SUP PEMBINA	10-34-47-4W5	At 2186.3 ft (A)	0.27	0.7	7.8	0.3
2.7			At 2186.3 ft (B)	0.18	2.0	10.0	0.7
2.8			40	0.36	7.3	2.5	0.8
2.9			41	0.29	5.7	6.2	0
2.10			50	0.29	0.3	7.8	7.2
2.11	IOE CDN-SUP PEMBINA	10-35-47-4W5	52	0.29	5.0	8.3	0.5
2.12			53	0.25	0.8	6.6	0.2
3.13			6	0.30	0.5	8.8	1.8
3.14			18	0.41	~1.0	1.3	39.7
3.15			20	0.33	11.7	4.8	0.7
3.16	IOE CDN-SUP PEMBINA	4-36-47-4W5	23	0.36	2.5	7.4	23.8
3.17			25	0.36	13.3	4.5	2.0
3.18			39	0.32	5.2	6.3	0.7
3.19			46	0.31	3.3	8.3	4.5
4.20			12	0.31	5.8	7.5	0.5
4.21	IOE CDN-SUP PEMBINA		16	0.36	9.3	5.8	1.0
4.22			18	0.30	7.3	6.5	1.3
4.23			19	0.32	6.5	4.7	1.3

.../Continued



TABLE 13. - Continued

Serial No.	Well Name	Location	Sample No.	Grain Mean Dia. (mm)	Observed T.S. Porosity	Kaolinite Cement	Other Cements
4.24	IOE CDN-SUP PEMBINA	4-36-47-4W5	23	0.29	3.3	6.7	1.0
4.25			25	0.29	3.8	8.7	0.2
4.26			35	0.36	0.8	5.5	8.2
4.27			37	0.30	2.2	9.8	1.8
5.28	IOE CDN-SUP PEMBINA	4-2-48-4W5	12	0.23	2.7	6.5	17.0
5.29			13	0.32	6.7	5.3	0.3
5.30			16	0.35	10.3	5.0	0.7
5.31			23	0.39	6.2	5.2	0
5.32			23	0.27	5.0	4.5	0.3
5.33			33	0.32	4.5	7.0	0.2
5.34			33	0.22	1.7	5.3	0.3
5.35			42	0.28	2.5	10.3	1.5
5.36			46	0.29	5.5	9.7	1.0
5.37			47	0.30	3.8	9.3	0.3
5.38			51	0.28	4.7	9.7	0.5

NB: A = Coarse part of slide  
B = Fine part of slide





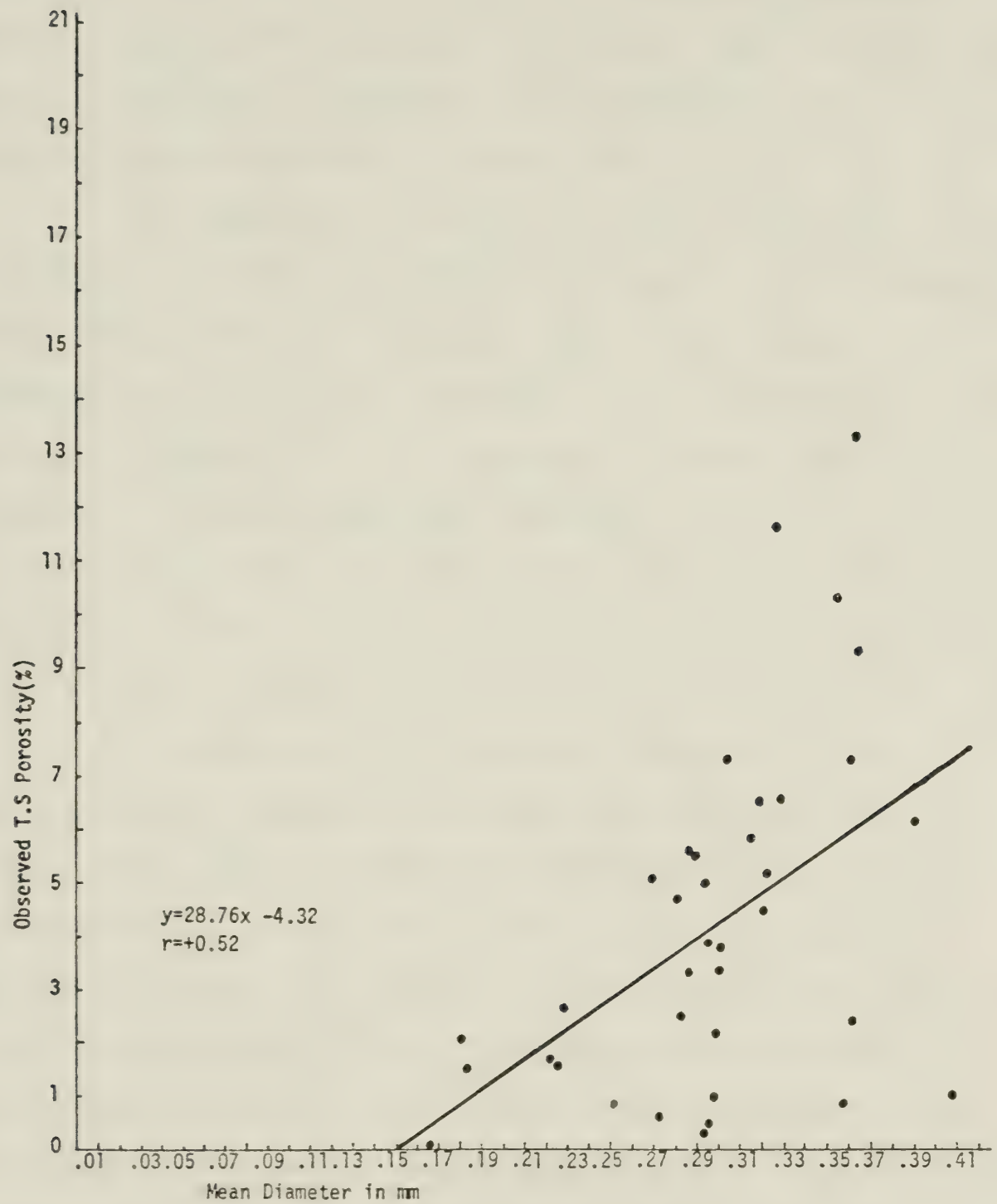


FIGURE 15. Grain Mean Diameter vs. Observed T.S. Porosity Plot.



In addition to the intergranular and intragranular microporosity (Plates 8B; 11E, F; 14F) most of the samples show submicroscopic porosity (pore spaces too small to be recognized with a light microscope at the normal magnifications of X50 to X150 at which counting of thin sections is generally performed) especially in the authigenic clay cement, as was documented in Chapter VI.

The observed thin section porosity values and the core analysis porosity values were also plotted as a scatter diagram (Figure 16). It shows an approximate linear relationship between the two variables. The correlation coefficient  $r$  value of +0.64 indicates a strong linear relationship. A linear regression equation of  $y = 0.77X + 13.18$  was also computed for the thin section and core analysis porosity data and was used to fit a regression line to the set of points (Figure 16).

The significant differences between the thin section porosity values and corresponding core analysis porosity values are due mainly to differences in the method of determination - thin section point counting versus summation of fluids. Thin section point counting has some obvious shortcomings in that it normally undermeasures the total porosity (ratio of the volume of all the pores to the bulk volume of the sample, regardless of size or interconnection of the pores) and overmeasures the grain and cement volumes of samples. This results from the non-recognition of submicroscopic pore spaces within solid



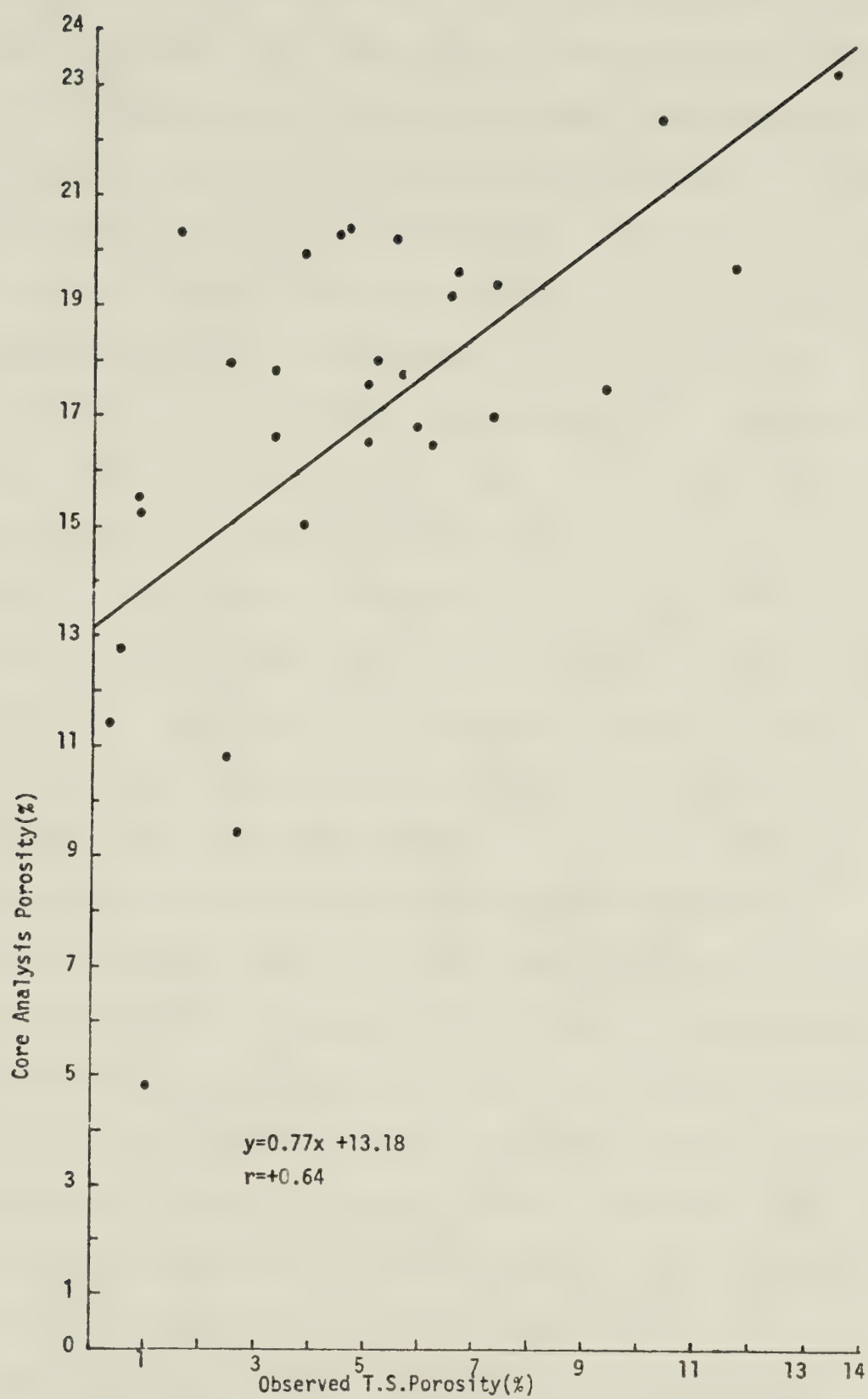


FIGURE 16. Core Analysis vs. Observed T.S. Porosity Plot.





volume, plus the "edge effect" caused by grain curvature within the thickness (30 microns) of the thin section. The edge error increases with decreasing grain size and sorting, and with increasing grain irregularity and tighter grain packing. In addition, the "edge effect" results in hiding pores which have maximum pore diameters less than the thickness of the thin section (Halley, 1978). In the present study, scanning electron micrographs revealed submicroscopic pores between the cement crystals in the authigenic clay cement (Plates 12A, B, C, D; 13A, D, E; 14A). Submicroscopic pores are also present between the component nanograins in the mudrock fragments. The edge effect error, which is due to the appreciable thickness of the thin section, and is complicated by packing and sorting variations and increased grain irregularities, is also revealed by the scanning electron microscope. A scanning electron micrograph of an apparently closely packed or tightly cemented sample often shows the existence of some pore space enveloping the detrital grains (Plate 14E). From scanning electron microscopy information, it is clear that submicroscopic pores in the authigenic clay cement, mudrock fragments and matrix, plus edge effect errors, none of which are obvious under the ordinary light microscope, are largely responsible for the underestimation of total porosity by thin section point-counting. The core analysis summation of fluids and mercury injection methods, on the other hand, measure all forms of pores (microscopic and submicroscopic)



down to less than one micron and are truer measures of total porosity (although they too do not measure pores which are not interconnected, but this is rare in detrital rocks).

In an attempt at evaluating the contribution of the submicroscopic pores to the total porosity of the samples, a visual estimate of the submicroscopic pore volume was made by examining scanning electron micrographs. About fifty percent of the bulk volume authigenic clay cement was estimated to be submicroscopic porosity and was added to the observed thin section porosity values (Table 14). The observed thin section porosity values plus 50 percent of authigenic clay cement were then plotted against core analysis porosity values (Figure 17). The general trend of the scatter can be approximated by a straight line. A correlation coefficient,  $r$ , of +0.71 was calculated for the set of points. A linear regression equation of  $y = 0.91X + 9.50$  was obtained, and based on the above equation, a regression line was fitted to the points. The observed thin section porosity plus 50 percent of authigenic clay cement versus core analysis porosity gives a stronger linear relationship than the observed thin section porosity versus core analysis porosity, and points to the fact that the submicroscopic porosity hidden between the cement crystals has contributed measurably to the core analysis porosity values. Unfortunately, the contribution of the "edge effect" to the total porosity value cannot be easily quantified by observation. Recourse was made to the



TABLE 14.

## Summary of Observed Thin Section Porosity, Submicroscopic

## Porosity, 'Edge Error' and Core Analysis Porosity

Serial No.	Sample No.	Grain Mean Dia. (mm)	Observed T.S. Porosity	Kaolinite Cement (%)	Observed T.S. Porosity + 0.5 Kaolinite Cement	Edge Error Estimate Using Halley's (1978) 'Edge Error' Curve		Core Analysis Porosity
						Edge Error as % of Void Space	Edge Error as Porosity (%)	
1.1	At 3212.8 ft	0.17	0	0.5	0.3	-	-	-
1.2	At 3215.4 ft	0.18	1.5	7.7	5.3	19.0	0.29	-
1.3	At 3215.4 ft	0.16	0.2	0.5	0.4	19.5	0.03	-
1.4	At 3219.1 ft	0.23	1.5	8.0	5.5	16.0	0.24	-
1.5	At 3233.8 ft	0.30	1.0	6.8	4.4	13.0	0.13	-
2.6	At 2186.3 ft	0.27	0.7	7.8	4.6	14.0	0.09	-
2.7	At 2186.3 ft	0.18	2.0	10.0	7.0	19.0	0.38	-
2.8	40	0.36	7.3	2.5	8.6	11.0	0.81	19.4
2.9	41	0.29	5.7	6.2	8.7	14.0	0.79	17.6
2.10	50	0.29	0.3	7.8	4.3	13.5	0.05	11.4
2.11	52	0.29	5.0	8.3	9.2	13.5	0.68	17.6
2.12	53	0.25	0.8	6.6	4.1	15.0	0.13	15.2
3.13	6	0.30	0.5	8.8	4.9	13.0	0.07	12.7
3.14	18	0.41	~1.0	1.3	1.7	10.0	0.1	4.8
3.15	20	0.33	11.7	4.8	14.1	12.5	1.46	19.7
3.16	23	0.36	2.5	7.4	6.2	11.0	0.27	10.8
3.17	25	0.36	13.3	4.5	15.6	11.0	1.47	23.3
3.18	39	0.32	5.2	6.3	8.3	12.5	0.65	18.0
3.19	46	0.31	3.3	8.3	7.5	13.0	0.43	16.6

.../Continued





TABLE 14. - Continued

Serial No.	Sample No.	Grain Mean Dia. (mm)	Observed T.S. Porosity	Kaolinite Cement (%)	Observed T.S. Porosity + 0.5 Kaolinite Cement	Edge Error Estimate Using Halley's (1978) 'Edge Error' Curve		Core Analysis Porosity
						Edge Error as % of Void Space	Edge Error as Porosity (%)	
4.20	12	0.31	5.8	7.5	9.6	13.0	0.76	16.8
4.21	16	0.36	9.3	5.8	12.3	11.0	1.03	17.5
4.22	18	0.30	7.3	6.5	10.6	13.0	0.95	16.9
4.23	19	0.32	6.5	4.7	8.8	12.0	0.78	19.2
4.24	23	0.29	3.3	6.7	6.7	14.0	0.47	17.8
4.25	25	0.29	3.8	7.7	8.2	14.0	0.54	15.0
4.26	35	0.36	0.8	5.8	3.6	11.0	0.09	15.5
4.27	37	0.30	2.2	9.8	7.1	13.0	0.28	14.8
5.28	12	0.23	2.7	6.5	5.9	16.0	0.43	9.4
5.29	13	0.32	6.7	5.3	9.3	12.5	0.83	19.6
5.30	16	0.35	10.3	5.0	12.8	12.0	1.24	22.4
5.31	23	0.39	6.2	5.2	8.8	10.5	0.65	16.5
5.32	23	0.27	5.0	4.5	7.3	14.5	0.73	16.5
5.33	33	0.32	4.5	7.0	8.0	12.0	0.54	20.3
5.34	33	0.22	1.7	5.3	4.3	16.0	0.27	20.3
5.35	42	0.28	2.5	10.3	7.7	14.0	0.35	17.9
5.36	46	0.29	5.5	9.7	10.3	14.0	0.77	20.2
5.37	47	0.30	3.8	9.3	8.5	13.0	0.50	19.9
5.38	51	0.28	4.7	9.7	9.5	14.0	0.65	20.4

NB: A = Coarse part of slide  
B = Fine part of slide



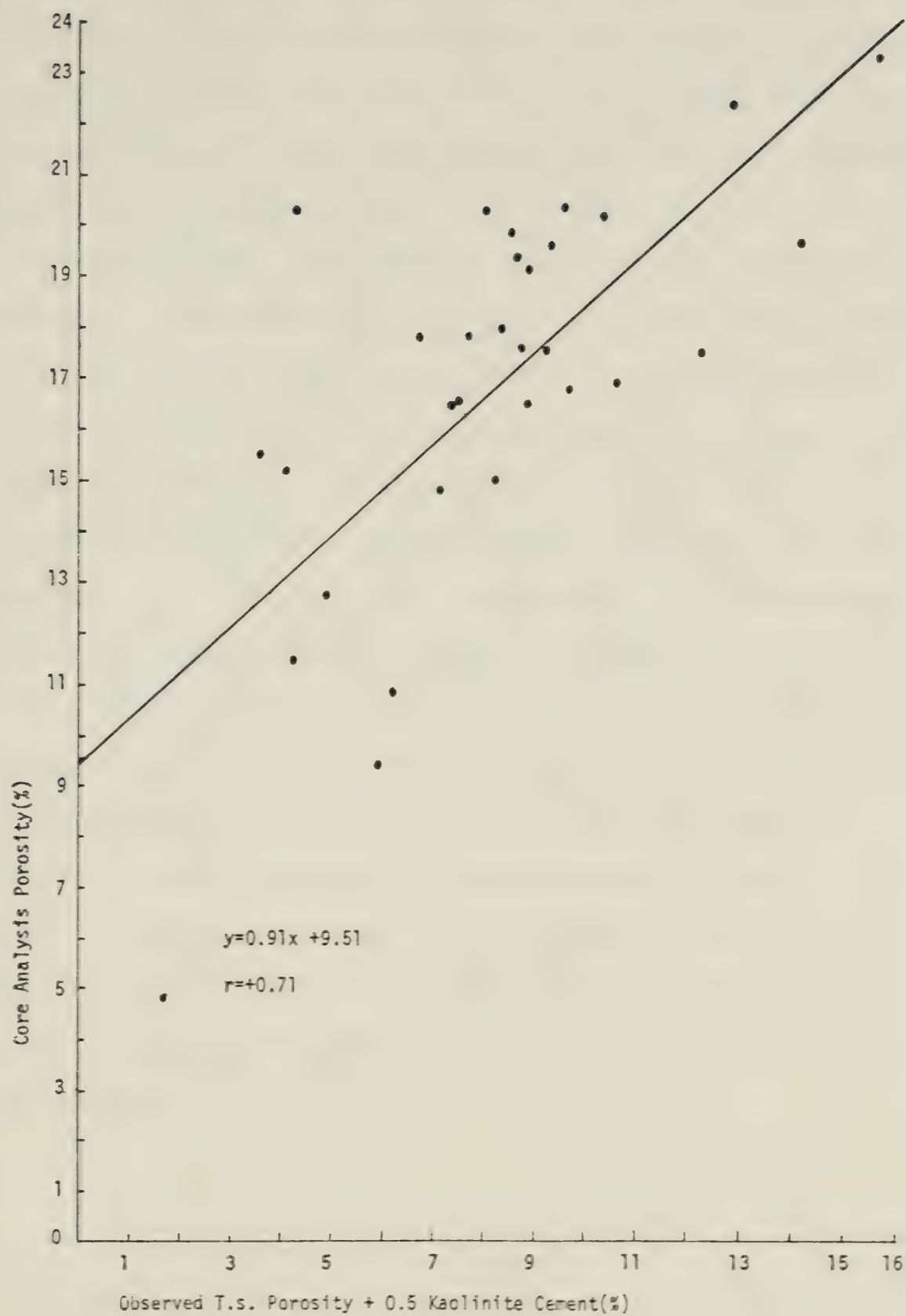


FIGURE 17. Core Analysis vs. Observed T.S. Porosity Plus 0.5 Kaolinite Cement Plot.



use of Halley's (1978) "edge error" curve (Figure 18) for the estimation of the contribution by "edge effect" to the total porosity. This curve is essentially an edge error versus grain diameter one. The "edge error" for the studied samples ranges from about 10.5 to 19 percent of the void space between grains. It therefore accounts for less than 1.5 percent of observed porosity (Table 14), indicating that edge error would not contribute greatly to the discrepancy between thin section and core analysis porosity values. The "edge effect" is not considered to be quantitatively significant in the present study, especially since all thin sections used in this study are impregnated with blue epoxy which helps to show up "edge covered" porosity.

A correlation coefficient value of  $+0.71$  shows a strong linear relationship for the variables under investigation (core analysis porosity and thin section porosity plus submicroscopic porosity). A y-intercept of 9.51, though an improvement on the initial value of 13.18 for the observed thin section porosity versus core analysis porosity plot, is still to be accounted for and will be discussed in the next Chapter.





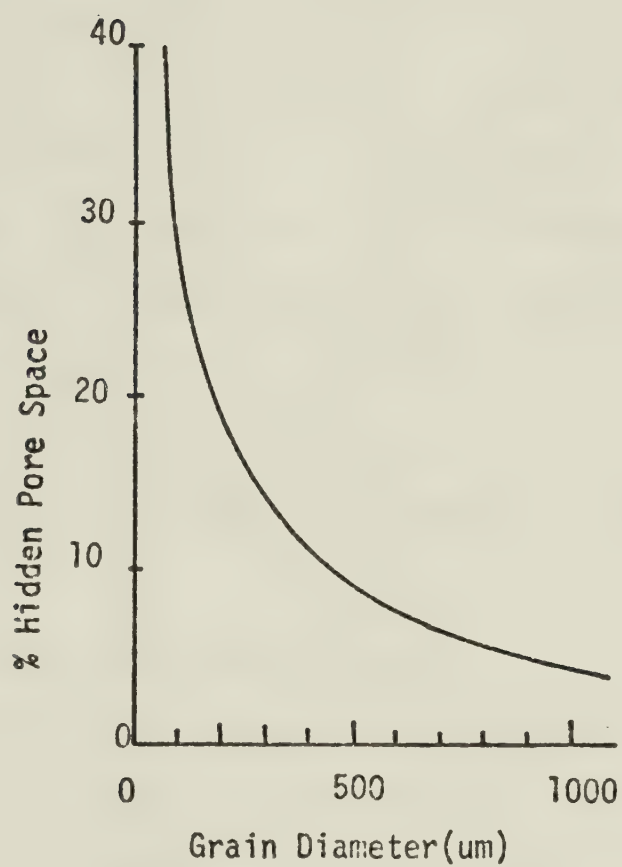


FIGURE 18. Edge error as percent of total obscured porosity plotted as a function of grain size for cubic-packed spheres. (From Halley, 1978).



## CHAPTER VIII.

### INTERRELATIONSHIPS OF AUTHIGENIC CLAY AND WATER SATURATION IN THE BASAL BELLY RIVER SANDSTONE

A comparison of Core Laboratory and observed petrographic data on the basal Belly River sandstone revealed a consistent disagreement between them. In addition, Core Laboratory water saturation values appear to be questionably high when considered in the light of oil/water production figures (Table 1). In the absence of production figures, the impression one would get from core analysis data is that the basal Belly River sandstone reservoir is characterized by high porosity but also high water saturation, and therefore of limited economic value. However, from the petrographic study, it is clear that these apparent discrepancies are largely the result of two main factors, namely:

1. presence of authigenic clay,
2. differences in the method of analysis (Core Laboratory versus thin section method). In the following pages an attempt will be made to explain these relatively high core analysis measurements in terms of the presence of authigenic clay and methods of core analysis.

#### Relatively High Core Analysis Porosity

The authigenic clay in the basal Belly River sandstone is characterized by very small crystal size, large inner surface area and submicroscopic porosity. The large



surface area of the clay renders it capable of adsorbing a large quantity of connate water. Connate water is here defined as water adsorbed on mineral "grains" of a reservoir and not produced with oil or gas (Dictionary of Geology, p. 90, 1976). Depending on the method of measurement of the porosity in the drilling core, the submicroscopic porosity and even the boundwater volume of the authigenic clay may be included in the porosity data.

A review of the Core Laboratory procedure for porosity determination shows that

1. two of the three variables - bulk volume, pore volume, and grain volume must be measured to determine porosity since

$$\begin{aligned} \text{Bulk volume} &= \text{Grain volume} + \text{Pore volume} \quad \text{and} \\ \text{Porosity} &= \frac{\text{Pore volume}}{\text{Bulk volume}} \times 100 \quad ; \end{aligned}$$

2. 'fresh' or prepared samples (plugs, sidewall cores, whole diameter cores and cuttings) may be used for the determination;
3. sample preparation involves thorough extraction of oil and brine by gas-driven solvent extractors, centrifugal extractors, and Soxhlet and Dean-Stark refluxing solvent extractors and vacuum retorts, followed by drying;
4. the methods of measurement of the three variables (bulk volume, pore volume and grain volume) vary and include the summation of fluids porosity procedure, use of various porosimeters to determine grain volume and pore volume (gas transfer methods) and the resaturation porosity procedure;





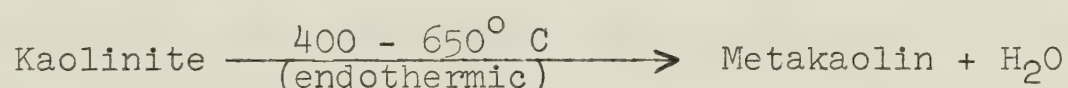
5. bulk volume is determined by displacement of a liquid, or by calipering a shaped sample and computation by the appropriate geometric formula (Fundamentals of Core Analysis).

The summation of fluids porosity procedure involves the independent determination of gas, oil and "pore water" volumes of a fresh core sample. The pore volume is determined by summing the three independent volumes. The gas transfer methods involve the compression of a gas into the pores or the expansion of gas from the pores of a prepared sample. The Boyle's Law method results in the determination of either the pore volume or grain volume. The Washburn-Bunting method, which is the vacuum extraction and collection of the gas (usually air) contained in the pores of a prepared sample, results in the determination of pore volume only. The liquid resaturation method involves the filling of the pores of a prepared sample with a liquid of known density and the division of the weight increase of the sample (weight of the saturating liquid) by the fluid density to get the pore volume (Fundamentals of Core Analysis).

With the above brief review of the Core Laboratory analysis procedures for porosity determination and the detailed petrography of the basal Belly River sandstone in mind, one finds some obvious limitations of these Core Laboratory methods and their possible effects on the reported Core Laboratory porosity data. In the case of the summation of fluids method, the "pore water" volume



determined in this way for the basal Belly River sandstone samples includes both the free pore water and boundwater (adsorbed water) of the clays because the operating temperature of  $650^{\circ}\text{C}$  ( $1200^{\circ}\text{F}$ ) is capable of liberating both. Grim (1968) defines adsorbed water as water held by clay materials only at relatively low temperatures, driven off by heating to about  $100$  to  $150^{\circ}\text{C}$ . It is regarded as nonliquid or nonordinary water in clay-water systems because it is in a physical state different from that of liquid water. In addition, at a temperature of  $650^{\circ}\text{C}$  (the Core Laboratory operating temperature) most of the clays lose their interlayer and OH lattice water as well. Mixed layer illite-montmorillonite clay loses most of its interlayer water between  $100$  and  $200^{\circ}\text{C}$ , and some of its OH lattice water at  $350$  to  $650^{\circ}\text{C}$ . Kaolinite dehydrates to metakaolin with loss of OH lattice water between about  $400$  and  $525^{\circ}\text{C}$ .



Chlorites also lose a good deal of their hydroxyl water between  $500$  and  $550^{\circ}\text{C}$ . But the detailed dehydration characteristics of these clay minerals vary with particle size, crystallinity and composition (Grim, 1968). These processes (loss of adsorbed, interlayer and OH lattice water) therefore result in higher than normal 'pore water' volume and porosity determinations. Sah (1977) defines total porosity as producible porosity plus boundwater volume and therefore recognizes the possible contribution of boundwater to porosity values determined by the summation of



fluids method. Therefore, boundwater and, if possible, interlayer and OH lattice water volume corrections should be applied to all core analysis porosity values determined for the basal Belly River sandstone samples by the summation of fluids method. The drying of samples in the gas transfer methods may also result in the liberation of the boundwater if a clay-bearing sample is not dried by the special humidity-controlled oven method. This increase in pore volume will be reflected in the porosity data determined subsequently by a gas transfer method. The resaturation method is greatly influenced by the drying of the sample, type of resaturating fluid, and the pressure applied in the resaturation process. Therefore it is possible to include the volume of the "ineffective" submicroscopic pores and the boundwater volume in the porosity values determined by this method. On the basis of the foregoing considerations, it is likely that the Core Laboratory analysis porosity values for the basal Belly River sandstone samples are total porosity values rather than only the economically important larger effective producible porosities measured in thin section. That is, the total porosity value determined by the Core Laboratory is equal to producible porosity plus submicroscopic porosity plus boundwater volume plus possibly interlayer and OH lattice water volumes. The roughly 10 percent difference between the core analysis porosity and the observed thin section porosity (corrected for submicroscopic porosity) described in Chapter VII may be mainly due to





boundwater, interlayer water and hydroxyl lattice water volumes of the authigenic clay. Reference to published dehydration data (Figures 19, 20, 21, 22 and 23) shows that appreciable quantities of water are lost by clays on heating to  $650^{\circ}$  C. Kaolinite loses about 13 percent by weight on heating to  $650^{\circ}$  C. Most montmorillonites lose approximately 8 to 10 percent by weight on similar treatment. Illites and chlorites also dehydrate with loss of about 6 and 9 percent by weight respectively on heat treatment to  $650^{\circ}$  C. Although Halley (1978) in his study of estimation of pore and cement volumes in thin section of oolite from Joulter's Cays thinks that as much as 7 percent porosity difference between bulk density porosity and thin section point count value is due to packing and sorting variations and grain irregularities, it seems that this is not the case in the present study and may account for only a small fraction of the 10 percent since the samples are fine to medium grained, very well to well sorted and moderately packed. The inference that an appreciable amount of the core analysis porosity is "ineffective" is suggested by the very low permeability values for sandstone samples with core analysis porosity values of less than 15 percent (Table 15). An examination of the Core Laboratory analysis data (Table 15) clearly shows that to have a permeability value greater than 1md, a core analysis porosity value of 14 percent is necessary, while observed thin section porosity values are only 2 to 4 percent for these types of samples. The Core



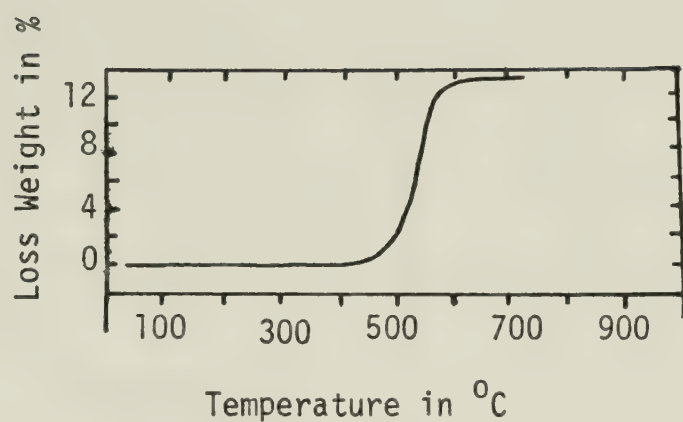


FIGURE 19. Idealized dehydration curve for kaolinite.  
(After Spiel et al. 1945).

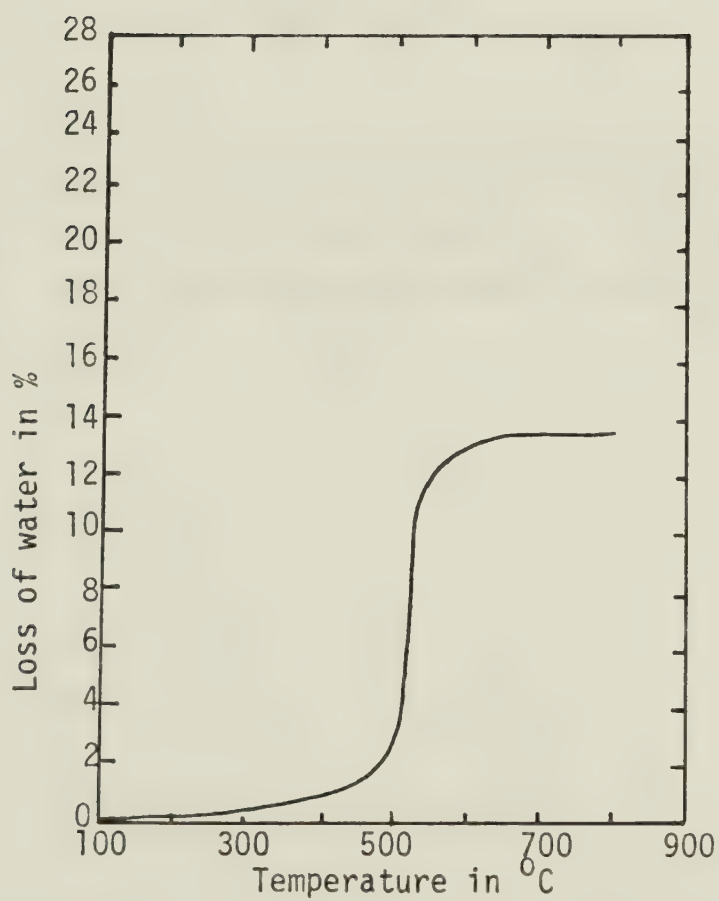


FIGURE 20. Dehydration curve for kaolinite, Ione, California.  
(From Ross and Kerr, 1931).



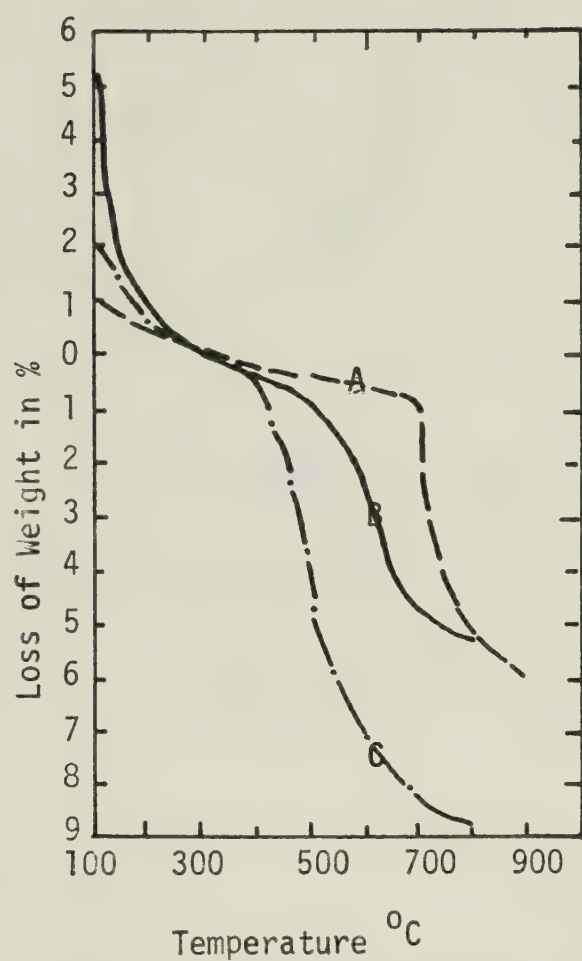


FIGURE 21. Dehydration curves, from Ross and Hendricks (1945).  
 (A) Hectorite, Hector, California; (B) Montmorillonite, Tatatilla, Mexico; (C) Montmorillonite, Pontotoc, Mississippi.





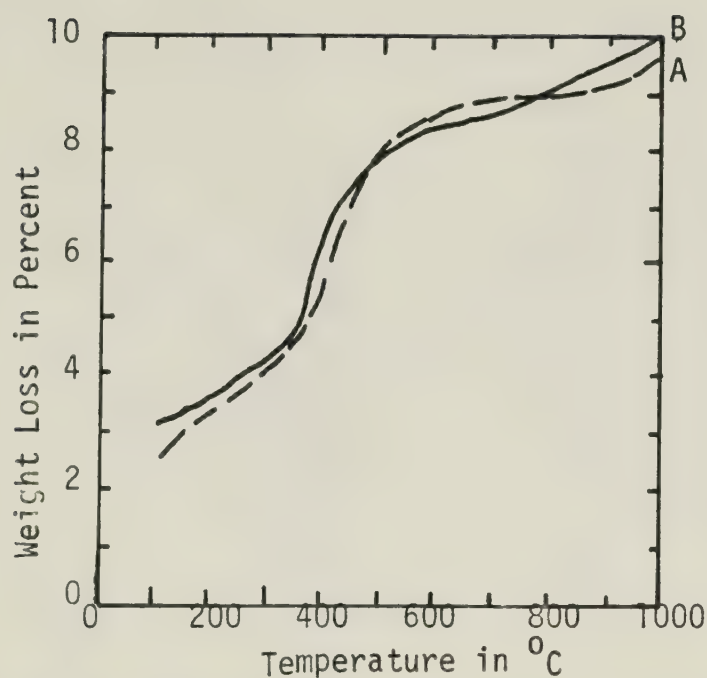


FIGURE 22. Dehydration curves, from Grim, Bray, and Bradley (1937).

- (A) Illite, Gilead, Calhoun County, Illinois;  
 (B) Illite, Fithian, Vermillion County, Illinois.

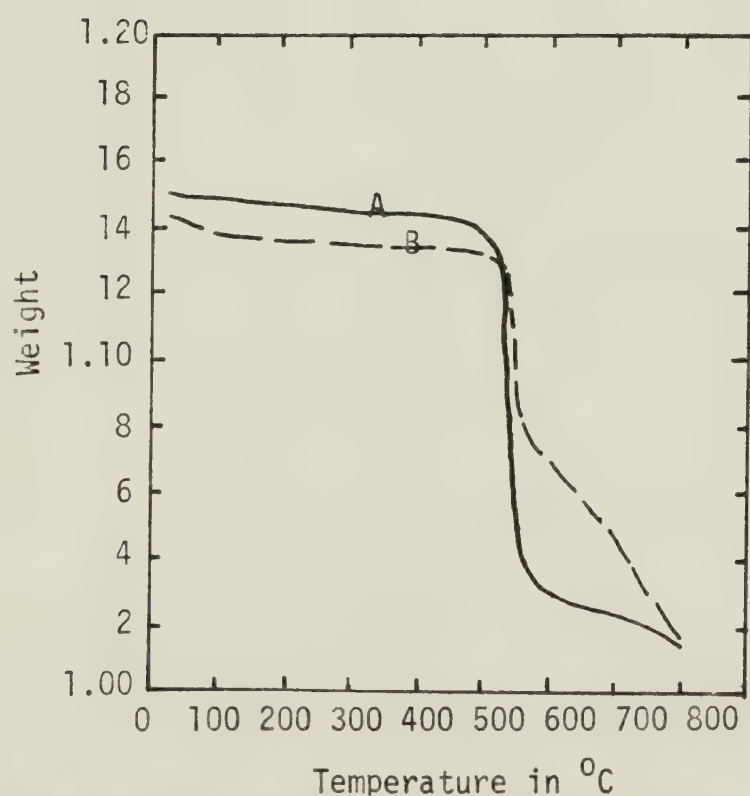


FIGURE 23. Dehydration curves, after Nutting (1943). The weight at 800 °C is taken as the base weight in plotting the curves.  
 (A) Penninite, Paradise Range, Nevada;  
 (B) Chlorite, Danville, Virginia.



TABLE 15.  
Core Laboratory Analysis Data and Observed Porosity

Serial No.	Well Name	Location	Sample No.	Plug Type†	Description of Sandstone Core Sample†	Max. Permeability (md)†	Core Analysis Porosity (%)†	Observed Porosity (%)	Pore Volume Saturation†	
									Oil	Water
1.1	IOE CDN-SUP PEMBINA	10-27-47-4W5	At 3212.8 ft	Full diameter	1,6,10,19,G	573.	19.4	0		
1.2			At 3215.4 ft (A)							
1.3			At 3215.4 ft (B)							
1.4			At 3219.1 ft							
1.5			At 3233.8 ft							
2.6	IOE CDN-SUP PEMBINA	10-34-47-4W5	At 2186.3 ft (A)	Cube (any size)	1,6,9,19	0.8	12.7	0.5	0.0	67.8
2.7			At 2186.3 ft (B)							
2.8			40							
2.9			41							
2.10			50							
2.11	IOE CDN-SUP PEMBINA	10-35-47-4W5	52	"	1,6,10,19,limy	193.0	19.7	11.7	13.7	46.3
2.12			53							
3.13			6							
3.14			18							
3.15			20							
3.16	IOE CDN-SUP PEMBINA		23	"	1,6,9,19,limy	0.3	10.8	2.5	0.0	64.0
3.17			25							
3.18			39							
3.19			46							

.../Continued



TABLE 15. - Continued

Serial No.	Well Name	Location	Sample No.	Plug Type†	Description of Sandstone Core Sample†	Max. Permeability (md)†	Core Analysis Porosity (%)†	Observed Pore Section Porosity (%)	Pore Volume Saturation†	
									Oil	Water
4.20	IOE CDN-SUP PEMBINA	4-36-47 -4W5	12	Full diameter	1,6,10,19,G,S	31.0	16.8	5.8	12.0	48.2
4.21			16	"	1,6,10,19,G,S	117.0	17.5	9.3	13.5	45.1
4.22			18	"	1,6,9,10,19,D,F,S,G	75.0	16.9	7.3	13.8	36.6
4.23			19	"	1,6,10,19,G,S	164.0	19.2	6.5	14.7	45.3
4.24			23	"	1,6,10,19,G,S	80.0	17.8	3.3	12.4	40.0
4.25			25	"	1,6,9,19,D,F,G,S	4.5	15.0	3.8	5.2	58.0
4.26			35	"	1,6,9,19,G,S	29.0	15.5	0.8	10.9	39.8
4.27			37	"	1,6,9,19,G,S	26.0	14.8	2.2	7.7	42.0
5.28	IOE CDN-SUP PEMBINA	4-2-48 -4W5	12	Cube (any size)	1,6,9,19,S	<0.1	9.4	2.7	5.3	50.0
5.29			13	"	1,6,10,19,S	123.0	19.6	6.7	10.2	50.5
5.30			16	"	1,6,10	313.0	22.4	10.3	19.7	48.2
5.31			23	"	1,6,10	234.0	16.5	6.2	9.1	46.1
5.32			23	"	1,6,10	234.0	16.5	5.0	9.1	46.1
5.33			33	"	1,6,10,19,S	249.0	20.3	4.5	7.9	51.9
5.34			33	"	1,6,10,19,S	249.0	20.3	1.7	7.9	51.9
5.35			42	"	1,6,10,19,S	10.0	17.9	2.5	8.4	61.0
5.36			46	"	1,6,10,19,S	26.0	20.2	5.5	8.0	62.4
5.37			47	"	1,6,10,19,S	51.0	19.9	3.8	10.1	57.4
5.38			51	"	1,6,10,19,S	37.0	20.4	4.7	10.9	54.3

.../Continued





TABLE 15. - Continued

NB:	A = Coarse part of slide
	B = Fine part of slide
	+ = Data compiled from Core Laboratory Analysis Sheet
	For Description of Sandstone Core Samples Column only:-
	1 = Grey
	6 = Medium Cemented
	9 = Fine Grain Size (<0.25 mm diameter)
	10 = Medium Grain Size (0.25 mm to 0.50 mm diameter)
	19 = Massive Sand (no visible shale)
	D = Pyrobitumen
	F = Silt or Clay
	G = ?
	S = Oil Stains



Laboratory analysis porosity values were plotted against permeability values (Figure 24), and both regression equation and correlation coefficient ( $r$ ) were computed for the set of points. The computed regression equation of  $y = 0.013X + 15.33$  was used to fit a regression line to the points (Figure 24). The correlation coefficient  $r$  of  $+0.56$  shows a fairly strong linear relationship between the two variables. However, a  $y$ -intercept of 15.3 shows the need for an initial core analysis porosity of about 15.0 percent for any measurable permeability to be achieved. It is pertinent to recall that a  $y$ -intercept of 13.1 was computed for the core analysis porosity versus observed porosity plot. The facts that:

- a) at zero observed porosity, the average core analysis porosity is 13.0 percent and
- b) at 15.0 percent core analysis porosity, the permeability of the sample is zero, show that the core analysis porosity values include 13.0 to 15.0 percent of essentially ineffective porosity. A plot of observed porosity against permeability (Figure 25) shows a better linear relationship ( $r = +0.67$ ) for the two variables and a smaller  $y$ -intercept of 3.3. This indicates that 4 percent observed porosity is capable of generating some measurable permeability.

#### High Core Analysis Water Saturation

The saturation of a reservoir rock is equivalent to its pore content and is basically made up of water saturation ( $S_w$ ) and hydrocarbon saturation ( $S_h$ ) (Gürr, 1976).



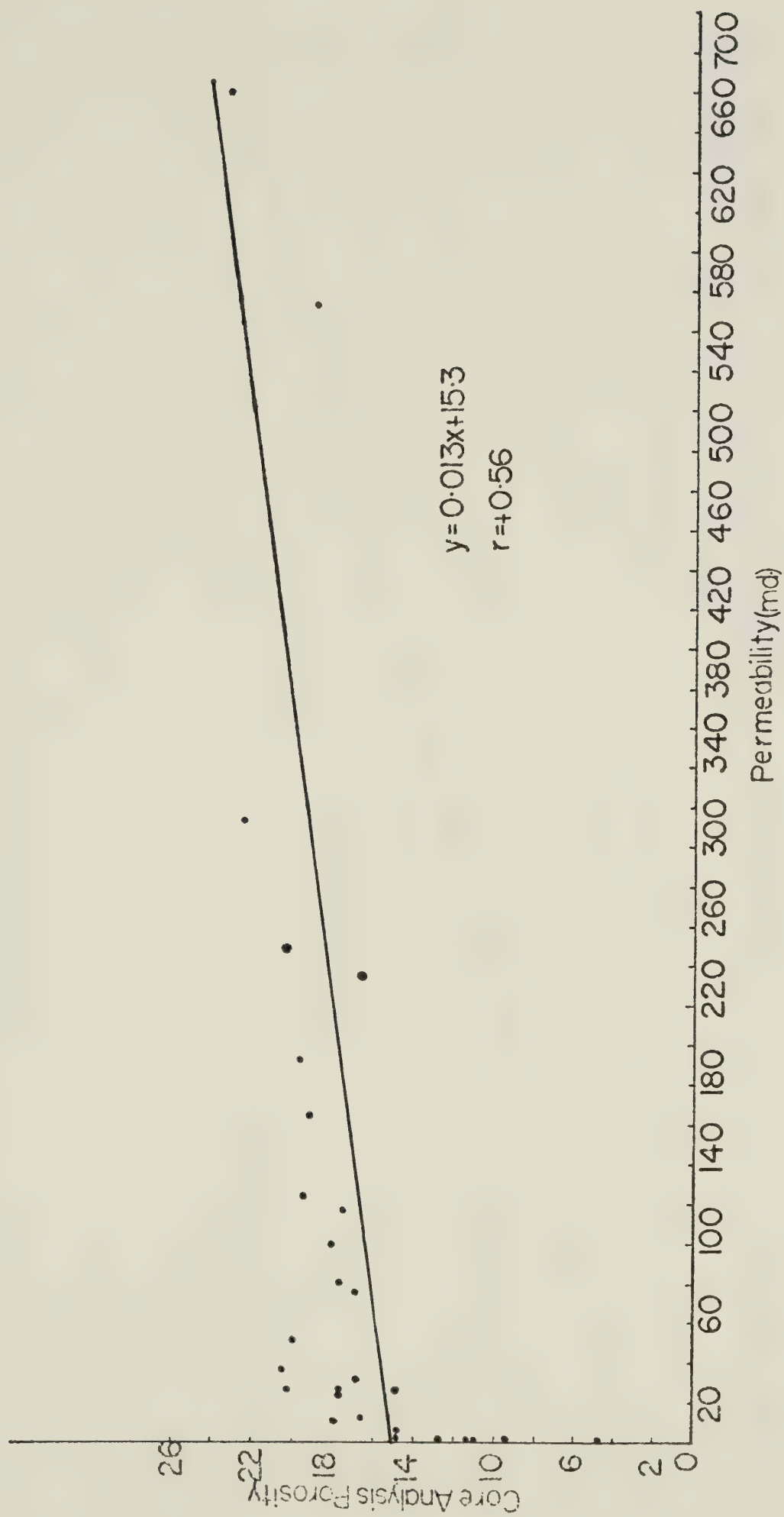


FIGURE 24. Core Laboratory Analysis Porosity vs. Permeability Plot.





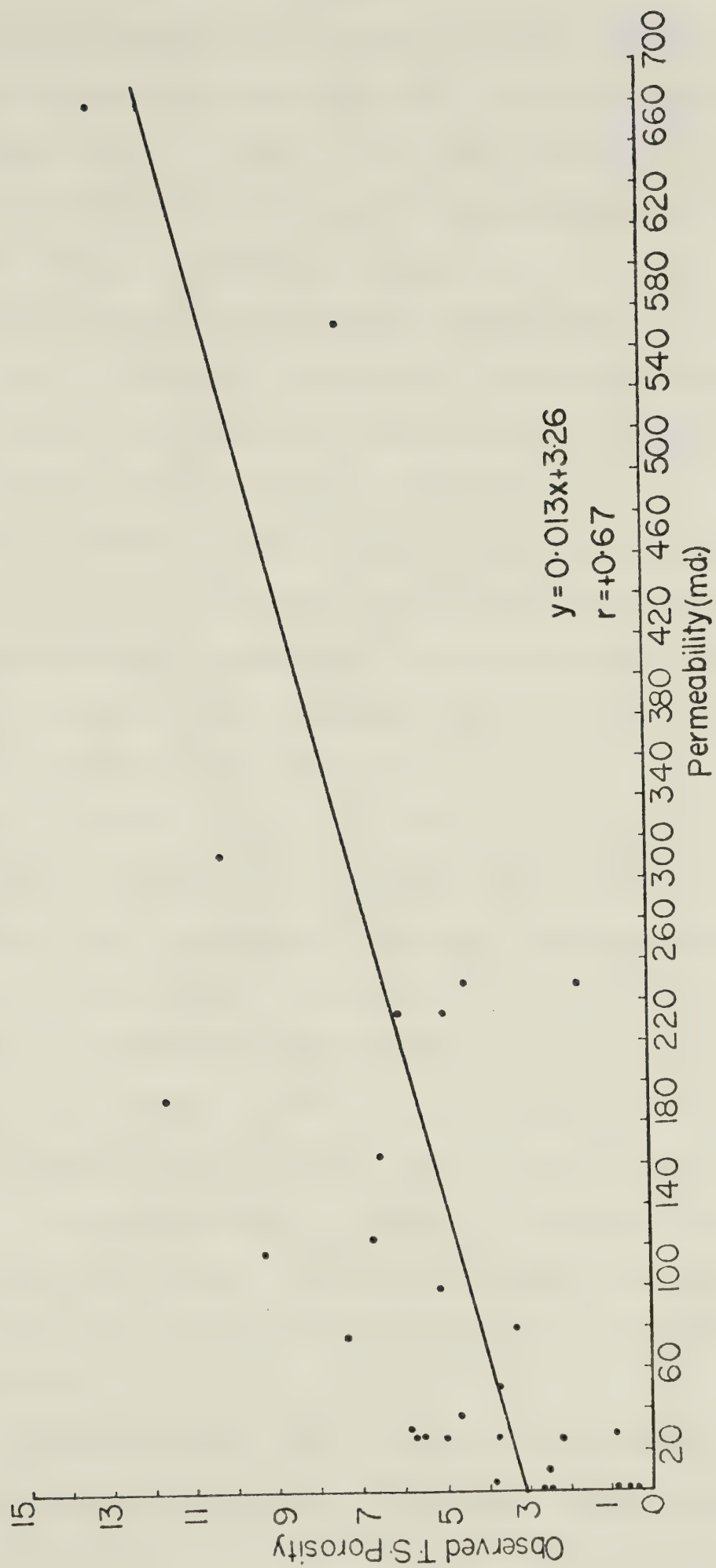


FIGURE 25. Observed thin section Porosity vs. Permeability plot.



The hydrocarbon saturation is made up of two components, oil saturation ( $S_o$ ) and gas saturation ( $S_g$ ) (Schlumberger Log Interpretation, Vol. 1, 1972). The water saturation ( $S_w$ ) is therefore the fraction of the pore volume occupied by formation water while hydrocarbon saturation ( $=1 - S_w$ ) is the fraction of the pore volume occupied by hydrocarbon. The determination of these two saturations is the main aim of both core analysis and borehole geophysical log interpretations. Decisions regarding the economic production of hydrocarbons from a reservoir largely depend on the reservoir rock saturation, and therefore it is important that accurate measurements be made and properly interpreted.

A survey of Core Laboratory procedures for water saturation determination shows that:

1. the water content of sidewall and conventional core samples (cubes or cylinders) is determined concurrently with the oil content by atmospheric distillation of the sample in a retort at a temperature of about  $1200^{\circ}\text{F}$  ( $650^{\circ}\text{C}$ );
2. the water distilled from the sample is collected in a calibrated receiving tube where its volume is measured;
3. a distinction is made between pore water and water of hydration or crystallization by a plot of the water recovered versus the elapsed time of retorting. The first plateau of this plot indicates the removal of the pore or uncombined water;
4. whole cores have their water content determined by vacuum distillation concurrent with the oil content deter-



mination at a maximum temperature of  $450^{\circ}\text{ F}$  ( $232^{\circ}\text{ C}$ );

5. a distinction between pore water and water of hydration or crystallization is not required in whole core water content determinations because the temperature is not high enough to free combined water;

6. the water content volume (determined from sidewall core, core samples or whole core) divided by the pore volume gives the water saturation in percent of pore space for the sample; and

7. there is no distinction between "free" and adsorbed (bound) water in the Core Laboratory report of analysis.

Consideration of the above conditions and methods of water saturation determination in the Core Laboratory, and characteristics of the authigenic clay show that the Core Laboratory water saturation values probably include, besides free pore water, adsorbed (bound) water and possibly interlayer and hydroxyl lattice water of the authigenic clay (i.e., total water). Boundwater, interlayer and OH lattice water should be regarded as part of the solid 'matrix' volume of the reservoir rock under subsurface conditions. The minute size of the authigenic clay crystals and the associated large inner surface area favor adsorption of a large amount of water; the larger the surface area the more the adsorbed connate water content of a reservoir rock. Numerous attempts by various investigators to estimate the thickness of adsorbed water with definite nonliquid characteristics have yielded no good agreement. Thickness





values of 7.5 Å (three molecular water layers) to several hundred angstroms have been reported (Grim, 1968). The inner surface area of a reservoir rock is therefore an important parameter when estimating its connate water content (Gürr, 1976). A plot of authigenic clay cement against core analysis water saturation (Figure 26) shows a linear trend. A computed regression equation of  $y = 0.13X + 0.05$  was used to fit a regression line to the points. The correlation coefficient of  $r = +0.49$  shows a good linear relationship between the two variables. The permeability/water saturation relationship (Figure 27) for the basal Belly River sandstone samples shows a negative correlation with a correlation coefficient ( $r$ ) of  $-0.40$ . Gürr (1976) made a similar observation and interpreted it to be due to connate water content of the reservoir. He stated that the smaller the permeability of a rock, the greater its connate water content. Wright et al. (1955) also demonstrated that poorly permeable rock bodies have high water saturations. A plot of permeability values against the authigenic clay cement (Figure 28) also shows a negative correlation with an  $r$  value of  $-0.55$ , indicating that the low permeability of the studied samples (which also corresponds to high connate water content) is also measurably due to authigenic clay. Wilson and Pittman (1977) stated that micropores occurring among clay particles are capable of holding irreducible water (water tightly held because of the physical attraction of the solid for the liquid), and that a reservoir con-



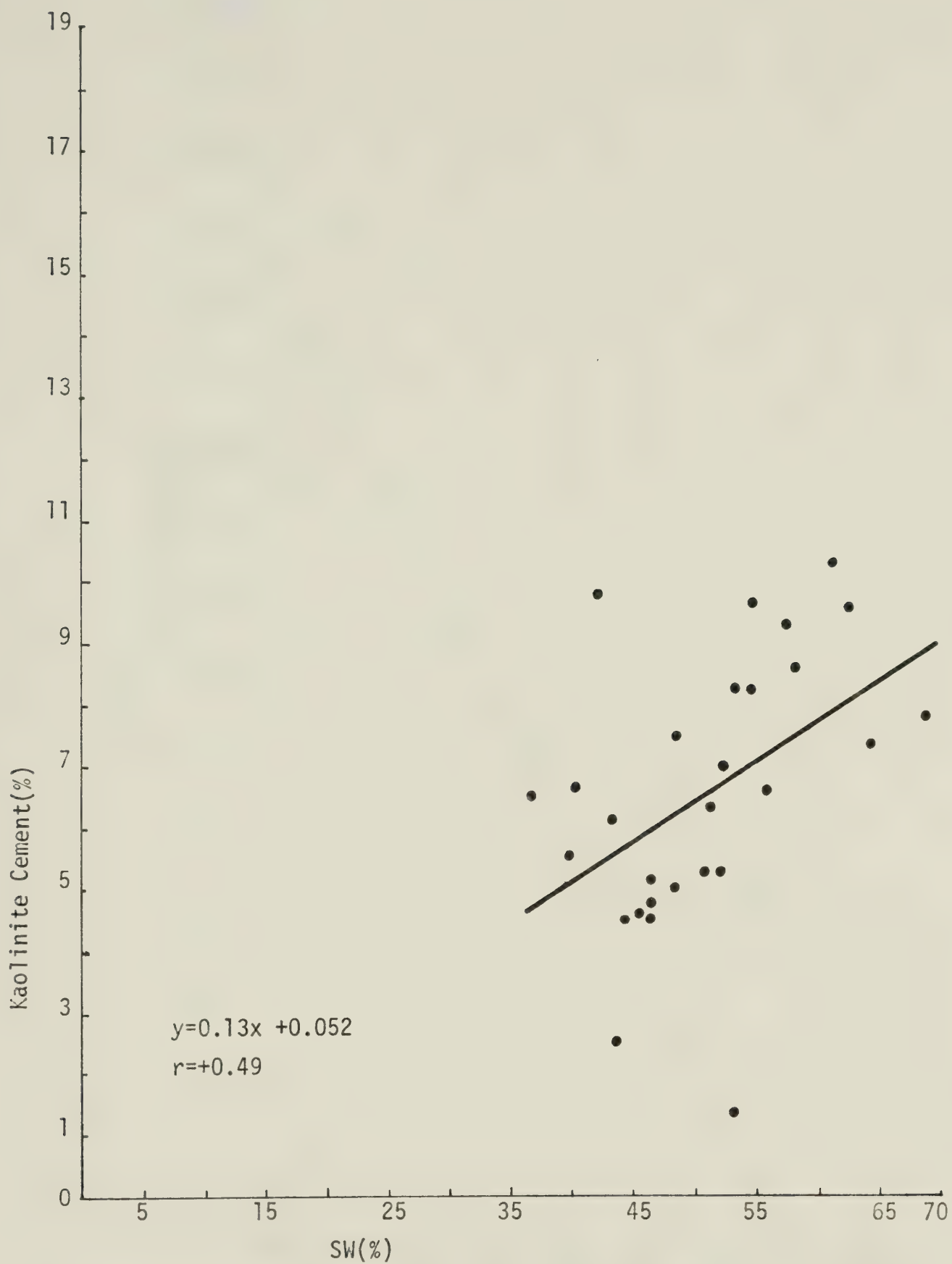


FIGURE 26. Kaolinite Cement vs. Core Analysis Water Saturation Plot.



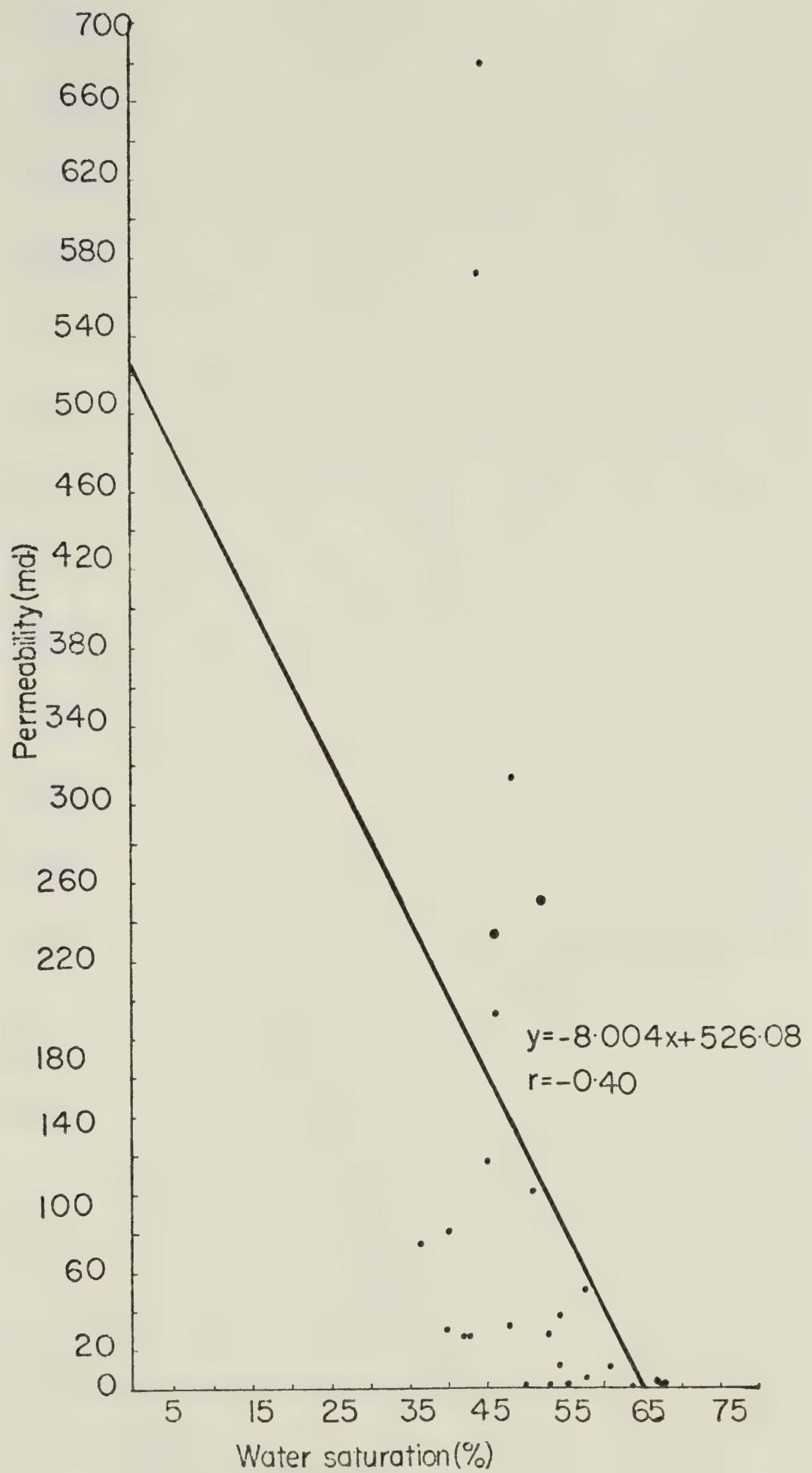


FIGURE 27. Permeability vs. Water saturation plot.





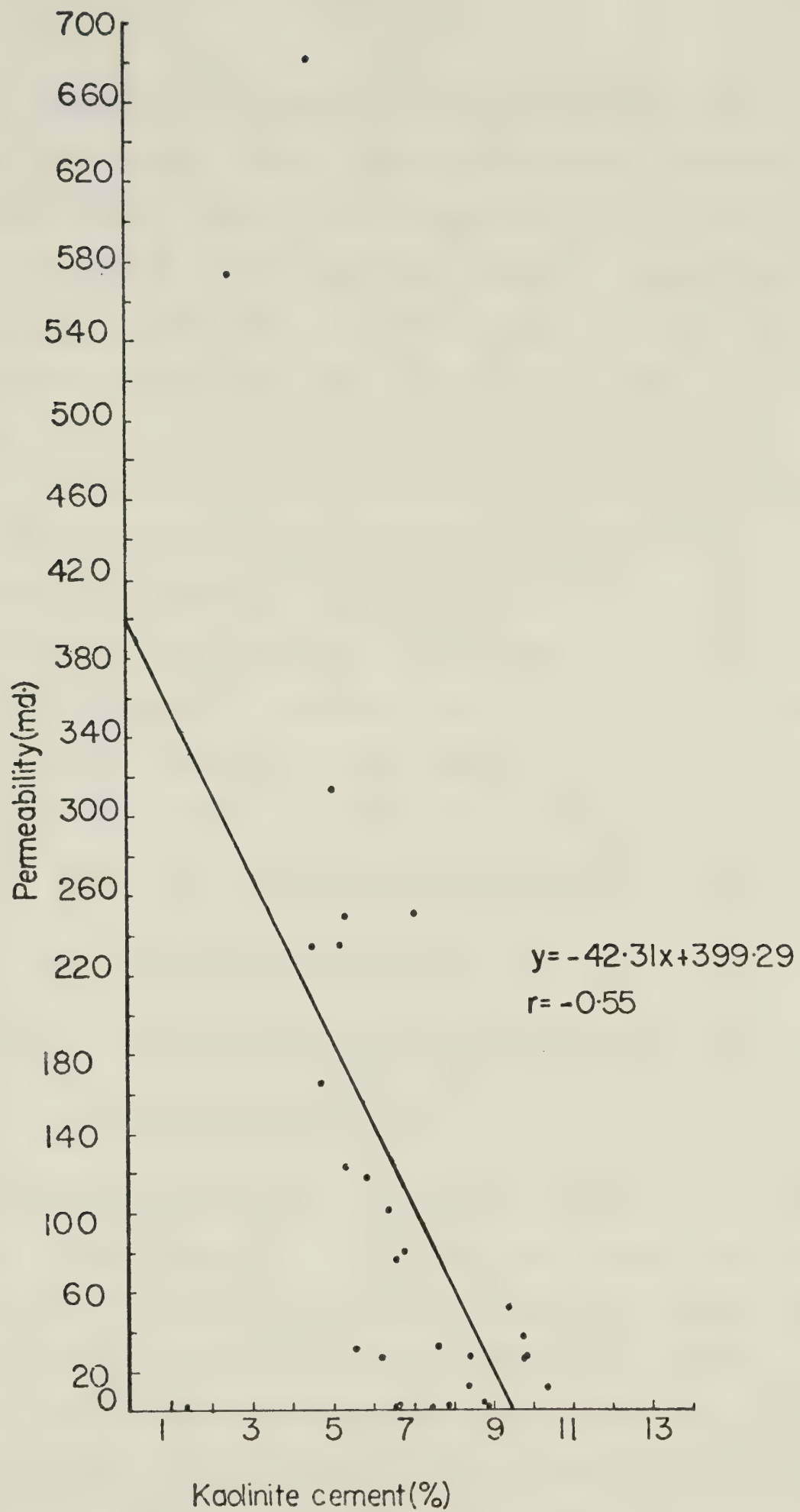


FIGURE 28. Permeability vs. Kaolinite cement plot.



taining abundant authigenic clays with associated micropores would be expected to have a long transitional oil-water or gas-water contact because of the adsorbed water associated with high surface area. They also commented that data from Gaida et al. (1973) show that low permeability and high surface area are associated with illite having lath-like projections.

Sah (1977) in his evaluation of parts of the shaly Colony Sand in Alberta observed that high boundwater saturation corresponds to poor permeability which is due to the presence of clay minerals. He recognizes two types of water - one of which is bonded to the shales and the other is in the pores. Based on this concept of two waters, he derived amongst others the following equations:

$$SWT = \frac{\text{Pore water volume} + \text{Boundwater volume}}{\text{Total Porosity}}$$

$$\begin{aligned} SW &= \frac{\text{Pore water volume}}{\text{Producibile Porosity}} \\ &= \frac{\text{Total water volume} - \text{Boundwater volume}}{\text{Producibile Porosity}} \end{aligned}$$

$$SBW = \frac{\text{Boundwater volume}}{\text{Total Porosity}}$$

where SWT (Total water saturation) is the fraction of total porosity filled with water, SW (Pore water saturation) is the fraction of producibile porosity filled with water and SBW (Boundwater saturation) is the fraction of total porosity filled with water bonded to the shale (Sah, 1977). Considering how water saturation is determined in Core Laboratories, it is obvious that both forms of Sah's water



and possibly the OH group water of the clays may be included in the core analysis water saturation values, with no corrections for boundwater and OH group water, especially when the presence of authigenic clay is not recognized. An examination of Core Laboratory data sheets (Table 15) also reveals that

1. some of the porosity and water saturation values were determined from full diameter cores;
2. most of the samples analyzed by Core Laboratories and examined in this present study were described as massive sand, which according to Core Laboratory terminology means no visible shale. The logical corollary to these two remarks is that no corrections were made for the presence of authigenic clay in the porosity and water saturation determinations despite its obvious presence and effect. Since the boundwater, interlayer water and lattice OH group water of the clays are part of the solid "matrix" of the reservoir rock under subsurface conditions, but included in the Core Laboratory water saturation values, they are responsible for the high Core Laboratory water saturation values and the low water recovery during production from the basal Belly River sandstone.





## CHAPTER IX. SUMMARY AND CONCLUSIONS

A detailed petrographic study of samples of the basal Belly River sandstone in the Keystone area of the Pembina field shows that:

1. This rock is a fine- to medium grained, very well to well sorted, mature lithic arenite.
2. Diagenesis has taken place mainly by mechanical compaction, carbonate, silica and authigenic clay cementation, and carbonate replacement.
3. The authigenic clay suite consisting of kaolinite, mixed-layer montmorillonite/illite and chlorite is characterized by minute crystal size and submicroscopic porosity.
4. The presence of significant quantities of authigenic clays results in large inner surface area and large quantities of adsorbed water in the reservoir.
5. The adsorbed (connate) water, interlayer water and possibly OH lattice water of the clays are liberated along with free pore water at Core Laboratory analysis temperatures.
6. These liberated water volumes measurably affect both core analysis porosity values and water saturations, and are responsible for high core analysis porosity and water saturation values, but low production water.
7. The Core Laboratory analysis porosity methods are better estimators of total porosity than is the thin section point-counting procedure, but includes 13 to 15 percent



"ineffective" or unusable porosity for an oil reservoir.

8. Core Laboratory permeability values and observed thin section porosity values are more reliable indicators of "effective" or usable porosity.

9. A core analysis porosity value of 13 to 15 percent or an observed thin section porosity value of 4 percent is necessary to generate any measurable permeability and permit oil production from this reservoir. But it is possible to have some commercial gas production at core analysis and observed thin section porosities of less than 13 and 4 percent respectively.

10. For thin sections to have maximum usefulness in the estimation of grain, cement and pore volumes of the basal Belly River sandstone they must be impregnated with a colored medium in order to maximize identification of microscopic pores and thereby minimize edge error effects.

11. Decisions on economic production of hydrocarbons from the basal Belly River sandstone should not be based solely on electrical log responses and Core Laboratory analysis, but should also consider evidence obtained from petrographic study. The same recommendation probably applies to all "shaly" sandstone reservoirs.



## BIBLIOGRAPHY

- Adams, J., 1977, Sieve size statistics from grain measurement: J. Geology, V. 85, p. 209-227.
- Allan, J. A., 1919, Sections along North Saskatchewan River and Red Deer and South Saskatchewan Rivers, between the third and fifth meridians: Geol. Surv. Canada, Summ. Rept., 1917, pt. C, p. 9-13.
- Bates, T. F., 1955, Electron microscopy as a method of identifying clays: Clays and Clay Technology, Calif. Div. Mines Bull. 169, p. 130-150.
- Blatt, H., Middleton, G. and Murray, R., 1972, Origin of Sedimentary Rocks: Englewood Cliffs, New Jersey, Prentice-Hall Inc., 634 p.
- Borst, R. L. and Keller, W. D., 1969, Scanning electron micrographs of A.P.I. reference clay minerals and other selected samples: Proc. Intern. Clay Conf., V. 1, p. 871-901.
- Bradley, W. F. and Grim, R. E., 1961, Mica clay minerals, in Brown, G. (ed.), X-ray identification and crystal structures of clay minerals: Mineralogical Soc. London, p. 208-241.
- Brindley, G. W., 1961, Kaolin, serpentine, and kindred minerals, in Brown, G. (ed.), X-ray identification and crystal structures of clay minerals: Mineralogical Soc. London, p. 51-131.
- \_\_\_\_\_, 1961a, Chlorite minerals, in Brown, G. (ed.), X-ray identification and crystal structures of clay minerals: Mineralogical Soc. London, p. 242-296.
- Carrigy, M. A. and Mellon, G. B., 1964, Authigenic clay mineral cements in Cretaceous and Tertiary sandstones of Alberta: J. Sed. Petrology, V. 34, p. 461-472.
- Carroll, D., 1974, Clay minerals: A guide to their X-ray identification: Geol. Soc. America, Sp. Paper 126, 80 p.
- Crook, K. A. W., 1960, Classification of arenites: Am. J. Sci., V. 258, p. 419-428.
- Dawson, G. M., 1883, Preliminary report on the geology of the Bow and Belly River region, North-west Territory, with special reference to the coal deposits:





Geol. and Nat. History Survey and Mus. Canada,  
Rept. Progress 1880-81-82, pt. B, p. 1-23.

Dictionary of Geological Terms, 1976: Am. Geol. Inst.,  
Garden City, New York, Anchor Press/Doubleday,  
p. 90.

Dowling, D. B., 1917, The Southern plains of Alberta: Geol.  
Surv. Canada, Mem. 93, 200 p.

Folk, R. L., 1955, Student operator error in determination  
of roundness, sphericity and grain size: J. Sed.  
Petrology, V. 25, p. 297-301.

\_\_\_\_\_, 1974, Petrology of Sedimentary Rocks: Austin,  
Texas, Hemphills Pub., 182 p.

Füchtbauer, H., 1967, Influence of different types of  
diagenesis on sandstone porosity: 7th World  
Petroleum Congress Proc., p. 353-369.

Fundamentals of Core Analysis, Mod II: Dallas, Texas, Core  
Laboratories Inc.

Gaida, K. H., Ruhl, W. and Zimmerle, W., 1973, Raster-  
elektronenmikroskopische Untersuchungen des  
Porenraumes von Sandsteinen: Erdoel Erdgas  
Zeitschrift, V. 89, p. 336-343.

Gilbert, C. M., 1954, Sedimentary Rocks, in Williams, H.,  
Turner, F. J. and Gilbert, C. M., Petrography:  
San Francisco, Calif., W. H. Freeman and Co.,  
p. 251-384.

Grim, R. E., Bray, R. H. and Bradley, W. F., 1937, The mica  
in argillaceous sediments: Am. Min., V. 22,  
p. 813-829.

\_\_\_\_\_, 1968, Clay Mineralogy: New York, McGraw-Hill  
Book Co., 596 p.

Gürr, A. M., 1976, Petroleum Engineering: New York-Toronto,  
John Wiley and Sons, 208 p.

Halley, R. B., 1978, Estimating pore and cement volumes in  
thin section: J. Sed. Petrology, V. 48, no. 2,  
p. 643-650.

Hildenbrand, F. A., 1960, Belly River Group, in Lexicon of  
Geological Names in the Western Canada Sedimentary  
Basin and Arctic Archipelago: Alberta Soc.  
Petroleum Geologists, p. 31-32.

Kahn, J. S., 1956, The analysis and distribution of the



properties of packing in sand-size sediments: J. Geology, V. 64, p. 385-395.

- Khamesra, D. S., 1963, Basal Belly River sandstone (Upper Cretaceous), Pembina Field, Alberta, Canada: M.Sc. thesis, Dept. of Geology, Univ. of Alberta.
- Krumbein, W. C., 1942, Physical and chemical changes in sediments after deposition: J. Sed. Petrology, V. 12, no. 3, p. 111-117.
- Lerbekmo, J. F., 1961, Porosity reduction in Cretaceous sandstones of Alberta: J. Alberta Soc. Petroleum Geologists, V. 9, no. 6, p. 192-199.
- \_\_\_\_\_, 1961a, Stratigraphic relationship between the Milk River Formation of the southern plains and the Belly River Formation of the southern foothills of Alberta, J. Alberta Soc. Petroleum Geologists, V. 9, no. 9, p. 273-276.
- \_\_\_\_\_, 1963, Petrology of the Belly River Formation, southern Alberta foothills: Sedimentology, V. 2, no. 1, p. 54-86.
- Le Ribault, L., 1975, L'exoscopie méthode et applications: Paris, Compagnie Française Des Pétroles, p. 164-165.
- Levorsen, A. I., 1967, Geology of Petroleum: San Francisco, Calif., W. H. Freeman and Co., 724 p.
- McLean, J. R., 1971, Stratigraphy of the Upper Cretaceous Judith River Formation in the Canadian Great Plains: Sask. Res. Coun., Geol. Div., Rept. 11, 96 p.
- Molloy, M. W. and Kerr, P. F., 1961, Diffractometer patterns of A.P.I. reference clay minerals: Am. Min., V. 46, p. 583-605.
- Nutting, P. G., 1943, Some standard thermal dehydration curves of minerals: U.S. Geol. Surv. Prof. Paper 197E, p. 197-216.
- Page, H. G., 1955, Phi-millimeter conversion table: J. Sed. Petrology, V. 25, no. 4, p. 285-292.
- Powers, M. C., 1953, A new roundness scale for sedimentary particles: J. Sed. Petrology, V. 23, no. 2, p. 117-119.
- Richardson, H. M., 1961, Phase changes which occur on heating kaolin clays, in Brown, G. (ed.), X-ray identification and crystal structures of clay



- minerals: Mineralogical Soc. London, p. 132-142.
- Ross, C. S. and Kerr, P. F., 1931, The Kaolin Minerals:  
U.S. Geol. Surv., Prof. Paper 165E, p. 151-175.
- 
- \_\_\_\_\_ and Hendricks, S. B., 1945, Minerals of the  
Montmorillonite Group: U.S. Geol. Surv., Prof.  
Paper 205B, p. 23-80.
- Russell, L. S. and Landes, R. W., 1940, Geology of the  
Southern Alberta Plains: Geol. Surv. Canada, Mem.  
221, 223 p.
- Sah, R. C., 1977, Shaly sand evaluation with total water:  
Trans. CWLS Sixth formation evaluation symposium,  
pt. 0, p. 1-7.
- Schedule of Wells Drilled for Oil and Gas, Province of  
Alberta, 1965: Calgary, Alberta, Oil and Gas  
Conservation Board, p. 154-155.
- Schedule of Wells Drilled for Oil and Gas, Province of  
Alberta, 1966: Calgary, Alberta, Oil and Gas  
Conservation Board, p. 124.
- Schlumberger Log Interpretation, V. 1, 1972: New York,  
Schlumberger Ltd., 113 p.
- Shaw, E. W. and Harding, S. R. L., 1949, Lea Park and Belly  
River Formations of east-central Alberta: Am.  
Assoc. Petroleum Geologists Bull., V. 33, no. 4,  
p. 487-499.
- Slipper, S. E. and Hunter, H. M., 1931, Stratigraphy of  
Foremost, Pakowki and Milk River Formations of  
southern plains of Alberta: Am. Assoc. Petroleum  
Geologists Bull., V. 15, no. 10, p. 1181-1196.
- Spiel, S., Berkelheimer, L. H., Pask, J. A. and Davies, B.,  
1945, Differential thermal analysis - its appli-  
cation to clays and other aluminous minerals:  
U.S. Bur. Mines, Tech. Paper 664.
- Taylor, J. M., 1950, Pore-space reduction in sandstones:  
Am. Assoc. Petroleum Geologists Bull., V. 34,  
no. 4, p. 701-716.
- Thiel, G. A., 1940, The relative resistance to abrasion of  
mineral grains of sand size: J. Sed. Petrology,  
V. 10, no. 3, p. 103-124.
- Travis, R. B., 1955, Classification of rocks: Quart. Colo.  
Sch. Mines, V. 50, no. 1, p. 13-25.





- Trollope, F. H., 1976, Personal Communication.
- Van Houten, F. B., 1968, Iron oxide in Red Beds: Geol. Soc. America Bull., V. 79, p. 399-416.
- Walker, T. R., 1967, Formation of red Beds in ancient and modern Deserts: Geol. Soc. America Bull., V. 78, p. 353-368.
- Williams, M. Y. and Dyer, W. S., 1930, Geology of southern Alberta and southwestern Saskatchewan: Geol. Surv. Canada, Mem. 163, 160 p.
- Wilson, M. D. and Pittman, E. D., 1977, Authigenic clays in sandstones: recognition and influence on reservoir properties and paleoenvironmental analysis: J. Sed. Petrology, V. 47, no. 1, p. 3-31.
- Wright, H. T. and Woody, H. D., 1955, Formation evaluation: AIME Symposium on Formation evaluation.

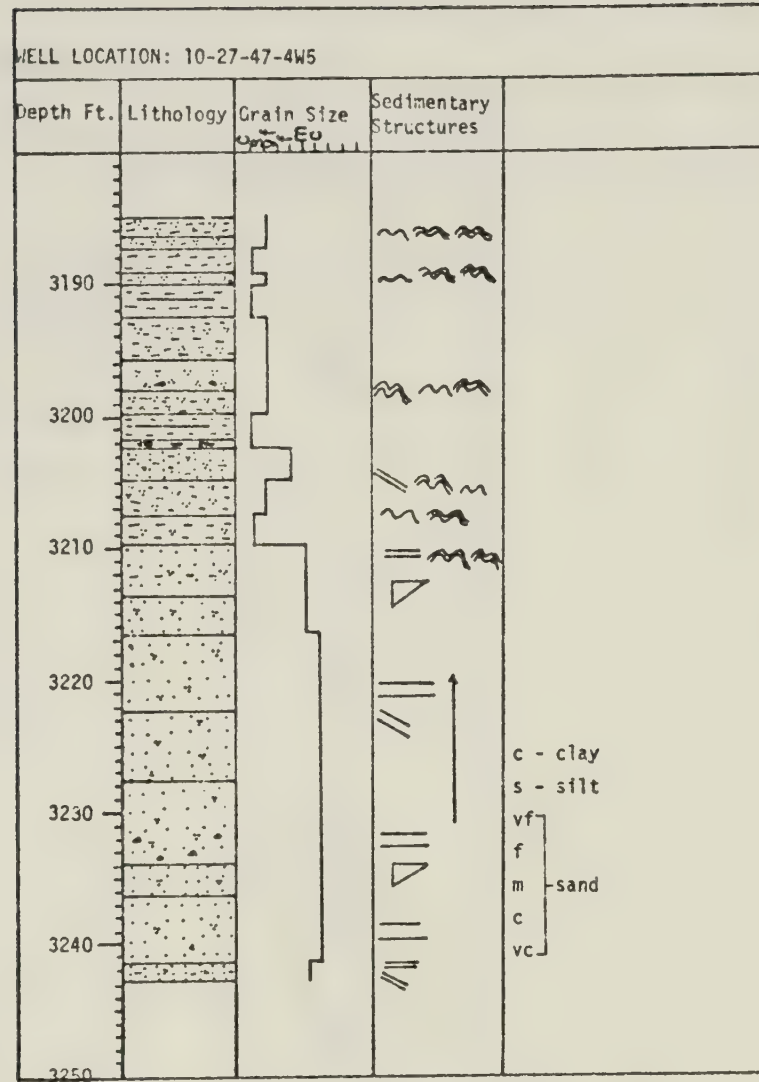




APPENDIX A

Megascopic Descriptions of Basal Belly River Core



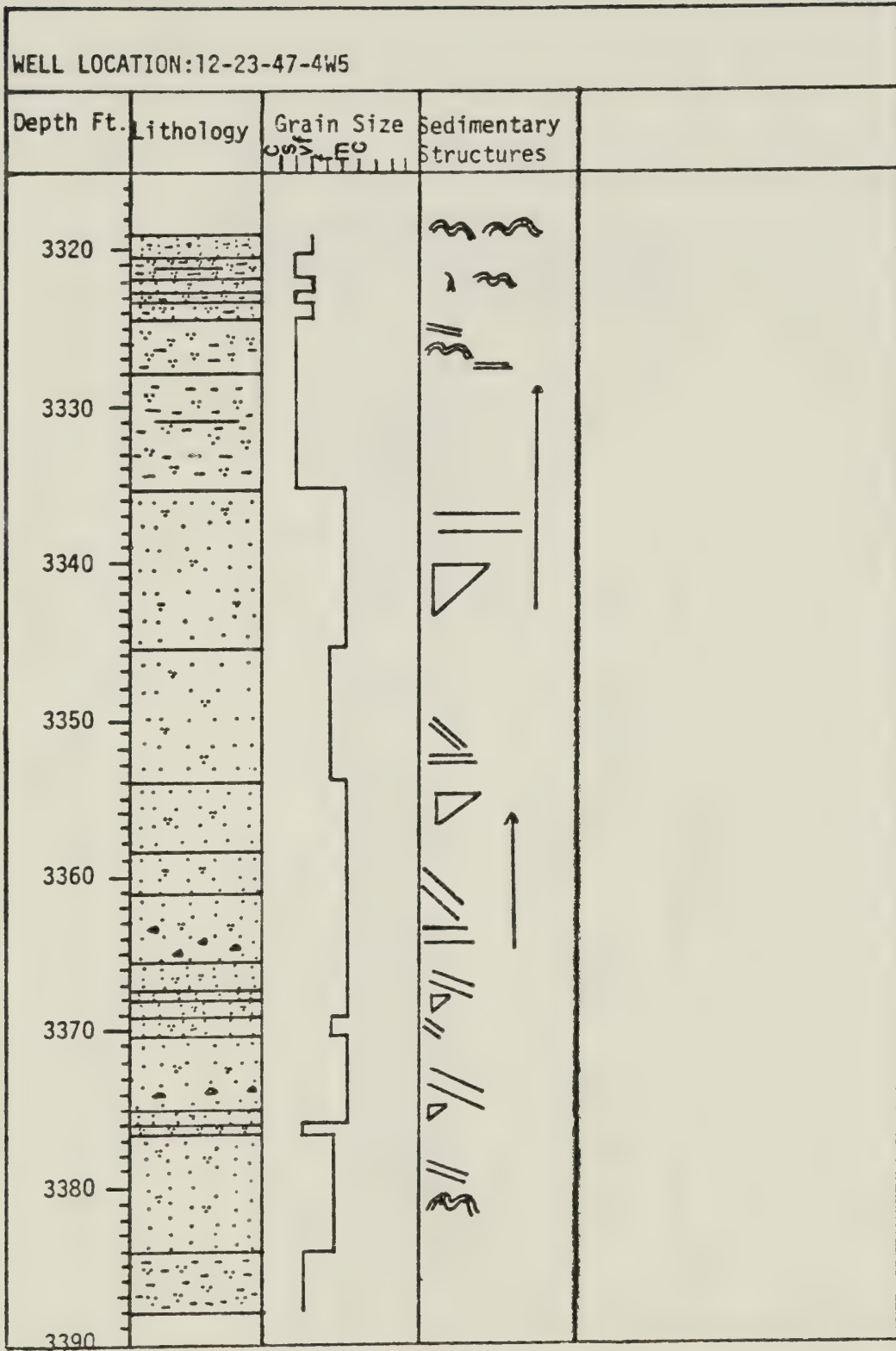


LEGEND:

- Sandstone
- Shaly Sandstone
- Shale
- Sandy Shale
- Siltstone
- Mudstone
- Coal
- Bentonitic Bed
- Pebbly

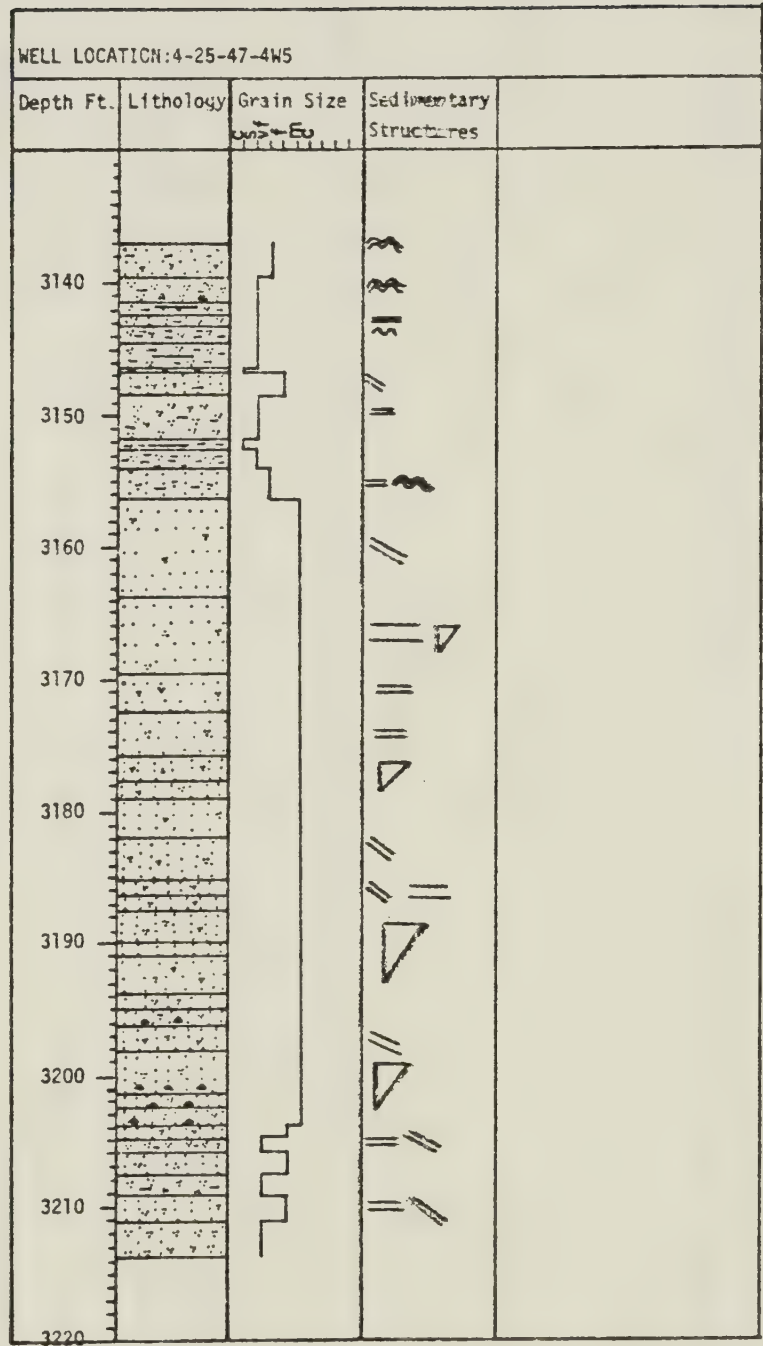
- Horizontal Bedding
- Thick Bedding
- Cross Stratification
- Parallel Lamination
- Cross Lamination
- Irregular Lamination
- Slump Structure
- Bioturbation (Churning)
- Rootlets
- Fining Upward
- Coarsening Upward



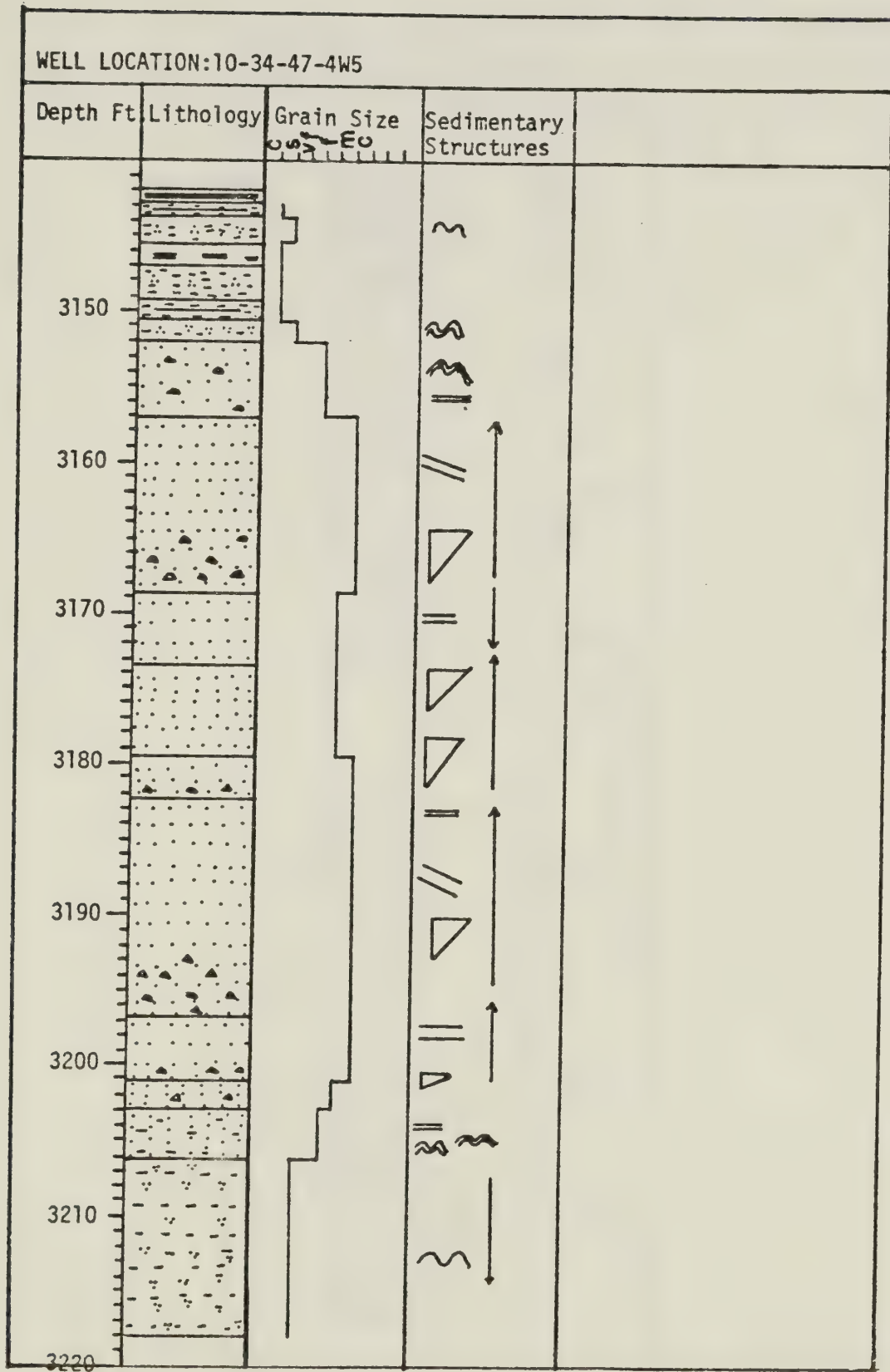




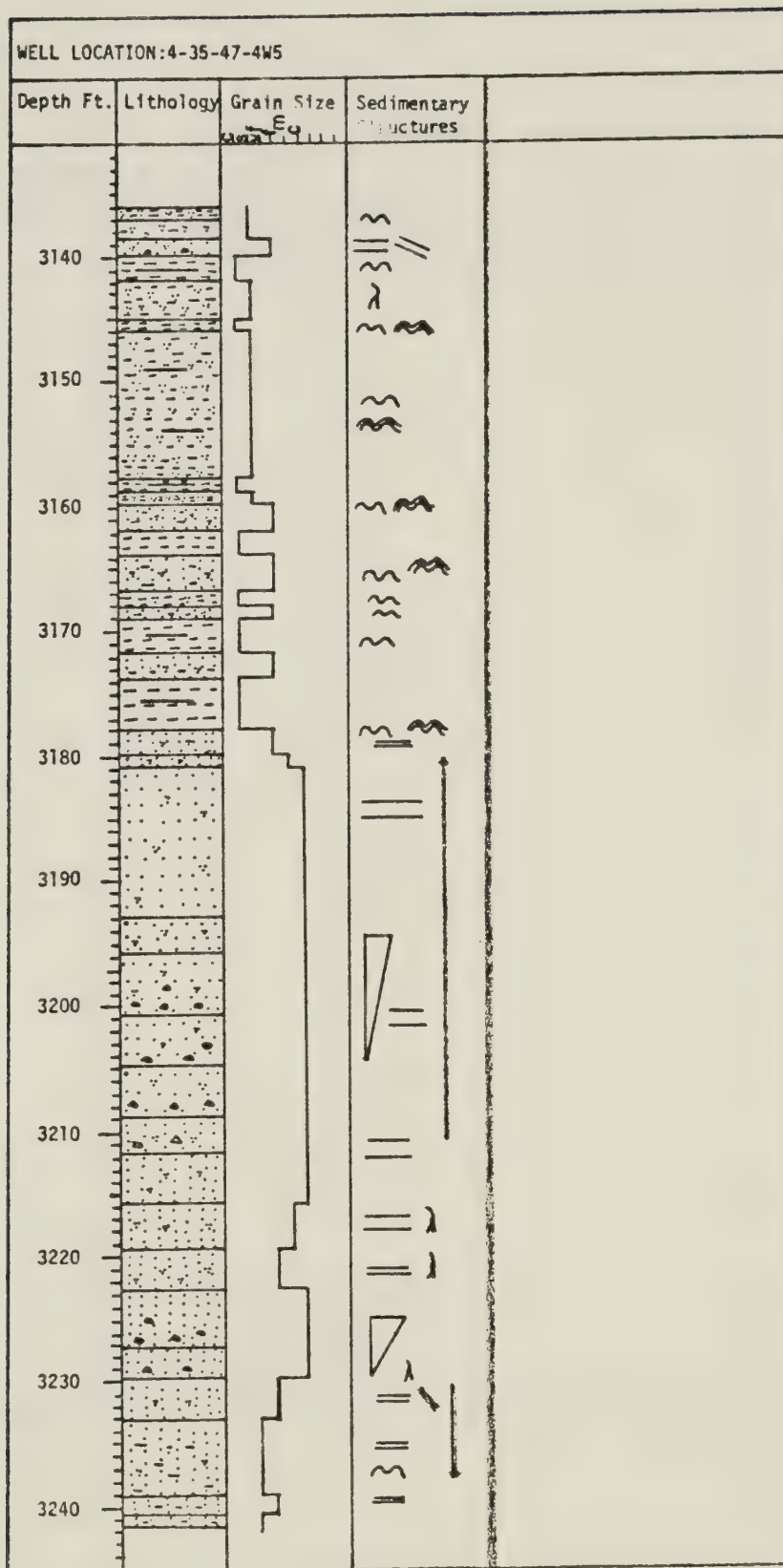




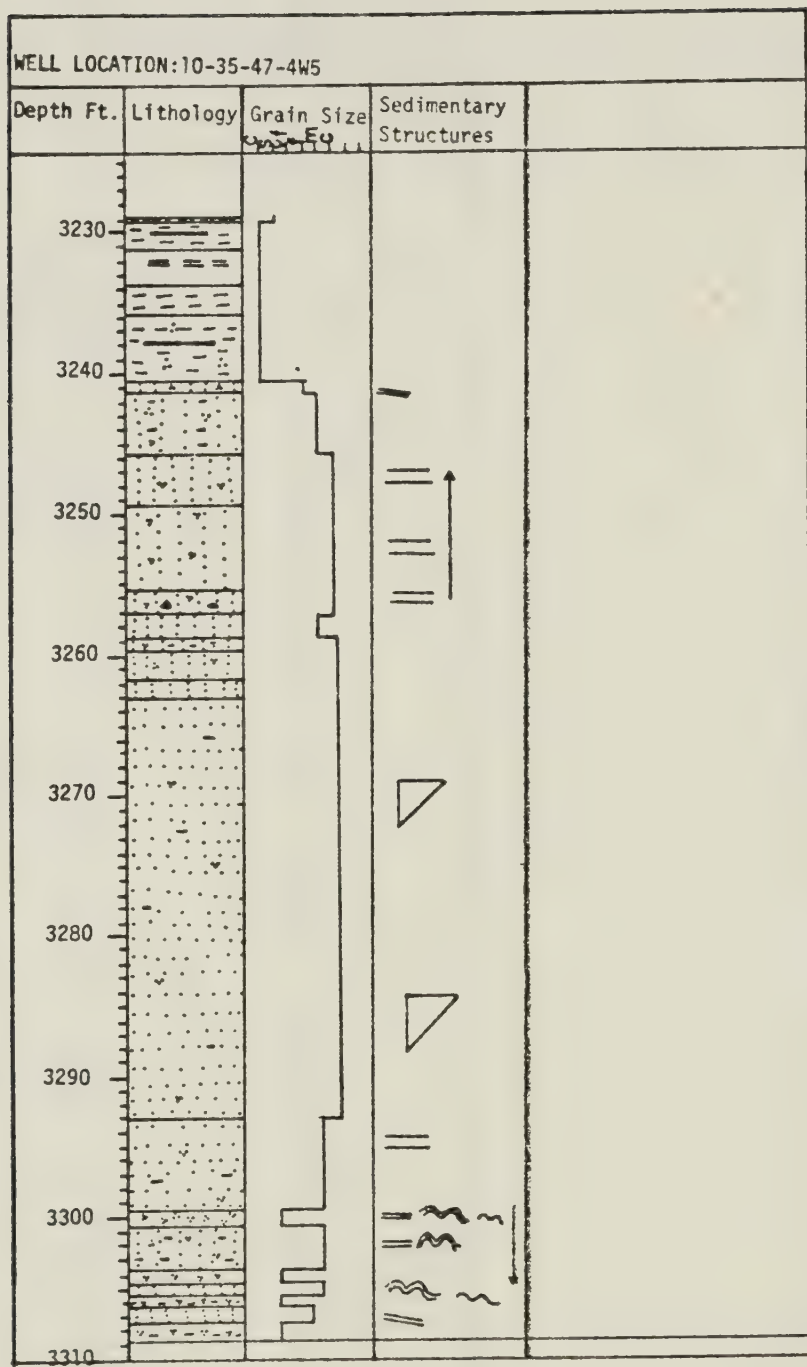






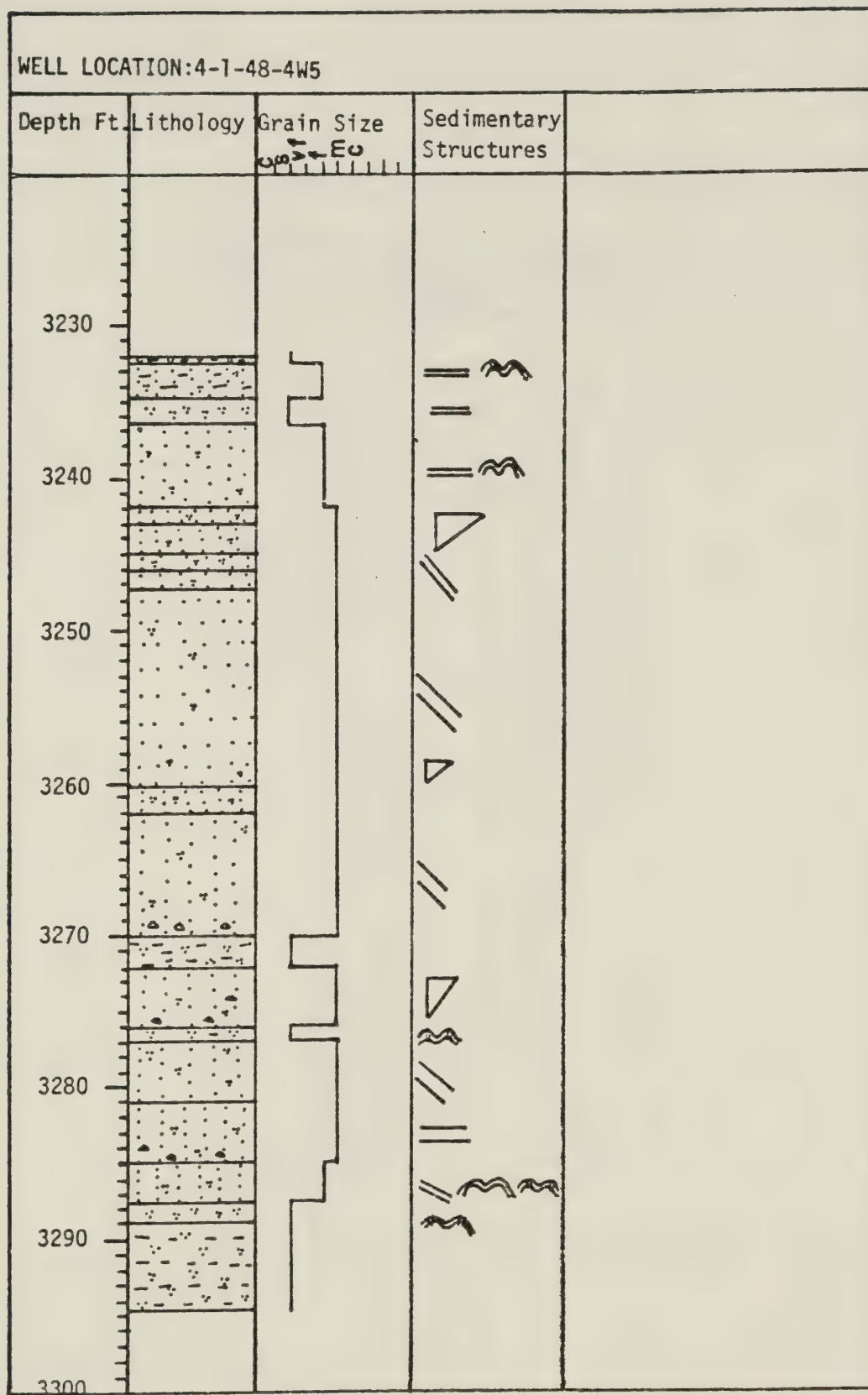




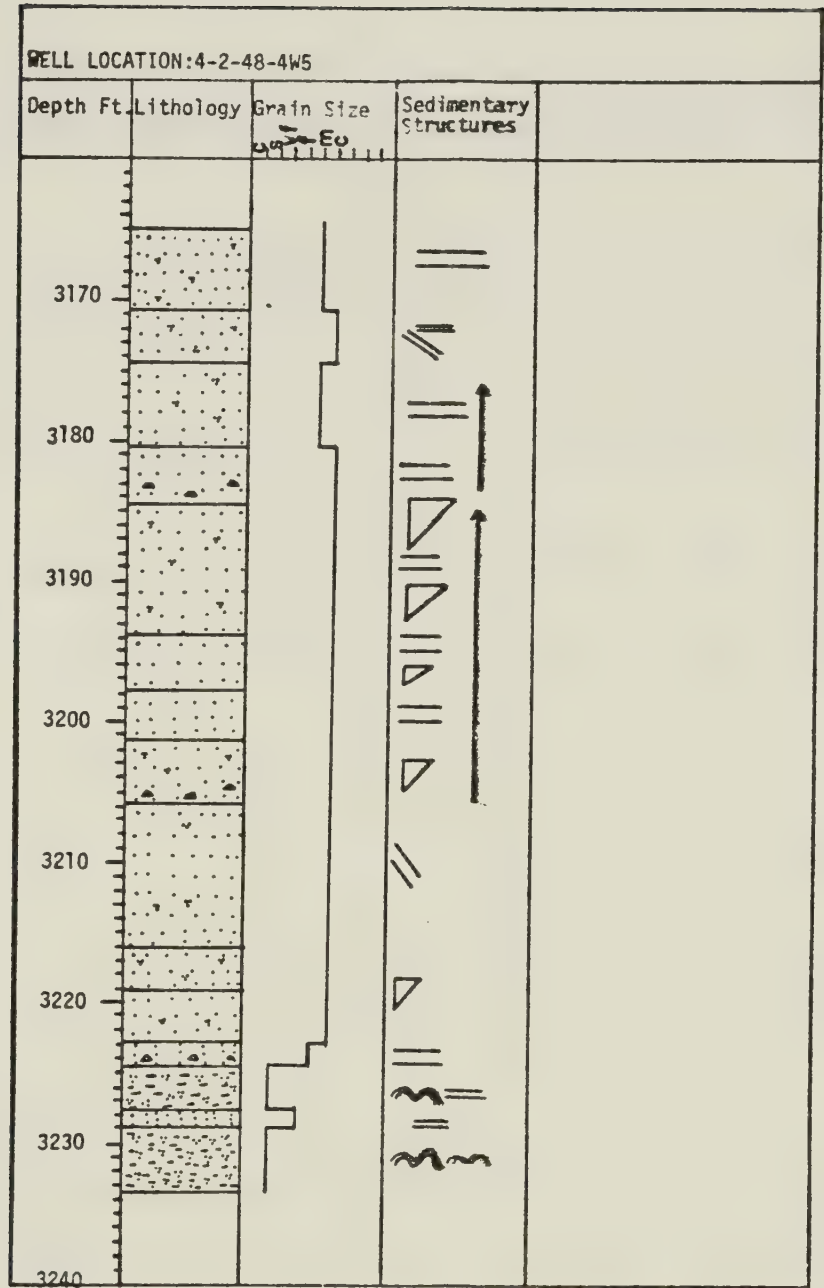














APPENDIX B.

Data Sheet for the Grain-Size Analyses (Using Humphries' Micrometer Eyepiece and the Counter Unit)

Serial No.	Well Name	Location	Sample No.	Counter No.	Grain No.	Grain %	Cumulative %	Corresponding Class Midpoints of Sizes ( $\phi$ )
1.1	IOE CDN-SUP PEMBINA	10-27-47-4W5	At 3212.8 ft	3	6	1.5	100	3.875
				4	21	5.3	98.8	3.625
				5	42	10.5	93.5	3.375
				6	47	11.8	83.0	3.125
				7	58	14.5	71.2	2.875
				8	55	13.8	56.7	2.625
				9	45	11.3	42.9	2.375
				10	48	12.00	31.6	2.125
				11	38	9.5	19.6	1.875
				12	26	6.5	10.1	1.625
				13	9	2.3	3.6	1.375
				14	4	1.0	1.3	1.125
				15	0	0	0.3	0.875
				16	1	0.3	0.3	0.625
1.2			At 3215.4 ft(A)	3	2	0.5	100	3.875
				4	6	1.5	99.5	3.625
				5	18	4.5	98.00	3.375
				6	30	7.5	93.5	3.125
				7	47	11.8	86.0	2.875
				8	75	18.8	74.3	2.625
				9	84	21.0	55.5	2.375
				10	64	16.0	34.5	2.125
				11	41	10.3	18.5	1.875
				12	23	5.8	8.3	1.625
				13	8	2.00	2.5	1.375
				14	2	0.5	0.5	1.125

.../Continued





APPENDIX B. - Continued

Serial No.	Well Name	Location	Sample No.	Counter No.	Grain No.	Grain %	Cumulative %	Corresponding Class Midpoints of Sizes ( $\phi$ )
1.3	IOE CDN-SUP PEMBINA	10-27-47 -4W5	At 3215.4 ft(B)	1	1	0.3	100	4.375
				2	4	1.0	99.8	4.125
				3	8	2.0	98.8	3.875
				4	11	2.8	96.8	3.625
				5	25	6.3	94.0	3.375
				6	53	13.3	87.8	3.125
				7	68	17.0	74.5	2.875
				8	89	22.3	57.5	2.625
				9	69	17.3	35.3	2.375
				10	45	11.3	18.0	2.125
				11	20	5.0	6.8	1.875
				12	5	1.3	1.8	1.625
				13	1	0.3	0.5	1.375
				14	1	0.3	0.3	1.125
1.4			At 3219.1 ft	3	1	0.3	100	3.875
				4	2	0.5	99.8	3.625
				5	12	3.0	99.3	3.375
				6	18	4.5	96.3	3.125
				7	26	6.5	91.8	2.875
				8	44	11.0	85.3	2.625
				9	47	11.8	74.3	2.375
				10	81	20.3	62.5	2.125
				11	83	20.8	42.3	1.875
				12	49	12.3	21.5	1.625
				13	23	5.8	9.3	1.375
				14	10	2.5	3.5	1.125
				15	4	1.0	1.0	0.875

.../Continued



## APPENDIX B. - Continued

Serial No.	Well Name	Location	Sample No.	Counter No.	Grain No.	Grain %	Cumulative %	Corresponding Class Midpoints of Sizes ( $\phi$ )
1.5	IOE CDN-SUP PEMBINA	10-27-47 -4W5	At 3233.8 ft	5	1	0.3	100	3.375
				6	3	0.8	99.8	3.125
				7	6	1.5	99.0	2.875
				8	15	3.8	97.5	2.625
				9	23	5.8	93.8	2.375
				10	57	14.3	88.0	2.125
				11	91	22.8	73.8	1.875
				12	86	21.5	51.0	1.625
				13	74	18.5	29.5	1.375
				14	27	6.8	11.0	1.125
				15	10	2.5	4.3	0.875
				16	5	1.3	1.8	0.625
				17	2	0.5	0.5	0.375
				4	2	0.5	100	3.625
				5	6	1.5	99.5	3.375
				6	12	3.0	98.0	3.125
2.6		10-34-47 -4W5	At 2186.3 ft (A)	7	16	4.0	95.0	2.875
				8	28	7.0	91.0	2.625
				9	41	10.3	84.0	2.375
				10	48	12.0	73.8	2.125
				11	55	13.8	61.8	1.875
				12	79	19.8	48.0	1.625
				13	60	15.0	28.3	1.375
				14	27	6.0	13.3	1.125
				15	16	4.0	6.5	0.875
				16	8	2.0	2.5	0.625
				17	2	0.5	0.5	0.375

.../Continued



APPENDIX B. - Continued

Serial No.	Well Name	Location	Sample No.	Counter No.	Grain No.	Grain %	Cumulative %	Corresponding Class Midpoints of Sizes (Ø)
2.7	IOE CDN-SUP PEMBINA	10-34-47 -4W5	At 2186.3 ft(B)	3	4	1	100	3.875
				4	10	2.5	99.0	3.625
				5	17	4.3	96.5	3.375
				6	24	6.0	92.3	3.125
				7	61	15.3	86.3	2.875
				8	75	18.8	71.0	2.625
				9	75	18.8	52.3	2.375
				10	65	16.3	33.5	2.125
				11	31	7.8	17.3	1.875
				12	24	6.0	9.5	1.625
				13	7	1.8	3.5	1.375
				14	5	1.3	1.3	1.125
				15	1	0.3	0.5	0.875
				16	1	0.3	0.3	0.625
				5	2	0.5	100	3.375
2.8			40	6	4	1.0	99.5	3.125
				7	2	0.5	98.5	2.875
				8	12	3.0	98.0	2.625
				9	28	7.0	95.0	2.375
				10	30	7.5	88.0	2.125
				11	29	7.3	80.5	1.875
				12	65	16.3	73.3	1.625
				13	90	22.5	57.0	1.375
				14	61	15.3	34.5	1.125
				15	39	9.8	19.3	0.875
				16	27	6.8	9.5	0.625
				17	11	2.8	2.8	0.375

.../Continued



APPENDIX B. - Continued

Serial No.	Well Name	Location	Sample No.	Counter No.	Grain No.	Grain %	Cumulative %	Corresponding Class Midpoints of Sizes ( $\phi$ )
2.9	IOE CDN-SUP PEMBINA	10-34-47-4W5	41	5	2	0.5	100	3.375
				6	7	1.8	99.5	3.125
				7	5	1.3	97.8	2.875
				8	23	5.8	96.5	2.625
				9	42	10.5	90.8	2.375
				10	61	15.3	80.3	2.125
				11	77	19.3	65.0	1.875
				12	70	17.5	45.8	1.625
				13	58	14.5	28.3	1.375
				14	37	9.3	13.8	1.125
				15	12	3.0	4.5	0.875
				16	5	1.3	1.5	0.625
				17	1	0.3	0.3	0.375
				4	1	0.3	100	3.625
				5	1	0.3	99.8	3.375
				6	2	0.5	99.5	3.125
2.10	50			7	6	1.5	99.0	2.875
				8	19	4.8	97.5	2.625
				9	32	8.0	92.8	2.375
				10	56	14.0	84.8	2.125
				11	80	20.0	70.8	1.875
				12	81	20.3	50.8	1.625
				13	75	18.8	30.5	1.375
				14	39	9.8	11.8	1.125
				15	7	1.8	2.0	0.875
				16	1	0.3	0.3	0.625

.../Continued





APPENDIX B. - Continued

Serial No.	Well Name	Location	Sample No.	Counter No.	Grain No.	Grain %	Cumulative %	Corresponding Class Midpoints for Sizes ( $\phi$ )
2.11	IOE CDN-SUP PEMBINA	10-34-47-4W5	52	5	1	0.3	100	3.375
				6	6	1.5	99.8	3.125
				7	10	2.5	98.3	2.875
				8	17	4.3	95.8	2.625
				9	27	6.8	91.5	2.375
				10	55	13.8	84.8	2.125
				11	85	21.3	71.0	1.875
				12	82	20.5	49.8	1.625
				13	67	16.8	29.3	1.375
				14	29	7.3	12.5	1.125
				15	16	4.0	5.3	0.875
				16	5	1.3	1.3	0.625
				5	3	0.8	100	3.375
				6	11	2.8	99.3	3.125
				7	20	5.0	96.5	2.875
				8	42	10.5	91.5	2.625
2.12			53	9	52	13.0	81.0	2.375
				10	72	18.0	68.0	2.125
				11	59	14.8	50.0	1.875
				12	69	17.3	35.3	1.625
				13	34	8.5	18.0	1.375
				14	28	7.0	9.5	1.125
				15	5	1.3	2.5	0.875
				16	4	1.0	1.3	0.625
				17	1	0.3	0.3	0.375

.../Continued



APPENDIX B. - Continued

Serial No.	Well Name	Location	Sample No.	Counter No.	Grain No.	Grain %	Cumulative %	Corresponding Class Midpoints for Sizes ( $\phi$ )
3.13	IOE CDN-SUP PEMBINA	10-35-47-4W5	6	6	2	0.5	100	3.125
				7	6	1.5	99.5	2.875
				8	20	5.0	98.0	2.625
				9	35	8.8	93.0	2.375
				10	57	14.3	84.3	2.125
				11	79	19.8	70.0	1.875
				12	89	21.8	50.3	1.625
				13	63	15.8	28.5	1.375
				14	27	6.8	12.8	1.125
				15	17	4.3	6.0	0.875
				16	4	1.0	1.8	0.625
				17	3	0.8	0.8	0.375
				5	1	0.3	100	3.375
				6	2	0.5	99.8	3.125
				7	7	1.8	99.3	2.875
				8	11	2.8	97.5	2.625
3.14			18	9	20	5.0	94.8	2.375
				10	24	6.0	89.8	2.125
				11	25	6.3	83.8	1.875
				12	33	8.3	77.5	1.625
				13	53	13.3	69.3	1.375
				14	74	18.5	56.0	1.125
				15	66	16.5	37.5	0.875
				16	60	15.0	21.0	0.625
				17	22	5.5	6.0	0.375
				18	2	0.5	0.5	0.125

.../Continued



APPENDIX B. - Continued

Serial No.	Well Name	Location	Sample No.	Counter No.	Grain No.	Grain %	Cumulative %	Corresponding Class Midpoints for Sizes ( $\phi$ )
3.15	IOE CDN-SUP PEMBINA	10-35-47-4W5	20	4	1	0.3	100	3.625
				5	2	0.5	99.8	3.375
				6	1	0.3	99.3	3.125
				7	8	2.0	99.0	2.875
				8	16	4.0	97.0	2.625
				9	23	5.8	93.0	2.375
				10	45	11.3	87.3	2.125
				11	56	14.0	76.0	1.875
				12	69	17.3	62.0	1.625
				13	83	20.8	44.8	1.375
				14	52	13.0	24.0	1.125
				15	28	7.0	11.0	0.875
				16	9	2.3	4.0	0.625
				17	7	1.8	1.8	0.375
				5	1	0.3	100	3.375
				6	3	0.8	99.8	3.125
3.16			23	7	4	1.0	99.0	2.875
				8	9	2.3	98.0	2.625
				9	18	4.5	95.8	2.375
				10	36	9.0	91.3	2.125
				11	51	12.8	82.3	1.875
				12	58	14.5	69.2	1.625
				13	71	17.8	55.0	1.375
				14	65	16.3	37.3	1.125
				15	47	11.8	21.0	0.875
				16	25	6.3	9.3	0.625
				17	11	2.8	3.0	0.375
				18	1	0.3	0.3	0.125
				.../Continued				





APPENDIX B. - Continued

Serial No.	Well Name	Location	Sample No.	Counter No.	Grain No.	Grain %	Cumulative %	Corresponding Class Midpoints for Sizes ( $\phi$ )
3.17	IOE CDN-SUP PEMBINA	10-35-47 -4W5	25	5	1	0.3	100	3.375
				6	1	0.3	99.8	3.125
				7	1	0.3	99.5	2.875
				8	5	1.3	99.3	2.625
				9	20	5.0	98.0	2.375
				10	33	8.3	93.0	2.125
				11	41	10.3	84.8	1.875
				12	79	19.8	74.5	1.625
				13	83	20.8	54.8	1.375
				14	69	17.3	34.0	1.125
				15	43	10.8	16.8	0.875
				16	18	4.5	6.0	0.625
				17	6	1.5	1.5	0.375
				5	1	0.3	100	3.375
				6	5	1.3	99.8	3.125
				7	10	2.5	98.5	2.875
3.18			39	8	23	5.8	96.0	2.625
				9	23	5.8	90.3	2.375
				10	30	7.5	84.5	2.125
				11	60	15.0	77.0	1.875
				12	75	18.8	62.0	1.625
				13	80	20.0	43.3	1.375
				14	44	11.0	23.3	1.125
				15	33	8.3	12.3	0.875
				16	14	3.5	4.0	0.625
				17	2	0.5	0.5	0.375

.../Continued



APPENDIX B. - Continued

Serial No.	Well Name	Location	Sample No.	Counter No.	Grain No.	Grain %	Cumulative %	Corresponding Class Midpoints for Sizes ( $\phi$ )
3.19	IOE CDN-SUP PEMBINA	10-35-47-4W5	46	4	1	0.3	100	3.625
				5	2	0.5	99.8	3.375
				6	6	1.5	99.3	3.125
				7	11	2.8	97.3	2.875
				8	13	3.3	95.0	2.625
				9	20	5.0	91.8	2.375
				10	46	11.5	86.8	2.125
				11	73	18.3	75.3	1.875
				12	82	20.5	57.0	1.625
				13	68	17.0	36.5	1.375
				14	53	13.3	19.5	1.125
				15	16	4.0	6.3	0.875
				16	8	2.0	2.3	0.625
				17	1	0.3	0.3	0.375
				5	1	0.3	100	3.375
				6	1	0.3	99.8	3.125
4.20		4-36-47-4W5	12	7	5	1.3	99.5	2.875
				8	12	3.0	98.3	2.625
				9	24	6.0	95.3	2.375
				10	52	13.0	89.3	2.125
				11	83	20.8	76.3	1.875
				12	84	21.0	55.5	1.625
				13	60	15.0	34.5	1.375
				14	37	9.3	19.5	1.125
				15	29	7.3	10.3	0.875
				16	11	2.8	3.0	0.625
				17	1	0.3	0.3	0.375

.../Continued



APPENDIX B. - Continued

Serial No.	Well Name	Location	Sample No.	Counter No.	Grain No.	Grain %	Cumulative %	Corresponding Class Midpoints for Sizes ( $\phi$ )
4.21	IOE CDN-SUP PEMBINA	4-36-47 -4W5	16	6	1	0.3	100	3.125
				7	1	0.3	99.8	2.875
				8	2	0.5	99.5	2.625
				9	14	3.5	99.0	2.375
				10	27	6.8	95.5	2.125
				11	50	12.5	88.5	1.875
				12	84	21.0	76.3	1.625
				13	94	23.5	55.3	1.375
				14	72	18.0	31.8	1.125
				15	37	9.3	13.8	0.875
				16	13	3.3	4.5	0.625
				17	5	1.3	1.3	0.375
				5	1	0.3	100	3.375
				6	3	0.8	99.8	3.125
				7	11	2.8	99.0	2.875
				8	20	5.0	96.3	2.625
				9	27	6.8	91.3	2.375
4.22		18		10	44	11.0	84.5	2.125
				11	70	17.5	73.5	1.875
				12	84	21.0	56.0	1.625
				13	81	20.3	35.0	1.375
				14	35	8.8	14.8	1.125
				15	14	3.5	6.0	0.875
				16	9	2.3	2.5	0.625
				17	1	0.3	0.3	0.375

.../Continued



## APPENDIX B. - Continued

Serial No.	Well Name	Location	Sample No.	Counter No.	Grain No.	Grain %	Cumulative %	Corresponding Class Midpoints for Sizes ( $\phi$ )
4.23	IOE CDN-SUP PEMBINA	4-36-47 -4W5	19	5	1	0.3	100	3.375
				6	4	1.0	99.8	3.125
				7	3	0.8	98.8	2.875
				8	6	1.5	98.0	2.625
				9	21	5.3	96.5	2.375
				10	44	11.0	91.3	2.125
				11	74	18.5	80.3	1.875
				12	98	24.5	61.8	1.625
				13	82	20.5	37.3	1.375
				14	46	11.5	16.8	1.125
				15	14	3.5	5.3	0.875
				16	5	1.3	1.8	0.625
				17	2	0.5	0.5	0.375
				4	1	0.3	100	3.625
				5	1	0.3	99.8	3.375
				6	7	1.8	99.5	3.125
				7	4	1.0	97.8	2.875
4.24			23	8	19	4.8	96.8	2.625
				9	33	8.3	92.0	2.375
				10	61	15.3	83.8	2.125
				11	88	22.0	68.5	1.875
				12	87	21.8	46.5	1.625
				13	53	13.3	24.8	1.375
				14	36	9.0	11.5	1.125
				15	8	2.0	2.5	0.875
				16	2	0.5	0.5	0.625

.../Continued





APPENDIX B. - Continued

Serial No.	Well Name	Location	Sample No.	Counter No.	Grain No.	Grain %	Cumulative %	Corresponding Class Midpoints for Sizes ( $\phi$ )
4.25	IOE CDN-SUP PEMBINA	4-36-47 -4W5	25	4	2	0.5	100	3.625
				5	3	0.8	99.5	3.375
				6	10	2.5	98.3	3.125
				7	11	2.8	96.3	2.875
				8	20	5.0	93.5	2.625
				9	41	10.3	88.5	2.375
				10	63	15.8	78.3	2.125
				11	59	14.8	62.5	1.875
				12	63	15.8	47.8	1.625
				13	55	13.8	32.0	1.375
				14	47	11.8	18.3	1.125
				15	16	4.0	6.5	0.875
				16	8	2.0	2.5	0.625
				17	2	0.5	0.5	0.375
				4	1	0.3	100	3.625
				5	1	0.3	99.8	3.375
				6	4	1.0	99.5	3.125
4.26			35	7	5	1.3	98.5	2.875
				8	6	1.5	97.3	2.625
				9	19	4.8	95.8	2.375
				10	30	7.5	91.0	2.125
				11	49	12.3	83.5	1.875
				12	68	17.0	71.3	1.625
				13	72	18.0	54.3	1.375
				14	71	17.8	36.3	1.125
				15	45	11.3	18.5	0.875
				16	20	5.0	7.3	0.625
				17	9	2.3	2.3	0.375

.../Continued



APPENDIX B. - Continued

Serial No.	Well Name	Location	Sample No.	Counter No.	Grain No.	Grain %	Cumulative %	Corresponding Class Midpoints for Sizes (Ø)
4.27	IOE CDN-SUP PEMBINA	4-36-47 -4W5	37	5	1	0.3	100	3.375
				6	3	0.8	99.8	3.125
				7	7	1.8	99.0	2.875
				8	21	5.3	97.3	2.625
				9	35	8.8	92.0	2.375
				10	53	13.3	83.3	2.125
				11	63	15.8	70.0	1.875
				12	90	22.5	54.3	1.625
				13	65	16.3	31.8	1.375
				14	44	11.0	15.5	1.125
				15	12	3.0	4.5	0.875
				16	4	1.0	1.5	0.625
				17	2	0.5	0.5	0.375
5.28	4-2-48 -4W5	12	3	2	0.5	100	3.875	
			4	2	0.5	99.5	3.625	
			5	1	0.3	99.0	3.375	
			6	14	3.5	98.8	3.125	
			7	17	4.3	95.3	2.875	
			8	41	10.3	91.0	2.625	
			9	82	20.5	80.8	2.375	
			10	89	22.3	60.3	2.125	
			11	74	18.5	38.0	1.875	
			12	44	11.0	19.5	1.625	
			13	21	5.3	8.5	1.375	
			14	10	2.5	3.8	1.125	
			15	2	0.5	0.3	0.875	
16	1	0.3	0.3	0.625				

.../Continued



APPENDIX B. - Continued

Serial No.	Well Name	Location	Sample No.	Counter No.	Grain No.	Grain %	Cumulative %	Corresponding Class Midpoints for Sizes (Ø)				
5.29	IOE CDN-SUP PEMBINA	4-2-48 -4W5	13	4	1	0.3	100	3.625				
				5	1	0.3	99.8	3.375				
				6	2	0.5	99.5	3.125				
				7	7	1.8	99.0	2.875				
				8	15	3.8	97.3	2.625				
				9	25	6.3	93.5	2.375				
				10	41	10.3	87.3	2.125				
				11	68	17.0	77.0	1.875				
				12	76	19.0	60.0	1.625				
				13	73	18.3	41.0	1.375				
				14	55	13.8	22.8	1.125				
				15	22	5.5	9.0	0.875				
				16	11	2.8	3.5	0.625				
				17	3	0.8	0.5	0.375				
				5.30			16	5	2	0.5	100	3.375
								6	1	0.3	99.5	3.125
								7	8	2.0	99.3	2.875
8	7	1.8	97.3					2.625				
9	8	2.0	95.5					2.375				
10	27	6.8	93.5					2.125				
11	50	12.5	86.8					1.875				
12	81	20.3	74.3					1.625				
13	92	23.0	54.0					1.375				
14	74	18.5	31.0					1.125				
15	34	8.5	12.5					0.875				
16	14	3.5	4.0					0.625				
17	2	0.5	0.5					0.375				
.../Continued												





## APPENDIX B. - Continued

Serial No.	Well Name	Location	Sample No.	Counter No.	Grain No.	Grain %	Cumulative %	Corresponding Class Midpoints for Sizes (Ø)				
5.31	IOE CDN-SUP PEMBINA	4-2-48 -4W5	23 (A)	6	3	0.8	100	3.125				
				7	5	1.3	99.3	2.875				
				8	13	3.3	98.0	2.625				
				9	16	4.0	94.8	2.375				
				10	17	4.3	90.8	2.125				
				11	38	9.5	86.5	1.875				
				12	61	15.3	77.0	1.625				
				13	62	15.5	61.8	1.375				
				14	68	17.0	46.3	1.125				
				15	56	14.0	29.3	0.875				
				16	47	11.8	15.3	0.625				
				17	12	3.0	3.5	0.375				
				18	2	0.5	0.5	0.125				
				5.32			23 (B)	4	2	0.5	100	3.625
								5	3	0.8	99.8	3.375
								6	5	1.3	98.5	3.125
								7	16	4.0	97.5	2.875
								8	29	7.3	93.5	2.625
9	43	10.8	86.3					2.375				
10	61	15.3	75.5					2.125				
11	80	20.0	60.3					1.875				
12	65	16.3	40.3					1.625				
13	48	12.0	24.0					1.375				
14	35	8.8	12.0					1.125				
15	11	2.8	3.3					0.875				
16	1	0.3	0.5					0.625				
17	1	0.3	0.3					0.375				

.../Continued

.../Continued



APPENDIX B. - Continued

Serial No.	Well Name	Location	Sample No.	Counter No.	Grain No.	Grain %	Cumulative %	Corresponding Class Midpoints for Sizes ( $\phi$ )
5.33	IOE CDN-SUP PEMBINA	4-2-48-4W5	33 (A)	6	3	0.8	100	3.125
				7	8	2.0	99.3	2.875
				8	16	4.0	97.3	2.625
				9	33	8.3	93.3	2.375
				10	32	8.0	85.0	2.125
				11	66	16.5	77.0	1.875
				12	84	21.0	60.5	1.625
				13	61	15.3	39.5	1.375
				14	61	15.3	24.3	1.125
				15	21	5.3	9.0	0.875
				16	11	2.8	3.8	0.625
				17	4	1.0	1.0	0.375
				3	1	0.3	100	3.875
				4	4	1.0	99.8	3.625
				5	7	1.8	98.8	3.375
				6	8	2.0	97.0	3.125
				7	27	6.8	95.0	2.875
5.34	33 (B)			8	48	12.0	88.3	2.625
				9	69	17.3	76.3	2.375
				10	87	21.8	59.0	2.125
				11	62	15.5	37.3	1.875
				12	52	13.0	21.8	1.625
				13	25	6.3	8.8	1.375
				14	7	1.8	2.5	1.125
				15	3	0.8	0.8	0.875
				3	1	0.3	100	3.875
				4	4	1.0	99.8	3.625
				5	7	1.8	98.8	3.375
				6	8	2.0	97.0	3.125

.../Continued



APPENDIX B. - Continued

Serial No.	Well Name	Location	Sample No.	Counter No.	Grain No.	Grain %	Cumulative %	Corresponding Class Midpoints for Sizes ( $\phi$ )
5.35	IOE CDN-SUP PEMBINA	4-2-48 -4W5	42	6	2	0.5	100	3.125
				7	9	2.3	99.5	2.875
				8	15	3.8	97.3	2.625
				9	42	10.5	93.5	2.375
				10	73	18.3	83.0	2.125
				11	84	21.0	64.8	1.875
				12	86	21.5	43.8	1.625
				13	49	12.3	22.3	1.375
				14	28	7.0	10.0	1.125
				15	8	2.0	3.0	0.875
				16	3	0.8	1.0	0.625
				17	1	0.3	0.3	0.375
				6	2	0.5	100	3.125
				7	10	2.5	99.5	2.875
				8	17	4.3	97.0	2.625
				9	27	6.8	92.8	2.375
5.36		46		10	66	16.5	86.0	2.125
				11	93	23.3	69.5	1.875
				12	85	21.3	46.3	1.625
				13	53	13.3	25.0	1.375
				14	29	7.3	11.8	1.125
				15	14	3.5	4.5	0.875
				16	2	0.5	1.0	0.625
				17	2	0.5	0.5	0.375

.../Continued



APPENDIX B. - Continued

Serial No.	Well Name	Location	Sample No.	Counter No.	Grain No.	Grain %	Cumulative %	Corresponding Class Midpoints for Sizes ( $\phi$ )
5.37	IOE CDN-SUP PEMBINA	4-2-48 -4W5	47	5	1	0.3	100	3.375
				6	3	0.8	99.8	3.125
				7	7	1.8	99.0	2.875
				8	8	2.0	97.3	2.625
				9	28	7.0	95.3	2.375
				10	68	17.0	88.3	2.125
				11	83	20.8	71.3	1.875
				12	85	21.3	50.5	1.625
				13	58	14.5	29.3	1.375
				14	30	7.5	14.8	1.125
				15	16	4.0	7.3	0.875
				16	9	2.3	3.3	0.625
				17	4	1.0	1.0	0.375
				5	1	0.3	100	3.375
				6	4	1.0	99.8	3.125
				7	6	1.5	98.8	2.875
5.38			51	8	32	8.0	97.3	2.625
				9	43	10.8	89.3	2.375
				10	75	18.8	78.5	2.125
				11	72	18.0	59.8	1.875
				12	65	16.3	41.8	1.625
				13	44	11.0	25.5	1.375
				14	40	10.0	14.5	1.125
				15	13	3.3	4.5	0.875
				16	4	1.0	1.3	0.625
				17	1	0.3	0.3	0.375

















**B30235**